

**The PM19 Protein: a Functional Analysis in *Arabidopsis thaliana***

**Omar M Alsaif**

A thesis submitted for the degree of

**Doctor of Philosophy**

**School of Life Sciences**

**Heriot-Watt University**

**Edinburgh, UK**

**September 2013**

**Copyright Statement:**

*“The copyright in this thesis is owned by the author. Any quotation from the thesis or use of any of the information contained in it must acknowledge this thesis as the source of the quotation or information.”*

---

## ABSTRACT

The amino acid sequence of the trans-membrane protein, PM19, unique to the plant kingdom has been highly conserved over 450 million years of evolution in all plant genera including ferns and mosses, but is not found in aqueous plants such as algae. Thus, the function of this protein is possibly linked to the plant ability to grow on land. We have investigated the PM19 protein using a number of molecular biological tools in *Arabidopsis thaliana*. Gene expression studies using bioinformatics, northern blotting and promoter-GUS fusions show that the AtPM19 gene is highly expressed in seeds and seedlings, in addition to expression observed in leaves under drought stress. A translational fusion with GFP reveals that the protein is located in the plasma membrane. T-DNA insertion mutants have a germination phenotype; the mutant is more sensitive to high levels of salts in the medium, and in addition, the mutant has a lower stomatal conductance indicative of reduced guard cell turgor. The predicted secondary structure of the protein and the mutant phenotype suggest that PM19 may be a cation transporter and this is being tested by functional complementation of yeast mutants.

---

## **DEDICATION**

I lovingly dedicate this thesis to my wife and parents.

---

## **ACKNOWLEDGMENT**

I would like to offer my sincerest gratitude to my supervisor, Dr. Peter Morris, who has supported me throughout my research project with his practical help and knowledge, without him this thesis would not have been completed.

In my daily work in T.23 lab I have been blessed with a friendly and helpful group of fellow students who in many ways I have learnt much from and because of them. A special thanks to Mohammed Abbas, Salem Rajab, Callum Scott, Bayani wan Omar and Monica Agarwal for their technical help and support.

The Saudi Government has funded my studies and the School of Life Sciences has provided the support and equipment I have needed to produce and complete my thesis.

I want to thank my parents, my family, relatives and friends for encouragement that was an important source of inspiration throughout all my studies in the UK. Finally, I am indebted to the endless love and countless help I received from Noor (my wife), Faris and Khalid (my sons). Also I want to send my love to Maryam (my soon coming baby in sha'a Allah).

---

## **DECLARATION STATEMENT**

I, Omar M Alsaif, hereby declare that I am the author of this thesis. All the work described in this thesis is my own, except where stated in the text. The work presented here has not been accepted in any previous applications for a higher degree. All the sources of information have been consulted by myself and are acknowledged by means of reference.

Omar Alsaif,

ACADEMIC REGISTRY  
**Research Thesis Submission**



Name:	Omar Mohammed A Alsaif		
School/PGI:	School of Life Sciences		
Version: <i>(i.e. First, Resubmission, Final)</i>	Final submission	Degree Sought (Award and Subject area)	PhD in Biotechnology

**Declaration**

In accordance with the appropriate regulations I hereby submit my thesis and I declare that:

- 1) the thesis embodies the results of my own work and has been composed by myself
- 2) where appropriate, I have made acknowledgement of the work of others and have made reference to work carried out in collaboration with other persons
- 3) the thesis is the correct version of the thesis for submission and is the same version as any electronic versions submitted\*.
- 4) my thesis for the award referred to, deposited in the Heriot-Watt University Library, should be made available for loan or photocopying and be available via the Institutional Repository, subject to such conditions as the Librarian may require
- 5) I understand that as a student of the University I am required to abide by the Regulations of the University and to conform to its discipline.

\* *Please note that it is the responsibility of the candidate to ensure that the correct version of the thesis is submitted.*

Signature of Candidate:		Date:	/ / 2014
-------------------------	--	-------	----------

**Submission**

Submitted By <i>(name in capitals)</i> :	OMAR MOHAMMED A ALSAIF
Signature of Individual Submitting:	
Date Submitted:	

**For Completion in the Student Service Centre (SSC)**

Received in the SSC by <i>(name in capitals)</i> :			
<i>Method of Submission</i> <i>(Handed in to SSC; posted through internal/external mail):</i>			
<i>E-thesis Submitted (mandatory for final theses)</i>			
Signature:		Date:	

---

## TABLE OF CONTENT

Copyright Statement: .....	II
ABSTRACT .....	III
DEDICATION .....	IV
ACKNOWLEDGMENT .....	V
DECLARATION STATEMENT .....	VI
TABLE OF CONTENT .....	VIII
LIST OF FIGURES: .....	XII
LIST OF TABLES .....	XV
ABBREVIATIONS AND SYMBOLS .....	XVI
1. INTRODUCTION: .....	2
1.1. Background: .....	2
1.2. Arabidopsis thaliana .....	4
1.3. Transmembrane proteins: .....	6
1.4. Protein sorting: .....	9
1.5. Transport through the cellular plasma membrane: .....	10
1.6. Potassium transport through plasma membrane: .....	14
1.7. Sodium transport through plasma membrane: .....	19
1.8. Abiotic stress: .....	20
1.9. Plant and water deficiency: .....	21
1.10. Drought stress tolerance mechanism in plant cell: .....	21
1.11. Salt stress tolerance mechanisms: .....	23
1.12. Abscisic acid: .....	25
1.13. Transformation .....	29
1.14. Methods for plant transformation: .....	30
1.15. <i>Saccharomyces cerevisiae</i> as a biotechnology tool .....	34
1.16. PM19 protein: .....	36
1.17. The plan of investigation: .....	38
2. MATERIALS AND METHODS: .....	41
2.1. Materials: .....	41
2.2. Centrifugation .....	41
2.3. Images .....	41



---

2.4. Source of seeds .....	41
2.5. Plant growth conditions .....	42
2.6. DNA methods .....	42
2.6.1. Extraction of genomic DNA from plant tissue .....	42
2.6.2. Plasmid DNA purifications.....	43
2.6.3. Restriction enzyme digests .....	43
2.6.4. DNA ligations .....	44
2.6.5. Standard PCR reactions preparation .....	44
2.6.6. Agarose gel electrophoresis of DNA .....	47
2.6.7. Gel purification of DNA .....	47
2.6.8. Preparation and transformation of E. coli competent cells:.....	47
2.7. RNA methods: .....	48
2.7.1. Preparation and quantifying of total RNA from Arabidopsis tissues: .....	48
2.7.2. From Arabidopsis leaves: .....	48
2.7.3. From Arabidopsis seeds:.....	49
2.7.4. Quantifying RNA concentration by spectrophotometer: .....	50
2.7.5. Preparation of RNA denaturing gel: .....	51
2.7.6. Northern blotting: .....	51
2.7.6.1. Preparation of RNA probe: .....	51
2.7.6.2. Transferring RNA to a Membrane (Capillary Transfer Method): .....	51
2.7.6.3. Fixing RNA to membrane.....	52
2.7.6.4. Pre-hybridization .....	52
2.7.6.5. Denaturation of the probe .....	52
2.7.6.6. Hybridization .....	53
2.7.6.7. Washing .....	53
2.7.6.8. Blocking.....	53
2.7.6.9. Washing .....	54
2.7.6.10. Detection.....	54
2.8. Characterization of mutants .....	54
2.8.1. Seed sterilization:.....	54
2.8.2. Sowing the seeds for germination percentage: .....	54
2.8.3. Drought experiments.....	55
2.8.3.1. Water loss: .....	55
2.8.3.2. Stomatal conductancy:.....	55
2.9. The floral dip <i>Agrobacterium</i> plant transformation:.....	57

---

---

2.10. Staining GUS-expressing plants: .....	57
2.11. Yeast methods:.....	57
2.11.1. Extraction of DNA from yeast:.....	57
2.11.2. Yeast Transformation (Electroporation):.....	58
3. RESULTS: .....	61
3.1. PM19 in evolution: .....	61
3.2. Prediction of protein localization:.....	73
3.3. <i>PM19</i> expression pattern .....	74
3.3.1. PM19 protein expression in different stages of plant life:.....	75
3.3.2. <i>PM19::GUS</i> fusion expression in plants under drought stress:.....	81
3.4. PM19 protein localisation in the cell: .....	83
3.4.1. Transformation of <i>A. thaliana</i> plants:.....	84
3.4.2. AtPM19-GFP expression analysis .....	84
3.4.3. Obtaining homozygous 35S::PM19-GFP .....	86
3.5. Molecular biological analysis of the transgenic plants:.....	88
3.5.1. PCR confirmation of the insertion mutation of AtPM19 DNA .....	88
3.5.2. Sequencing the mutant AtPM19 gene: .....	90
3.5.3. Left border/forward: .....	90
3.5.4. Left border/reverse:.....	90
3.5.5. Northern blot confirmation of the silencing of <i>AtPM19</i> gene expression: ....	91
3.5.6. Overexpression of <i>AtPM19</i> gene: .....	92
3.6. Physiological analysis of <i>AtPM19</i> under different abiotic stresses: .....	95
3.6.1. Analysis of the germination percentage of wildtype and <i>atmp19</i> mutants under different abiotic stresses: .....	95
3.6.2. Alkali metals .....	95
3.6.3. Low water availability .....	97
3.6.4. Abscisic acid .....	97
3.6.5. Stomatal conductancy:.....	104
3.6.6. Analysis of leaf weight loss:.....	106
3.7. Yeast functional complementation: .....	107
3.7.1. Cloning of <i>AtPM19</i> into yeast plasmid vector.....	107
3.7.2. Confirmation of pYES2-PM19 cloning [digestion with <i>XbaI</i> + <i>BamH1</i> ]: ....	109
3.7.3. Transformation of the yeast vector pYES2 containing <i>AtPM19</i> into yeast strains:.....	110
3.7.4. Yeast in SDAP media containing 75 mM NaCl pH 5.8: .....	110

---

---

4. DISCUSSION:.....	113
4.1. Molecular characterization of the <i>A. thaliana</i> PM19 gene and its expression: .....	113
4.2. AtPM19 protein localisation:.....	120
4.3. Physiological analysis of germination:.....	123
4.4. Yeast functional complementation:.....	127
4.5. Conclusions:.....	130
5. REFERENCES:.....	131

---

## LIST OF FIGURES:

Figure 1: World population presented on a logarithm scale over the past 10,000 years..	2
Figure 2: <i>Arabidopsis thaliana</i> plant (Meinke et al. 1998).....	5
Figure 3: Different ways in which proteins interact with plasma membrane bilayer. ....	7
Figure 4: Molecules or ions can pass through the membrane via simple diffusion, passive transport where there is no atp required, or via active transport when the transport is against the concentration gradient where atp is required.....	13
Figure 5: The structural modelling of plant K <sup>+</sup> channels and transporters obtained from (Chen et al. 2008).....	18
Figure 6: The figure shows transport proteins that appear to be involved in the influx and efflux of potassium and sodium ions through the plasma membrane of <i>S.</i> <i>Cerevisiae</i> . ....	35
Figure 7: A graph of the primers used in this study. ....	46
Figure 8: The picture explains the concept of the soil drying drought experiment. ....	56
Figure 9: Multiple protein sequence alignment for PM19 homologues from different plant species showing the degree of conservation of the amino acids.....	67
Figure 10: The PM19 protein sequence is conserved in plant groups for over four hundred million years.. ....	68
Figure 11: A phylogenetic tree comparing the amino acids sequences of PM19 from representative plant species, and illustrating that although the <i>A. thaliana</i> PM19 protein may share common ancestors with higher plants such as rice, there are also roots that are shared with other more primitive plants like mosses, club mosses, and pine trees (Dereeper et al., 2008).....	69
Figure 12: PM19 multiple protein sequence alignment for different plant species showing the hydrophobicity of the amino acids. ....	70
Figure 13: Predicted transmembrane tendency of AtPM19.....	71
Figure 14: PM19 multiple protein sequence alignment for different plant species showing the secondary structure of the amino acids. ....	72
Figure 15: A schematic map of the <i>PM19 promoter-gus</i> system made by (Pons 2005)	75
Figure 16: Crushed dry seeds of columbia (0) wild type (top) and <i>PM19::gus</i> (bottom) plant stained for gus activity.....	77
Figure 17: Cotyledons of wild type (top) and <i>pm19::gus</i> (bottom) plant stained for gus activity after 7 days in plant media. ....	78
Figure 18: primary roots of <i>pm19::gus</i> plant stained for gus activity after 7 days in plant media.....	79
Figure 19: primary root of <i>pm19::gus</i> plant stained for gus activity after 11 days in plant media.....	80
Figure 20: Cotyledon and leaves of <i>pm19::gus</i> plant stained for gus activity after 11 days in plant media. ....	80
Figure 21: Leaf of <i>PM19::gus</i> plant stained for gus activity after 15 days in plant media .....	81
Figure 22: Root of <i>pm19::gus</i> plant stained for gus activity after 15 days in plant media .....	81
Figure 23: Leaves from 2 weeks old <i>pm19::gus A. thaliana</i> plants stained for gus activity. ....	82

Figure 24: The plasmids used for the localisation experiments of pm19 protein in the plant cell.....	83
Figure 25: Confocal microscopy of <i>A. thaliana</i> root cells from transformed plants with <i>35s::gfp</i> .....	85
Figure 26: Confocal microscopy of <i>A. thaliana</i> root cells from transformed plants with <i>35s::pm19-gfp</i> .....	85
Figure 27: 1% agarose gel electrophoresis for PCR amplifications based on genomic dna from T <sub>1</sub> <i>35S::PM19-GFP</i> plants.....	86
Figure 28: 1% agarose gel electrophoresis for pcr amplifications based on genomic DNA from <i>35S::PM19-GFP</i> plants.....	87
Figure 29: Gel electrophoresis photo showing PCR products produced using genomic DNA of wild type and mutant <i>atpm19</i> <i>A. thaliana</i> plants.....	89
Figure 30: A schematic graphic of the mutant <i>atpm19</i> gene in the genomic DNA of <i>A. thaliana</i> .....	89
Figure 31: Northern blot for RNA extracted from wildtype and <i>atpm19</i> mutant from seeds.....	92
Figure 32: Cloning plan for overexpression of the <i>ATPM19</i> ORF into a binary vector.	93
Figure 33: Confirmation of the transformed <i>Arabidopsis</i> plants with the pBinar plasmid DNA carrying the <i>35S::PM19</i> fragment.....	94
Figure 34: RNA denaturing gel of total RNA from leaves of different genotypes of <i>A. thaliana</i> plants.....	94
Figure 35: Germination percentage of wild type, mutant <i>AtPM19</i> and <i>35S::PM19-GFP</i> seeds on media containing H <sub>2</sub> O.....	98
Figure 36: Germination percentage of wild type, mutant <i>AtPM19</i> and <i>35S::PM19-GFP</i> seeds on media containing different concentrations of KCl.....	98
Figure 37: Germination percentage of wild type, mutant <i>AtPM19</i> and <i>35S::PM19-GFP</i> seeds on media containing different concentrations of NaCl.....	99
Figure 38: Germination percentage of wild type, mutant <i>AtPM19</i> and <i>35S::PM19-GFP</i> seeds on media containing different concentrations of mannitol.....	100
Figure 39: Germination percentage of wild type, mutant <i>AtPM19</i> and <i>35S::PM19-GFP</i> seeds on media containing different concentrations of ABA.....	101
Figure 40: Germination percentage of wild type, mutant <i>AtPM19</i> and <i>35S::PM19-GFP</i> seeds on media containing different concentrations of CsCl.....	101
Figure 41: Germination percentage of wild type, mutant <i>AtPM19</i> and <i>35S::PM19-GFP</i> seeds on media containing different concentrations of LiCl.....	102
Figure 42: Germination percentage of wild type, mutant <i>AtPM19</i> and <i>35S::PM19-GFP</i> seeds on media containing different concentrations of RbCl.....	103
Figure 43: Stomatal conductancy of wildtype, mutant <i>AtPM19</i> and <i>35S::PM19-GFP</i> plants under normal watering and drought conditions.....	105
Figure 44: Leaf weight loss over 6 hours.....	106
Figure 45: The plasmid vector used to insert <i>AtPM19</i> cDNA into the plasmid contains the selectable marker URA3 for selection in yeast.....	108
Figure 46: A DNA gel electrophoresis showing DNA fragments of yes2- <i>AtPM19</i> construct after digestion with <i>Xba</i> I and <i>Bam</i> HI.....	109

---

Figure 47: WT yeast, *trk1* and *tok1* mutants, mutants with pYes2 vector and with yes2-  
AtPM19 were diluted to  $10^0$ ,  $10^{-1}$ ,  $10^{-2}$  and  $10^{-3}$  then spotted on sdap media  
containing 0 mM KCl at pH 5.83. .... 111

---

## LIST OF TABLES

Table 1: Potassium transport proteins in <i>arabidopsis</i> species involved in $k^+$ responses and their function. ....	17
Table 2: <i>A. thaliana</i> mutants that are known to affect ABA sensitivity.....	27
Table 3: Transgenic <i>A. Thaliana</i> lines used in the study .....	42
Table 4: Restriction and modifying enzymes and buffers used in this study. ....	44
Table 5: Primers used in this study. ....	46
Table 6: Identified species after a protein blast search using atpm19 amino acid sequence.....	65
Table 7: Protein sequences used in the protein sequence alignment. ....	66
Table 8: PCR reactions carried out to confirm the presence and the orientation of the inserted T-DNA in the <i>Atpm19</i> gene. (F): is the forward <i>atpm19</i> primer, (R): is the reverse <i>Atpm19</i> primer (Prok-LB): is the T-DNA left border primer.....	89

---

## ABBREVIATIONS AND SYMBOLS

°C	Degree Celsius
%	percent
µg	Microgram
µl	Microliter
µm	Micromole
µM	Micromolar
ATP	Adenosine triphosphate
bp	Base pair
CaMV 35S	Cauliflower Mosaic Virus 35S promoter
cDNA	Complementary DNA
DEPC	Diethyl pyrocarbonate
dH <sub>2</sub> O	Distilled water
DIG	Digoxigenin
DNA	Deoxyribonucleic acid
DNase	dioxyribonuclease
dNTP	Deoxyribonucleoside 5'-triphosphate
<i>E.coli</i>	<i>Escherichia coli</i>
EDTA	Ethylene diamine tetra acetic acid
<i>et al.</i>	and others
etc.	et cetera
eV	electron volt
Fig.	Figure
g	Gram
<i>g</i>	Gravitational force
<i>hpt</i>	hygromycin phosphotransferase gene
kbp	Kilo base pair
kDa	Kilo Dalton
l	litre
LB	Luria Bertani broth or left border
M	Molar
MS	Murashige and Skoog basal salt mixture
MES	4-morpholinoethanesulphonic acid
mg	miligram



ml	mililiter
mM	mili Molar
mm	milimeter
mRNA	messenger-RNA
NaCl	Sodium chloride
NBT	nitrotetrazolium blue chloride
ng	nanogram
nm	nanomolar
OD <sub>600</sub>	Optical density at 600 nm
ORF	Open reading frame
PCR	polymerase chain reaction
pH	a measure of the acidity or alkalinity of a solution
pmol	picomolar
RB	right border
RNA	ribonucleic acid
RNase	Ribonuclease
rpm	Rotation per minute
RCF	Relative centrifugal force
SDS	Sodium dodecyl sulfate
SOD	Superoxide dismutases
T <sub>0</sub>	regenerated transgenic plant
T <sub>1</sub>	progeny derived from self-pollination of T <sub>0</sub>
<i>Taq</i>	<i>Thermus aquaticus</i>
T-DNA	transfer-DNA
Ti	Tumor inducing
Tris	2-Amino-2-hydroxymethylpropane-1.3-diol
u	unit
UV	Ultraviolet
V	Volt
v/v	volume to volume
w/v	weight to volume
WT	wild-type plant

---

**CHAPTER 1: INTRODUCTION**

## 1. INTRODUCTION:

### 1.1. Background:

A number of reasons have an influence on the availability of commodity crops to cover human consumption. For instance, in 2011 the world population reached 7 billion according to the World Bank (<http://search.worldbank.org/all?qterm=world%20population>) and The United Nations Population Fund (<http://www.7billionactions.org/>) (Figure 1). This high population density as well as being required to be fed, also influences negatively the plant population, as pointed out by Thompson and Jones (1999).

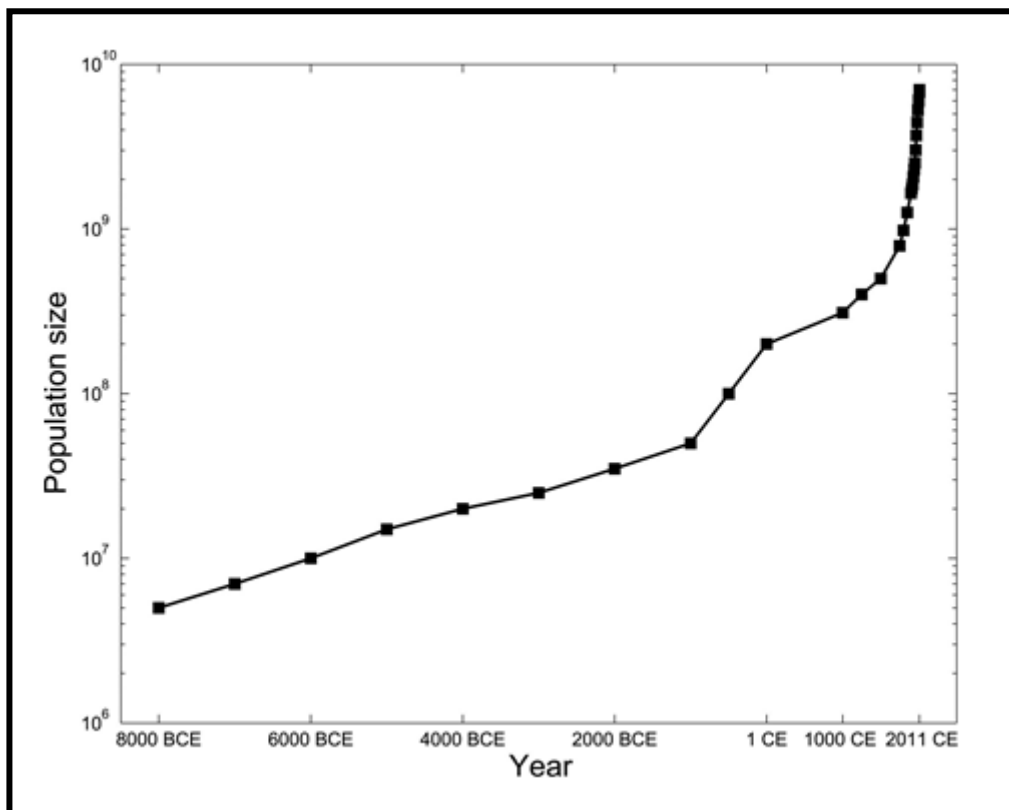


Figure 1: World population presented on a logarithm scale over the past 10,000 years. the population was about 5 million at 8000 BCE and about 7 billion today. The linear increase (on the log scale) through most of the presented periods represents exponential growing of rather persistent ratio growth in population mass each year. A quickening increase of that growth starting in the Common Era is noticeable. The graph is taken from (Keinan and Clark 2012).

Climate change is another factor that has a major influence on the world crop production (Jones and Davis 2000). According to The National Aeronautics and Space Administration (NASA), global warming happens as a result of the increase of the certain gasses (such as water vapour, CO<sub>2</sub>, methane, nitrous oxide and chlorofluorocarbons). These gasses block the heat that is reflected from the surface of the earth from escaping from the atmosphere and then causing increase in the atmospheric temperature (Pachauri and Reisinger 2007). The impact of this global warming is on a wide range of life aspects, starting from impact on the environment and ending on impact on agricultural and social life. An example of the impact of global warming on the environment is shrinkage in the glaciers which causes increase in the sea level and in turn causing more frequent floods. These frequent floods, for instance, have a severe challenge on the agricultural soil. It also was reported that an increase in the temperature has a negative effects on the yield of corn and rice (Parry 2007, Lal et al. 2005)

If we look at the example of China, its population represents almost 20% of the world's population which puts a higher demand on household and agricultural water which, in turn, put a major pressure on food security. In addition, the growing industry of China has a major effect on the climate change. Climate change effects on China include more frequent heat waves and a reduction in the annual cold days. The temperature has raised 1.2 °C in the last 5 decades. Drought is one of the most concerning signs of climate change in China. Severe droughts hit China four times in the last 6 decades (Piao et al. 2010).

Araus et al. (2002) suggested that in order to overcome the high demand levels for production of commodity crops, a global production increase of up to 2.6% annually is needed. To reach the required level of production, however, it is essential to study the

crops yield traits on the molecular level by making use of the power of biotechnology (Araus et al. 2002).

Knowing the regulatory genes, signalling pathways and the resulting proteins expression patterns that affect the way plant respond to those stresses are vital to select the appropriate traits that help engineering abiotic stress tolerant crops with better yield (Araus et al. 2002). As an example, studies identifying proteins associated with barley drought tolerance (Wendelboe-Nelson and Morris (2012), help in understanding the biochemical processes that take place when plant cells encounter different environmental stresses and may point the way forward for improved barley varieties.

### **1.2. Arabidopsis thaliana**

*Arabidopsis thaliana* is a dicotyledonous weed that belongs to the *brassicaceae*. Although the *brassicaceae* contains highly economically important plants - such as cabbage and broccoli-, *A. thaliana* has no economic value. The *Arabidopsis* genome consists of 5 chromosomes with a total of 25498 genes (Initiative 2000).

However, this model plant is very important for researchers for different advantages. These advantages include not only the small size or the short life cycle of this model plant, but also include the usefulness of the plant in genetic mapping and sequencing. The full sequence of *A. thaliana* was published in 2000, by the Arabidopsis Genome Initiative. The availability of *A. thaliana* T-DNA knockouts and more diverse online resources and data bases are another attractive for plant molecular biologists (Meinke et al. 1998).



Figure 2: *Arabidopsis thaliana* plant (Meinke et al. 1998)

**1.3. Transmembrane proteins:**

Transmembrane proteins are well described and explained in terms of their synthesis and processing and topology in number of cell molecular biology textbooks such as (Lodish et al. 2008a, Alberts et al. 2008).

As far as the plasma membrane of the cell is concerned, it is the barrier between the extracellular surroundings and the cytosol. The plasma membrane bilayer consists of phospholipids, and each of those phospholipid molecules consists of a hydrophilic (polar) head and two or three hydrophobic (non-polar) fatty acid tails. The polar head group is variable and may consist of choline, phosphate and glycerol while the hydrophobic tails consist of fatty acids. The group of phospholipid molecules spontaneously arrange to hide the fatty acids from water. This arrangement can make two forms. One is when the tails are inward which are called spherical micelles. Second is when two layers of phospholipid molecules arrange where the hydrophobic tails are sandwiched between the hydrophilic heads (Alberts et al. 2008). This bilayer carries proteins that regulate many cellular functions such as transport, signalling, stress responses, etc. Therefore, the plasma membrane protein composition differs in relation to the species, tissue and also on the stage of development (Lüthje et al. 2009) ; (Komatsu 2008). Some plasma membrane proteins are imbedded within the plasma membrane lipid while others have a temporal attachment by reversible interactions to the plasma membrane with some parts of their sequence in the cellular cytosol or the extracellular matrix (Komatsu 2008).

Membrane proteins represent 30% of the total proteins in the cell (Xiong 2006). According to their interaction with the plasma membrane, transmembrane proteins can be classified into two categories, peripheral membrane proteins and integral membrane proteins. The former is when the protein does not pass through the hydrophobic region



of the plasma membrane and instead they are attached - by interactions with an integral protein of a lipid head group - to either the extracellular surface or the intracellular surface of the membrane. The integral membrane proteins are those that extend into the phospholipid bilayer and have domains at the extracellular matrix and at the intracellular cytosol. Integral membrane proteins are found in a form of single or multiple  $\alpha$  helices strands or  $\beta$  barrel strands (Alberts et al. 2008, Lodish et al. 2000) .

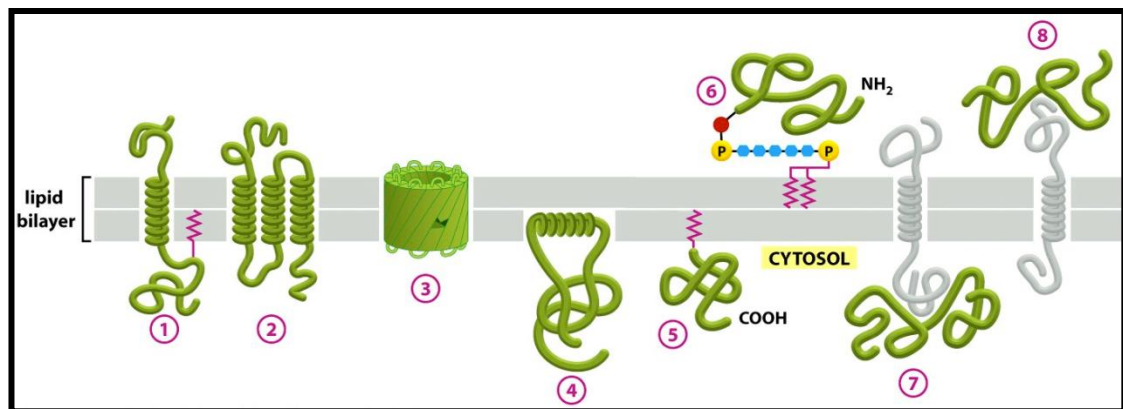


Figure 3: Different ways in which proteins interact with plasma membrane bilayer. Some membrane proteins extend through the membrane, for example the protein in (1) represents a transmembrane protein with a single  $\alpha$  helix pass, (2) is a multiple pass through the membrane while (3) shows  $\beta$  sheet (or  $\beta$  barrel). Other membrane proteins are anchored towards the cytosol by an  $\alpha$  helix (4). Some proteins are attached to the bilayer by a lipid in the cytosol (5), or by an oligosaccharide to the outer side of the membrane (6). Other proteins attach to the membrane via other integral proteins (7, 8). The figure is taken from (Alberts et al. 2002)

With respect to the topology, there are two main types of transmembrane plasma membrane protein. One is alpha helical in structure, the second has a beta barrel structure. According to Singer (1990), the alpha helical transmembrane proteins are also classified into bitopic and polytopic. Bitopic are those proteins that have a single pass through the plasma membrane bilayer, while the polytopic proteins are the ones that have multiple passes through the plasma membrane bilayer. Bitopic are divided into

type I and type II, where type I proteins are those that have their N terminus exposed to the extracellular matrix and type II are the ones that have their N terminus towards the cytoplasm. Type I transmembrane proteins are subdivided into type Ia and type Ib. It is called type Ia when it has a cleavable signal sequence and is called type Ib when it lacks this sequence.

Polytopic proteins are divided into type III and type IV, where type III proteins are those that have multiple transmembrane domains. Type IV transmembrane proteins have multiple passes through the membrane. Transport proteins and membrane receptors usually belong to this type of membrane proteins. Type III proteins are subgrouped into type IIIa proteins where they are cleavage signal sequence similar to type Ia, while type IIIb proteins have their N terminus oriented towards outside the cell and lack cleavage signal sequence similar to type Ib and type II (Singer 1990, Nakai 2000).

**1.4. Protein sorting:**

In eukaryotic cells, proteins are transported to their destinations by either containing the protein in a transport vesicle, which then called the vesicular pathway, or directly through the cytosol when they may be targeted to the nucleus, mitochondria and chloroplasts. The vesicular pathway is usually used when the translated protein is to be secreted outside of the cell or to be integrated in one of the cellular membranes.

The vesicular pathway takes place in the same time when the protein is being translated by the ribosome. The first 15 to 20 amino acids that emerge from the ribosome are called the signal sequence. As the signal sequence emerges from the ribosome it is recognised by signal recognition particle (SRP). The SRP then guide the ribosome to bind to a SRP receptor associated with the translocon apparatus on the endoplasmic reticulum (ER), after which the SRP is released. After that, the signal sequence enters the ER translocon and the translation of the polypeptide continues. In some proteins the signal peptide is cleaved from the polypeptide by a signal peptidase enzyme that is located in the ER lumen. Once the translation terminates the protein is released inside the ER lumen if it is a secretory protein or integrated in the ER membrane if it is an integral membrane protein. After that the protein is transported from the lumen of the ER to the Golgi apparatus where it is further processed and sorted into the appropriate vesicle for the final destination. Then is released in the lumen of Golgi to be released outside the cell or vesicle fusion in the plasma membrane (Nakai 2000, Nakai 1991). The fusion of those vesicles to the plasma membrane is thought to be via SNARE proteins. SNAREs are membrane protein on the vesicles that mediate interaction between the vesicle and target membrane, or v-SNARE and t-SNARE (Chen and Scheller 2001).

Integral proteins are inserted in the ER membrane and embedded within the membrane by hydrophobic regions that are usually  $\alpha$  helices. There are different ways in which proteins are inserted in the ER membrane. The simplest way is when the translated protein contains a cleavable site in the signal sequence and one  $\alpha$  helix region in the sequence (called stop-transfer sequence). The signal peptide is cleaved once it enters the ER lumen and the stop-transfer sequence stops the translocon from the translocation of the polypeptide inside the ER lumen. This results in a membrane protein with one transmembrane domain. Another way is when the protein contains a noncleavable signal sequence. That is when the orientation of the resulted polypeptide can be either amino terminus towards the cytosol or towards the ER lumen. The signal sequence in this case acts as a transmembrane domain (Nakai 2000, Nakai 1991).

Some other polypeptides span the membrane multiple times. It is thought that this happens due to the presence of multiple noncleavable signal sequences and multiple stop-transfer sequences. Since these sequences act as transmembrane anchors, they result in the production of proteins with multi transmembrane domains (Nakai 2000, Nakai 1991).

### **1.5. Transport through the cellular plasma membrane:**

Control and facilitation of transport of compounds into and out of the plant cell is one of the important roles that cell plasma membrane plays. In addition to the import and export of mineral ions to the cell required for growth and development, these ions are essential in maintaining the turgor pressure of the plant cell. Turgor pressure is the turgidity that occurs when the cellular contents such as vacuole pushes the plant cell membrane against the cell wall. This happens when the osmotic pressure increases inside the cell by the accumulation of ions and thus water in the vacuole. The consequence of enhanced intracellular osmotic potential is the vacuole will enlarge with

water which will increase the cell's turgor. This turgor pressure is important to maintain the shape of the cell and, in turn, the shape of the plant (Glass 1983), (Xiong and Zhu 2002) and (Grefen et al. 2011).

Transmembrane transport of compounds happens by a number of different ways. These are passive diffusion across the lipid bilayer, passive diffusion through selective membrane channels or through active transport that depends on energy through membrane transporters. The transport of molecules such as amino acids, drugs and other nutrients usually happens through the channels. Also sometimes transport of molecules depends on the charge on the molecule, and its relative hydrophobicity (Wang et al. 2010).

Passive transport of molecules through the plasma membrane is a way of transport that does not require energy (ATP) and is totally driven by the concentration gradient. This energy-independent transport can happen in number of ways; diffusion through the bilayer, diffusion through membrane pores or gated channels, facilitated diffusion (a passive transport system by which molecules or ions can pass spontaneously) or by osmosis.

Gases and some other small molecules can diffuse through the phospholipid bilayer because of their relatively small size or their non-polarity. Examples of those molecules are oxygen, carbon dioxide. However, charged ions and sugars such as glucose cannot pass through the lipid bilayer.

Water passage in and out of plant cells happens either to a minor extent by diffusion through the phospholipid bilayer or to a greater extent via special plasma membrane proteins called aquaporins (Maurel and Chrispeels 2001). Water transport through aquaporins depends on passive transport where water moves from the concentration of

the solutes, from high to low. The first plasma membrane aquaporins in plants were identified in *Arabidopsis* root cells (Kammerloher et al. 1994). The transmembrane water flux might be controlled by controlling the number or the activity of the aquaporins. In addition, the plant cell may accommodate the water potential gradient by accumulating or removing osmotically active compounds to change the osmotic potential in favour of influx or efflux of water (Johansson et al. 2000).

Charged ions such as  $\text{Na}^+$  and  $\text{K}^+$  pass through the plasma membrane by means of ion channels. Gated channels open when they bind to signals or when they experience changes in voltage. Different from ion transporters and  $\text{H}^+$ -coupled transporters that are highly specific, ion channels have relatively poor ability to distinguish between ions. For instance the  $\text{Ca}^{2+}$  channels are also permeable to  $\text{Ba}^{2+}$ . Those channels occur often in low abundance (estimated between 100 and 200 ion channels in a single cell at the plasma membrane). However, they contribute substantially to the charge balance between the inside and outside the cell membrane (Blatt 2008).

Another way of transport through the plasma membrane is used by some molecules (e.g. glucose) that bind with the transporters proteins that change their shape to facilitate their movement. These transporters (sometimes called passive carriers) are a type of facilitated diffusion transport systems. A passive carrier is a transport system that does not require energy and transport its molecule down a concentration gradient (Mueckler 1994).

Active transport of molecules or ions requires energy (ATP) to move chemicals against the concentration gradient. An example of active transport proteins are the ion transport plasma membrane proteins. Transporters cannot work in ionic equilibrium and also the charge across the membrane cannot change without an external influence. That is why transporters transfer  $\text{H}^+$  (from inside the cell to outside) to change the charge voltage

across the cell membrane in order for ions (such as  $K^+$  and  $Na^+$ ) to transfer back inside the cytosol.

Although these movements of  $H^+$  and metal cations across the two sides of the plasma membrane occur at the same time, they are physiologically separate, with the  $H^+$  movement taking place by means of ATPase protein pump. Reported findings in *Neurospora* showed that high-affinity  $K^+$  uptake was associated with neutralisation of the membrane polarity and making the cytosol more alkaline. Results of the voltage clamp analysis revealed that  $K^+$  uptake is association with two charges (1  $K^+$  and 1  $H^+$ ). This influx is in harmony with the output of two  $H^+$  by the ATPase thus changing the pH in cytosol for 1  $K^+$  to go in. This shows that the mechanisms of energy-based  $H^+$  efflux and  $K^+$  uptake could work in the same time across the membrane but be mechanistically separate, a process similar to the generation of the  $H^+$  electrochemical gradient and production of ATP in mitochondria and chloroplasts are separate processes (Blatt 2008) and (Palmgren 2001).

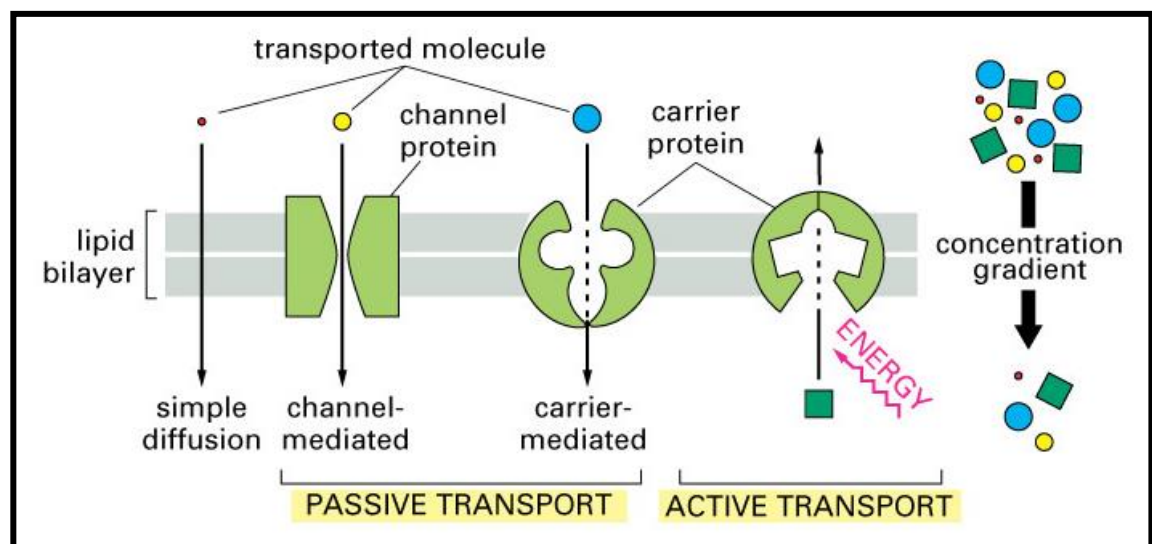


Figure 4: Molecules or ions can pass through the membrane via simple diffusion, passive transport where there is no ATP required, or via active transport when the transport is against the concentration gradient where ATP is required. The figure is obtained from (Alberts 2004)

**1.6. Potassium transport through plasma membrane:**

Potassium ( $K^+$ ) is considered one of the vital nutrients for plants in order for their optimal growth and development. It composes 10 % of the plant dry weight and is the most common cation in plant cells (Pyo et al. 2010, Szczerba et al. 2009, Britto and Kronzucker 2008, Grabov 2007, Gambale and Uozumi 2006). It is been reported that provision of more  $K^+$  can helps the recovery of plants affected by metal toxicity (Szczerba et al. 2009), pest and diseases in plants (Amtmann et al. 2008).

Potassium plays a major role in a number of the biochemical processes in the plant cell. For instance,  $K^+$  deficiency affect the photosynthesis mechanism in the chloroplasts (Hartt 1969). It is also involved in driving the movement of the opening and closure of the stomatal guard cells (Hosy et al. 2003) and in enzyme activation (Suelter 1970). Furthermore,  $K^+$  is essential for the equilibrium of the osmotic pressure inside and outside the cell (Gambale and Uozumi 2006, Maathuis and Sanders 1996, Mengel and Arneke 1982).

The extensive research on potassium kinetics including Epstein's experiments that was the first to establish that there are at least two ways of potassium movement across plants roots cells (Epstein et al. 1963, Britto and Kronzucker 2008). Those were then called HATS (high affinity transport system) and LATS (low affinity transport system). At very low  $K^+$  extra cellular concentrations ( $< 1$  mM) the HATS  $K^+$  influx turns to its maximum capacity. While when the extra cellular  $K^+$  concentration increases to  $>1$  mM the  $K^+$  influx through HATS decreases to its minimum and LATS takes over (Britto and Kronzucker 2008, Szczerba et al. 2009).

Each of the HATS and LATS transporter system has unique characteristics. For instance, there seem to be different mechanisms by which HATS and LATS transporters catalyse the flux of  $K^+$  across the plasma membrane. In HATS, it is proposed that  $K^+$



enters the cell through symports with  $H^+$ . Using an ATP molecule, transmembrane protons pump two  $H^+$  against the electric gradient outside the cell to make a charge imbalance that drives  $K^+$  inside the cell.


In LATS, on the other hand,  $K^+$  seem to be transported via ion channels that are either  $K^+$  specific or non-specific, which can initiate passive transport higher than those catalysed by pumps and carriers. The activity of those channels depends on electrochemical potential gradients of  $K^+$  to drive transport. A variety of factors may affect the regulation of the activity of those channels including membrane voltage, pH and  $K^+$  itself (Britto and Kronzucker 2008, Szczerba et al. 2009, Fox and Guerinot 1998).

There are several plant genes that have been reported that seem to encode potassium transport through plasma membrane proteins. Some have grouped these transporters into four main families (Britto and Kronzucker 2008, Szczerba et al. 2009). One is the HAK/KUP/KT group which consists of  $K^+/H^+$  symporters (transporters that allow two or more ions or molecules to move through the plasma membrane phospholipid bilayer). The members of this family are involved with the majority of HATS-mediated influx, especially under conditions of low  $K^+$ . Pyo et al. (2010) described that potassium transporters AtHAK5 and AKT1 are major plasma membrane structures of this first group mediating high-affinity  $K^+$  uptake into roots during and after seedling establishment. The second group is HKT/TRK which consists of  $K^+/H^+$  or  $K^+/Na^+$  symporters. KCO channels form the third group. The function of this group in plant cell is not known Véry and Sentenac (2003). Shaker channels are the fourth group. These channels are very similar to the animal Shaker family, consisting of six transmembrane (TM) domains with a highly conserved loop between the fifth and sixth TM domain (Véry and Sentenac 2003). In addition Shaker family channels share a common

structure in plants and animals that is containing four  $\alpha$  subunits. Each subunit contains six hydrophobic transmembrane domains and a positively charged amino acid stretch involved in voltage sensing (Britto and Kronzucker 2008, Szczerba et al. 2009).

There are three types of low affinity  $K^+$  channels described. Those are the inward rectifying channels (KIRC), the outward rectifying channels (KORCs) and the non-selective outward rectifying conductance (NORC). KIRC channels, such as AKT1, catalyse  $K^+$  influx via the hyperpolarization of plasma membrane. AKT1 channels can select between  $K^+$  and  $Na^+$  at physiological  $K^+$  and  $Na^+$  external concentrations. By knocking AKT1 out in *Arabidopsis* (*akt1-1*), although its involvement in the  $K^+$  intake when surrounded by low  $K^+$  concentrations (micromoles) was reported, there were no phenotypes to suggest that it has a function in  $Na^+$  intake (Spalding et al. 1999) (Blumwald 2000).

Table 1: Main potassium transport proteins in *Arabidopsis* species that are thought to be involved in low affinity  $K^+$  responses and their proposed function. Obtained from (Véry and Sentenac 2003, Ashley et al. 2006).

Protein	Expression location	Proposed function
AKT1	Root cap, epidermis, cortex, endodermis, stele	$K^+$ uptake
ATKC1	Meristem, epidermis, cortex, endodermis	$K^+$ uptake
GORK	Epidermis	$K^+$ efflux during stomatal closure
SKOR	Pericycle and stellar parenchyma	$K^+$ efflux to the xylem
AKT2/AKT3	Phloem	Phloem loading and unloading
AtHAK5	Epidermis of main and lateral roots, stele of main roots	High affinity $K^+$ uptake
TRH1 (AtKT3/AtKUP4) AtKUP1	 Root cap	$K^+$ transport, root hair development, gravitropic responses
AtKUP1		$K^+$ transport
AtKUP2		Root tip, root–hypocotyl junction
AtKUP3		
AtKUP12		
KEA5		
AtCHX17	Cortex and epidermis	$K^+$ uptake
KAT1	Guard cells	$K^+$ influx during stomatal opening
AtKUP1	Root	High affinity $K^+$ uptake

Chen et al. (2008) have grouped potassium transporters in plants to six gene families, suggesting that there are more than 70 potassium ion transporters and channels that have been identified so far in *Arabidopsis*. Those six gene families include three channel families (Shaker, TPK and Kir-like families) and three transporter families (KUP/HAK/KT, HKT and CPA families).

The structure of those plasma membrane transporters varies considerably see (Figure 5). Kir-like transporters, for instance, have two transmembrane domains, while the KUP/HAK/KT group can have up to 14 transmembrane domains. Some of those proteins have pore loops in between the membrane domains. The transporter HKT contains four pore loops, while the TPK channel has two (Chen et al. 2008).

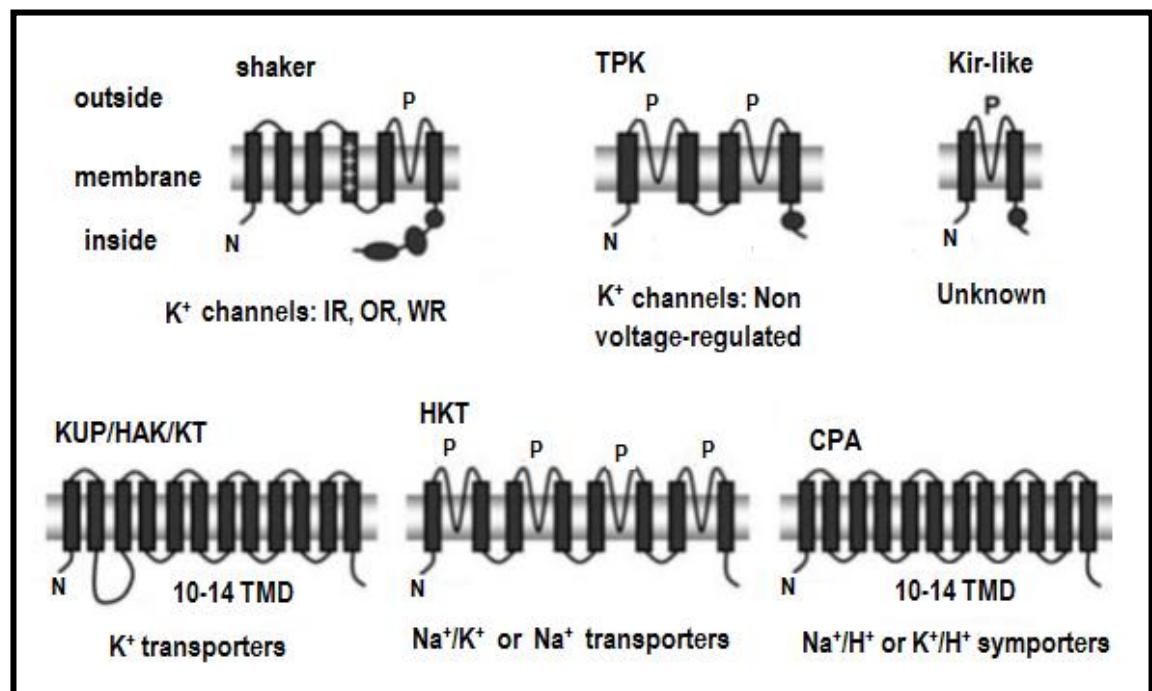


Figure 5: The structural modelling of plant K<sup>+</sup> channels and transporters obtained from (Chen et al. 2008). IR: inward-rectifying K<sup>+</sup> channel, OR: outward-rectifying K<sup>+</sup> channel, WR: weakly-rectifying K<sup>+</sup> channel, N: N-terminal, P: pore loop.

**1.7. Sodium transport through plasma membrane:**

The transport of sodium within the plant cell has extensively been studied in the context of salt stress and the mechanism of salinity tolerance. This is because of a number of reasons. One of those reasons is the abundance of sodium in the environment. For instance sodium chloride makes up to 3.5% w/v of the sea water (Castro and Huber 1992). This high environmental availability is a limiting factor for the overall plant health. Excess of sodium in soil negatively affects the growth rate, causes damage to leaves and changes the plant's root:shoot ratio (Blumwald et al. 2000).

Thus, mentioning the mechanisms that plants adopt to tolerate salinity is unavoidable. Excess salt in the soil can stress the plant cell by two ways. The first is by limiting water availability as a result of the relative high solute concentrations around the roots. The other way is by ionic toxicity which is a result from changing  $K^+/Na^+$  ratios and the increasing intracellular  $Na^+$  and  $Cl^-$  ion concentrations. This unfavourable change of ion ratios in the plant is caused by the entry of sodium through transporters that are for potassium intake. The reason of the leakage of sodium into the cell is the similarity between ionic size of sodium and potassium, making it difficult for the transporters to differentiate between the two ions (Blumwald et al. 2000, Zhu 2001).

In the optimal environmental conditions, the  $K^+/Na^+$  ratio inside the plant cell is high with an average concentration of  $K^+$  of 150 mM and  $Na^+$  of 5 mM. Assuming the negative membrane potential difference inside the plasma membrane, the high  $Na^+$  electrochemical potential gradient, will cause a passive transport of  $Na^+$  into the cell (Blumwald et al. 2000). Thus the cell must have mechanisms for removing excess  $Na^+$ .

When it comes to  $Na^+$  uptake and efflux from the cell, apart from the plasma membrane  $Na^+/H^+$  antiporter. This Na/H antiporter is called SOS1 and located the plasma membrane and in the tonoplast and is responsible for the  $Na^+$  homeostasis in the plant

cell. SOS1 regulates the Na export in the root cells in addition to its involvement in the transport of Na from roots to shoots in *Arabidopsis* (Elmahi et al. 2010). Sodium can also move in and out of the cell membrane through the K<sup>+</sup> channels (Blumwald 2000, Mäser et al. 2002, Marschner et al. 1981). Thus, it is essential to explain K<sup>+</sup> transporters in the transport of Na<sup>+</sup>.

K<sup>+</sup> outward rectifying channels might have a function in facilitating Na<sup>+</sup> intake, as has been suggested by (Wegner and Raschke 1994). When the electrical potential difference of the plasma membrane is changed to be more positive, KOR channels pass K<sup>+</sup> outside the cell and mediate Na<sup>+</sup> influx. The non-selective outward rectifying channels cannot distinguish between cations and can be activated when the Ca<sup>2+</sup> concentrations is increased in the cytosol (Blumwald 2000, Rodríguez-Navarro and Rubio 2006).

### **1.8. Abiotic stress:**

Since plants are non-motile organisms, so they are exposed to variety of harsh stresses. Abiotic stresses (stresses that are caused by environmental factors (Cushman and Bohnert 2000)) are responsible for considerable losses to agricultural sector. The estimated area that is affected by drought only were over 25% of the US soils (Boyer 1982) and costs that reached to over US\$1 billion within 24 years (Mittler 2006). By the year 2050 it is anticipated that more than 50% of the arable lands will encounter serious salinization losses (Wang et al. 2003).

Different types of abiotic stress, such as drought, salinity, freezing and high temperature can stimulate similar effects on the plant cell. For instance, both drought and high salt soils effect as osmotic relation, making the study of a specific abiotic stress a rather complex task (Wang et al. 2003).

In order for the plant to survive those extreme conditions they have developed sophisticated systems to respond to such stresses. Plant hormones such as salicylic acid (SA), jasmonic acid (JA), ethylene (ET) and abscisic acid (ABA) are responsible for the regulation of the protection of plant against abiotic –as well as biotic – stresses and (Peleg and Blumwald 2011).

ABA in particular plays an essential role in number of biochemical processes during the plant development. For instance, ABA helps in the closure of the stomata by changing the ion flux in guard cells. In addition, it is been reported that it is essential to regulate seed dormancy and germination (Leung and Giraudat 1998). More about ABA and its role in plant development is discussed in a separate section below.

### **1.9. Plant and water deficiency:**

Stresses due to water deficiency are the most important among the abiotic stresses. In a wider context, water stress includes both drought and salt stress (Zhu 2002). Water deficiency can lead to two different physical results to the plant; osmotic stress and ionic stress. In both cases plants have strategies to tackle those stresses. When encountered by osmotic stress, plants reduce cell elongation in the root tip, which might have an influence on the stomata to close (Munns and Tester 2008). However, drought may also cause high  $\text{Na}^+$  concentration in the plant cells. When plants encounter high  $\text{Na}^+$  medium, root cells start to exclude  $\text{Na}^+$  from the cell to avoid the accumulation of to toxic levels of  $\text{Na}^+$ . Plants also adopt compartmentalisation of  $\text{Na}^+$  inside the cellular cytosol during salinity stress (Munns and Tester 2008).

### **1.10. Drought stress tolerance mechanism in plant cell:**

The response to water loss depends on its rate. Too high a rate of water loss can cause a major impact and the plant may not be able to acclimate and protect itself from the effect. While when the rate is lower this allows the plants to adapt the water deficiency.

However, this principle may not be applied on all plant species. For instance, some sensitive plant species can be susceptible to injury and their protection strategy would fail when exposed to the same water loss rate (Yamaguchi-Shinozaki and Shinozaki 1994).

The perception of water deficiency by the plant cell can be obtained by number of cellular changes. Those changes include decrease of turgor, decrease of the volume of the cell, changes in water ion movement patterns and alteration in the membrane stretch. Plants have multiple stress perception and signal transduction pathways, some of which are not stress specific while others are specific. The signal transduction pathway from different abiotic stresses is complex, and these pathways are not yet fully elucidated (Huang et al. 2012).

However a general understanding of the process has been developed by many studies. After the abiotic stress perception take place by membrane receptors (such as perhaps calcium channels and changes in plasma membrane composition), secondary messages, such as calcium sensors and reactive oxygen species (ROS), are generated. After that, numbers of signal transduction and transcription events take place resulting in the expression of stress responsive genes. The final product of these signal transduction transcription pathways is a physiological stress resistance phenotype (Huang et al. 2012).

Abscisic acid is an essential signalling pathway that mediate the expression of gene products that are involved in water deficiency tolerance responses (Huang et al. 2012, Kline et al. 2010).

A number of DNA elements and sequence-specific DNA binding proteins also seem to be involved in the regulation of signalling pathways during low water availability



stresses responses (Huang et al. 2012). The identified promoter elements are divided into two classes; ABA-response elements ABRE and dehydration responsive elements (DRE). The (ABRE) can be recognised by the shaded core sequence, RYACGTGGYR, where R refers to a nucleotide with a purine base and Y refers to a nucleotide with a pyrimidine base. The (DRE) sequence is TACCGACAT (Bray 1997). These sequences are frequently to be found in the upstream promoter regions of abiotic stress induced genes.

### **1.11. Salt stress tolerance mechanisms:**

Plant use different strategies to respond to salt stress. Examples of those strategies are prevention or elimination of the damage (detoxification), bringing back the homeostatic balance and to restart growth under the stressful conditions even with a lower growth rate.

High sodium concentrations can cause damage to the cellular membranes' robustness, enzyme activities and function of the cell organelles. One of the important damage causing elements appears to be reactive oxygen species (ROS). Organic compounds that affect osmotic balance (such as mannitol) and some amino acids (such as proline) seem to act as detoxifying agents by scavenging ROS to prevent them from damaging the structure of the cell, as well as acting as osmosis active agents (Zhu, 2001).

The other approach plant cells employ is rebalancing the osmosis around the cell membrane (Zhu 2001). The plant cell carries out this homeostasis rebalance by number of ways. Those are restriction of Na<sup>+</sup> influx, sodium efflux and by intracellular compartmentalisation.

The key process for salt (Na<sup>+</sup>) efflux is facilitated by the plasma membrane ATPase driven sodium transporters. The H<sup>+</sup>-ATPase uses ATP molecules to create the energy to

pump  $H^+$  out of the cell. This increasing  $H^+$  out of the cell generates electrochemical  $H^+$  gradient. This high positive charge out of the cell generated by the  $H^+$ -ATPase activates the  $Na^+/H^+$  antiporters located in the plasma membrane, which couples the movement of  $H^+$  into the cell (with its electrochemical gradient) to the extrusion of  $Na^+$  (against its electrochemical gradient) (Blumwald 2000, Blumwald et al. 2000). The salt overlay sensitive 1 (*SOS1*) gene, a gene believed to be associated with high salt tolerance, has been shown to encode a putative plasma membrane  $Na^+/H^+$  antiporter (Shi et al. 2000, Zhu 2001).

Compartmentalization minimise the toxic effect of  $Na^+$  accumulation in the cytosol by accumulating the  $Na^+$  into the vacuole. In addition, it helps balancing the osmotic potential by using the compartmentalized  $Na^+$  and  $Cl^-$  in the vacuole to attract water in the cytosol by releasing those elements in the cytosol (Blumwald 2000).

Salinity inhibits plant growth as an adaptive feature to survive under unfavourable conditions. The slower growth rate allows the plant to depend on different resources (e.g. building blocks and energy) to combat stress. In nature, the extent of salt or drought tolerance often appears to be inversely related to growth rate. One of the causes of reduced growth rate under salt stress is photosynthesis inadequacy. This is due to the closure of stomatal apparatus and, in turn, limited carbon dioxide uptake. However, stress could inhibit cell division and expansion directly. Even slight increase in salinity or drought stress could cause lower growth losses in productivity.

A possible link between abiotic stress and cell proliferation was found when the expression of *ICK1* was induced in *Arabidopsis* by abscisic acid. The cyclin-dependent-protein-kinase (*ICK1*) inhibitor might obstruct cell division by decreasing the actions of cyclin-dependent protein kinases that is involved in the cell cycle process. Salinity and

drought might deter cell division due to abscisic acid accumulation which, in turn, induces *ICK1* (Zhu, 2001).

Overexpression of some abiotic stress related genes such as *CBF1*, *DREB1A*, and *ATHB7* has revealed that they cause slower growth of transgenic plants. Those genes are induced by drought and are not expressed under normal conditions. Therefore, their final gene product might be a stress signal to inhibit growth (Zhu 2001).

### **1.12. Abscisic acid:**

Abscisic acid (ABA) is a plant hormone that has essential functions in a wide number of physiological and biochemical processes in seed germination and in the plant abiotic stress responses. ABA has wide range of roles that been discussed in the literature (Raghavendra et al. 2010, AbuQamar et al. 2009). Those roles include the opening and closure of the stomata by the rapid changing of ion concentrations inside and outside the guard cells. In addition, ABA roles include alterations of gene expression. Research has led to significant results in characterization of its role in signalling.

After the isolation and identification of ABA in the 1960s, mutants that are affected by ABA biosynthesis were start to be identified in different plant species. The characterization of these mutants has helped to explain the ABA pathways in higher plants like *Arabidopsis* and maize. below, (Bewley 1997, Rock and Quatrano 1995, Li and Foley 1997, Leung and Giraudat 1998, Finkelstein et al. 2002, Koornneef et al. 2002, AbuQamar et al. 2009).

Table 2 shows ABA mutants that helped in understanding the role of ABA in seed dormancy and germination.

ABA contents in the cell increase dramatically during the maturation of the seed and before germination. This indicates that ABA plays significant roles for the developmental stage of the seed embryo. These roles include the dormancy of the seed, intake of the stored nutrients and the dehydration tolerance (Bewley 1997).

Table 2: The table shows *A. thaliana* mutants that are known to affect ABA sensitivity. Obtained from (Leung and Giraudat 1998).

<b>Mutation</b>	<b>Phenotype</b>	<b>Protein function</b>
<i>abi1</i>	ABA insensitivity	Protein phosphatase C 2 (PPC2)
<i>abi2</i>	ABA insensitivity	Protein phosphatase C 2 (PPC2)
<i>abi3</i>	ABA insensitivity in seeds	Seed transcription factor
<i>abi4/5</i>	ABA insensitivity in seeds	
<i>era1</i>	ABA hypersensitivity	Negative regulator of ABA signalling by adding $\beta$ subunit farnesyl transferase.
<i>era2/3</i>	ABA hypersensitivity	
<i>gca1/8</i>	ABA insensitivity	
<i>axr2</i>	resistance to ABA	
<i>jar1</i>	Resistance to ABA	
<i>jin4</i>	Resistance to ABA	
<i>bri1</i>	Hypersensitivity to ABA	

ABA plays essential roles in seed dormancy and germination. Clarifying what is dormancy and what is germination is important to set the baseline. Seed dormancy can be defined as the failure of an intact viable seed to complete germination under favourable conditions (Koornneef et al. 2002, Bewley 1997). Germination, however, can be explained as the events that start with water uptake by the dry seed and ends with protrusion of the embryonic axis (Bewley 1997). Dormancy and germination are complex processes that are influenced by different physiological and biochemical factors.

It was reported that added ABA can inhibit precocious germination in immature embryo culture (Rock and Quatrano 1995), embryos from ABA-biosynthetic mutants from maize and *A. thaliana* showed inhibition of their precocious germination (McCarty 1995, Marin et al. 1996). Precocious germination is the germination of the embryos while still attached to mother plant (Bewley 1997). These results suggest that ABA is a key element in the seed dormancy processes.

ABA is also involved in the seed uptake of stored nutrients and desiccations tolerance response. The accumulation of soluble nutrients and the acquisition of desiccation tolerance take place by the involvement of specific mRNAs expression. It was reported that the expression of late-embryogenesis-abundant (LEA) proteins - that are associated with extreme environment tolerance such as freezing, salinity and dehydration (Hundertmark and Hinch 2008) - can be induced by adding exogenous ABA to cultured embryos (Ingram and Bartels 1996, Leung and Giraudat 1998). In addition, Bartels et al. (1992) reported that ABA is associated together with light in the regulation of a desiccation-related gene from *Craterostigma plantagineum*.

Recent developments helped understanding ABA hormone perception mechanisms. One of which is a signalling pathway known as (The RCAR/PYR/PYL —| PP2C —| SnRK2 signalling pathway) (Weiner et al. 2010). RCAR/PYR/PYL is an ABA receptor; PP2Cs are negative regulators of ABA responses while SnRK2 kinases are positive regulators of ABA responses. When ABA is absent, PP2C activity is high preventing the accumulation of SnRK2 kinases by dephosphorylation. When ABA is present, RCAR/PYR/PYL bind to PP2Cs and inhibits it. This leads to the activation of SnRK2s. The SnRK2s then phosphorylate downstream targets that are involved with ABA responses, such as the inhibition of OST1 that leads to the activation of some ion channels - such as the potassium channel (KAT1) - in a mechanism that is not fully understood so far (Raghavendra et al. 2010, Weiner et al. 2010).

### **1.13. Transformation**

Plant genetic transformation has been developing widely since the first successful gene transfer to plant (Hilder et al. 1987). "Transformation" is the scientific term used in molecular biology for the modification of the genetic material of a cell as a result of an intake of an external fragment of DNA (Duffus et al. 2007). In some cases transformation happens naturally in some species of bacteria. In order for transformation to take place, bacteria must be in a condition that enables them to uptake the exogenous piece of DNA. This condition is known as "competence". Competence can be induced in the laboratory by treating the bacteria to make them permeable to uptake a foreign DNA (Smith et al. 1999, Davison 1999).

In microorganisms transformation is one of the physiological processes in which they transfer the genetic materials to other bacteria. Conjugation - in which the DNA is transferred from a bacterium to another via direct attachment - and transduction - where

the DNA is injected by a virus known as bacteriophage into the recipient bacterium - are also means to transfer genetic materials (Davison 1999).

The term "transformation" can also be used in one of the key genetic engineering processes in plants by which a foreign DNA is transferred into a mammalian and plant cells. However, the same process when applied in mammalian cells is called "transfection" (Gasser and Fraley 1989). This is to avoid the confusion with the term "transformation" that is used to describe cells that change to become in a cancerous state (Hynes 1976).

Plant genetic transformation is used for a variety of different purposes. Some of those purposes are of interest to scientists and researchers while others are more interesting to the commercial sector. For instance, transformation is widely used by molecular biologists as a tool to understand biochemical and physiological properties in the plant cell, such as signalling and the role of proteins in plant development, biotic or abiotic stress responses.

The interest in gene transformation research by the commercial sector is because of the expectations that gene transformation technology can enhance crop plant properties by a way that is not attainable by conventional breeding methods. In addition, genetic transformation may be able to correct the faults in cultivars in a more efficient manner. In addition, genetic manipulation is a faster method for the production of novel plant lines than the conventional plant breeding (Birch 1997).

#### **1.14. Methods for plant transformation:**

*Agrobacterium tumefaciens* is a Gram negative, rod shaped bacteria. It is a common bacterium that occurs naturally in soil and causes crown gall disease in plant. It can transfer parts of its DNA materials into the infected plant cells. The DNA sequence that



is transferred is called T-DNA and is located in a plasmid known as a tumour inducing (Ti) plasmid.

*Agrobacterium* can transfer its genetic material to a wide range of organisms. This includes a variety of dicotyledonous and monocotyledonous angiosperm species and gymnosperms. Moreover, *Agrobacterium* can transform fungi, including yeasts. *Agrobacterium* has also been reported to transfer DNA to human cells (Klee et al. 1987).

Because of its natural ability to change the genetic structure of the host plant *Agrobacterium* has been called the "smallest genetic engineer" and that was the basis of using it in plant transformation. Now, *Agrobacterium*-mediated transformation is the most common genetic engineering method that is used in plants. The reason for that is the high efficiency when compared with the other transformation techniques.

The basis in which *Agrobacterium* plant transformation occurs is the transfer of Ti plasmid from the *Agrobacterium* to be integrated into the plant's DNA inside the plant cell nucleus. The Ti plasmid is composed of the T-DNA region, virulence genes region, an origin of replication and opine catabolism region (a region responsible for encoding enzymes to break down the opine compounds induced by the Ti plasmid). The T-DNA region is composed of left border, right border and central region between the two borders. The central region naturally contains three genes, which induce cell division and proliferation and opine synthesis. This central region is the sequence that caused the plant disease by encoding proteins that induce tumor to the plant cell. The virulence region is composed of eight operons that are responsible for the successful transfer and integration of the T-DNA into the plant cell DNA material. The Ti plasmid can be "disarmed" to make it useful as a plant biotechnology tool. This is done by the removal

of the central region between the left border and right border (Klee et al. 1987, Gelvin 2003).

Plasmid vectors are essential when it comes to *Agrobacterium* transformation. One of the reasons of their importance is they contain selectable markers. A selectable marker is gene that confers a distinct phenotype, such as a resistance to certain herbicide or antibiotic, making it easy to select the positively transformed organisms (Miki and McHugh 2004).

As far as plasmid vectors are concerned, they are essential for obtaining a successful transformation. Binary vectors the most useful plasmid vector systems for plant transformation. This is because of their ability to replicate in a wide range of host organisms. The reason for that is they contain DNA sequences that enable them to replicate in those organisms, called the "origin of replication". One of the advantages of binary vectors is their independence from a specific Ti plasmid. In other words, they can be introduced into any *Agrobacterium* host as long as it contains Ti plasmid (Klee et al. 1987, Gelvin 2003, Tzfira and Citovsky 2003, Hooykaas and Schilperoort 1992).

Another method of plant transformation is biolistic bombardment (or gene gun approach). In 1987, Klein with his team reported that tungsten particles can behave as carriers to deliver genetic materials into onion cells and expression of this transferred genetic materials can be observed. A year later, Sanford (1988) explained the concept in more details and pointed out that the inventors of this approach have named it with the term 'biolistic' (biological ballistics). This is to refer to the method and the device used to bombard the biological materials into living cells or tissues (Sanford 1988, Klein et al. 1987).

The biolistic technique was presented as a new approach to the difficulty of the delivery of external genetic materials into living cells and tissues. The process uses highly dense particles "microprojectiles" and accelerates them by a device "gun" to a high velocity. These microprojectiles are used to carry DNA or other substances and are introduced into cell walls and membranes (Klein et al. 1987).

As for any technique, there are advantages and disadvantages of the biolistics transformation approach. The advantages of this technique over other plant transformation techniques include its effectiveness regardless of which species or tissue type is used for. In addition, it is relatively simple and straightforward. Furthermore, the biolistic process appears to be uniquely suitable for organelle transformation (Potrykus 1991, Christou 1992).

One of the disadvantages of the biolistics process is the need of special and expensive instruments. Moreover, researchers may need to optimise their protocols in terms of species or tissue being targeted. Besides when looking at it from cost benefit perspective, one of the major drawbacks of this approach include its high costs with its efficiency in terms of obtaining stable positive transformants (Klein et al. 1988, Christou 1992).

Protoplast plant transformation methods are an approach that needs a high degree of delicacy. Protoplasts are plant cells that have their cell wall removed. They can be isolated by processing plant tissue with enzymes to break down the cell wall. This reaction produces a suspension that contains individual cells. These cells can be used as single cell targets (Potrykus 1991, Hansen and Wright 1999). Protoplasts can be obtained from leaf, callus and suspension culture (Meyerowitz and Somerville 1994).

Protoplasts can be transformed by different approaches. These approaches might be indirect, such as *Agrobacterium*-mediated transformation, or directly by genetic material uptake methods. Direct methods can be carried out by treatment of the protoplasts by polyethylene glycol (PEG) or by electroporation (Shillito 1999).

Approaches where viruses were employed for gene transfer to plants have also been successful. In 1984, Brisson and his coworkers have published their work on transferring bacterial antibiotic resistance gene by infecting the plant with the cauliflower mosaic virus (Brisson et al. 1984).

### **1.15. *Saccharomyces cerevisiae* as a biotechnology tool**

*Saccharomyces cerevisiae*, or "baker's yeast" as it is called, has a number of features that made it an essential tool for biotechnologists. *S. cerevisiae* is fully sequenced containing 12000 kilo base pairs, more than 6000 genes on 16 chromosomes (Sychrova 2004). It can be used to analyse the expression of foreign proteins, particularly for higher eukaryotes. Since *S. cerevisiae* is considered a food organism, it is found acceptable to be produced in high quality for research, industry and pharmaceutical purposes. Moreover, yeast can be grown quickly on simple media and to high cell density. In addition, its genetics are well understood than any other eukaryote (Romanos et al. 1992, Sychrova 2004), so that it can be manipulated almost as easily as *E. coli* (Romanos et al. 1992). Although it is a unicellular creature *S. cerevisiae* is very similar to higher eukaryotic organisms in terms of the structure and the physiology of the cell (Cereghino and Cregg 1999, Romanos et al. 1992). This wealth of data makes it the organism of choice especially when it comes to understanding cellular functions including ion transport mechanisms (Sychrova 2004).

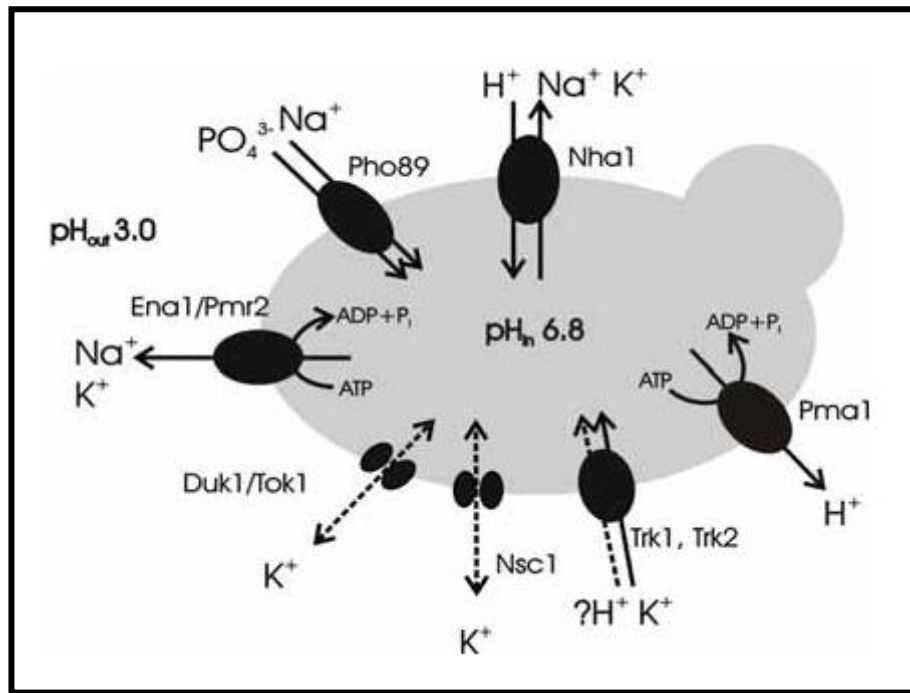


Figure 6: The figure shows transport proteins that appear to be involved in the influx and efflux of potassium and sodium ions through the plasma membrane of *S. cerevisiae*. Pma1: outward  $\text{H}^+$  active pump; Trk1, Trk2, high affinity potassium active intake proteins, Nsc1: low affinity  $\text{K}^+$  uptake channel, Duk1/Tok1: potassium channel, Ena1/Pmr2:  $\text{Na}^+$  active outward pump, Nha1,  $\text{Na}^+/\text{H}^+$  antiporter, Pho89:  $\text{Na}^+/\text{Pi}$  cotransporter. Obtained from (Sychrova 2004).

**1.16. PM19 protein:**

The PM19 protein is a highly conserved putative plasma membrane protein of unknown function found in all higher plant species. Functional analysis of the Arabidopsis homologue of the PM19 protein is the subject of this PhD thesis.

Koike and his team (1997) were the first to identify PM19 when a 19-kDa (AWPM19) plasma membrane protein was accumulated after exposing wheat suspension cultured cells to different ABA concentrations (from 1  $\mu$ M and up to 200  $\mu$ M). Cells that were exposed to 50  $\mu$ M ABA showed the highest freezing tolerance.

Then, Koike et al. (1997) isolated plasma membrane proteins of the wheat cultured cells at different times and compared between them in the presence and absence of 50  $\mu$ M ABA by the observation of their pattern by SDS-PAGE analysis. In the exposure to the 50  $\mu$ M ABA, the band of the 19 kDa protein showed the highest intensity on day 5. However, on the group that is not exposed to ABA, the intensity of the bands increased slightly. The increase in the intensity of the 19 kDa band correlates with the increase in the freezing tolerance.

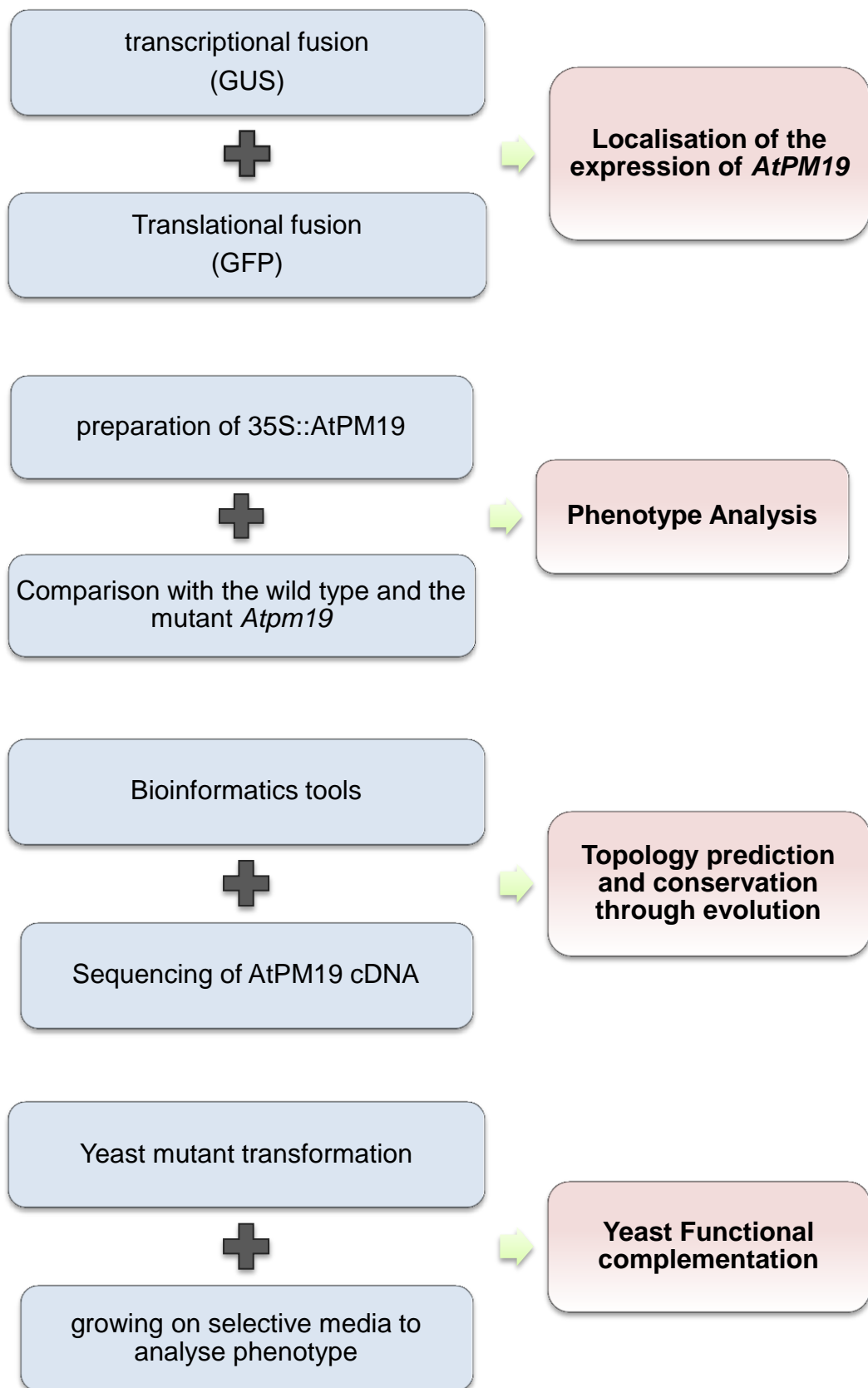
After that, the Koike et al. (1997) isolated the ABA-induced wheat plasma membrane protein (AWPM19) and the N-terminus amino acid sequence was determined. Then primers based on the N-terminal amino acid were designed that then were used for a PCR on cDNA from RNA extracted from the wheat cell suspension. Then another PCR was carried out using gene specific primers for WP-1 and  $\lambda$ ZAP vector to obtain the full length cDNA sequence of the WPM-1 then the full amino acid sequence encoding AWPM-19 (Koike et al. 1997).

Analysis of the AWPM-19 amino acid sequence showed that the first 34 amino acid in the mature polypeptide are present in the full length amino acid sequence, indicating

that it is not cleaved. In addition amino acid sequence has four hydrophobic regions suggesting it is located in the plasma membrane (Koike et al. 1997).

Ranford et al. (2001) screened dormant wild oat embryo cDNAs library - with DIG-labelled heterologous cDNA probes obtained from dormant and non-dormant barley - in order to isolate cereal embryo genes associated with dormancy. The one oat clone that was detected showed homology to (AWPM19) that was isolated by Koike et al. (1997). PM19, the barley homologue of AWPM19, has high homology with protein sequences encoded from seeds of *A. thaliana*, rice embryo (*Oryza sativa*) and soybean (*Glycine max*). The expression of *PM19* gene in barley during different stages of development was analysed by RT-PCR and northern blot. Although the expression analysis may indicated its association with seed dormancy, embryo development and abiotic stress, the function of PM19 protein was not clear from their experiments (Ranford et al. 2001).

Pons (2005) carried out expression analysis experiments to investigate the function of AtPM19 protein in *Arabidopsis*. He produced some constructs such as a transcriptional fusion of PM19 promoter-GUS and another translational fusion *35S::PM19-GFP*. He carried out transient expression analysis on onion tissues by bombardment and found that when PM19 protein is fused with *GFP* the green florescence appear in the plasma membrane of the onion cells. However, when the GFP protein is on its own the florescence spread all over the cytoplasm and the nucleus. With respect to the transcriptional fusion of PM19 promoter-GUS, Pons (2005) made the cloned the promoter of *AtPM19* gene in the binary vector pPR97 just before the gene *Gus*.

**1.17. The plan of investigation:**



The main findings in this PhD research project can be summarised as the following: PM19 protein has been conserved in terrestrial plant species, and not in algae, for more than 400 million years ago through plant evolution. The location of the AtPM19 protein was detected in the plasma membrane of transgenic *A. thaliana* cells containing translational fusion with GFP protein under confocal microscopy of *A. thaliana* seedlings that contain the overexpressed *AtPM19* gene.

The seedlings containing overexpressed *AtPM19* showed higher tolerance - than wild type and mutant *atpm19* seedlings - to relatively higher concentrations of sodium in the germination medium. They also showed tolerance to in medium containing potassium, mannitol and rubidium. Interestingly, when grown on medium containing caesium, the overexpressed *AtPM19* containing seedlings were able to tolerate relatively high concentrations while the mutant *atpm19* showed high sensitivity indicating that PM19 protein is helping the cell to expel those toxic ions outside it. The *AtPM19* gene was shown to be highly expressed during the early stages of seed germination. Moreover, AtPM19 protein was shown to express in *A. thaliana* leaves tissues during drought stress. Attempts to complement the loss of function in several yeast mutants were carried out.

At the beginning of this thesis the materials and methods will be outlined before presenting the obtained results. After that the results will be discussed in the discussion chapter.

**CHAPTER 2: MATERIALS AND METHODS**

**2. MATERIALS AND METHODS:****2.1. Materials:**

Unless otherwise stated, chemicals and reagents were supplied from Sigma-Aldrich (UK) or Fisher Scientific (UK). All chemicals, reagents, enzymes and other materials were stored and maintained as recommended by the manufacturer.

**2.2. Centrifugation**

Centrifugation of small volume samples were carried out in 1.5 or 2.0 ml Eppendorf tubes using a Micro Centaur Microfuge (MSE) at RCF 12000 x *g* at room temperature. Larger volume samples were centrifuged in an Avanti J-26 XP Centrifuge (Beckman Coulter) at the stated speed and temperature.

**2.3. Images**

Images of GFP expressing plants were taken using a Leica DMIRE2 confocal microscope with an HCV PL APO CS 40X 1.25 oil immersion lens. GFP excitation wavelength was 488 nm, emission 500-550 nm. Calcofluor excitation wavelength was 405 nm and emission 420-450 nm. FM4-64 excitation wavelength was in 561 nm emission 650-740 nm.

Images of the GUS plants tissues were taken using a Leica DFC320 microscope.

**2.4. Source of seeds**

*Arabidopsis thaliana* ecotype Columbia (Col 0) was the genetic background for all the *PM19* mutant plants. The T-DNA insertion into the *PM19* gene (At1g04560) was obtained from Salk Institute Genomic Analysis Laboratory. The 35S-*PM19*-GFP plants were constructed by (Pons 2005).

Plant Line	Resistance gene
T-DNA in <i>PM19</i>	Kan
35S-PAPIII-GFP	Amp/ Kan
35S –GFP	Amp/ Kan
PM19 promoter-GUS	Kan

Table 3: Summary of information on transgenic *A. thaliana* lines used in the study

### 2.5. Plant growth conditions

Seeds were sown on a petri dish containing plant medium [0.35 % Phytigel, 0.5 x Murashige and Skoog medium, 10 mM MES pH 5.8], then were stratified for a uniformed breakage of seed dormancy at 4 °C for two days. Then they were kept in a growth room at 25 °C under an 18 h/6 h light/dark cycle. One week after germination, seedlings were transplanted from the petri dish to the mix of compost (John Innes No. 2) and grown under the same conditions. The seedlings were covered by a plastic lid to keep the humidity high for the early stages of the seedlings' growth in soil.

### 2.6. DNA methods

#### 2.6.1. Extraction of genomic DNA from plant tissue

About 100 mg of leaves were ground in 0.4 ml of Edwards extraction buffer [200 mM Tris-Cl, pH 7.5, 250 mM EDTA, 0.5 % SDS] using a plastic pestle for about 10 seconds then vortex mixed. After that, the mixture was centrifuged at RCF 12000 x g for 1 minutes. Then, 0.3 ml of the supernatant was transferred to a fresh tube and an equal volume of isopropanol was added. The samples then were centrifuged at RCF 12000 x g for 1 minutes. Then, after the supernatant was removed and the pellet was dried at 70° C for 5 minutes, and resuspended in 100 µl of TE buffer [10 mM Tris, pH 8.0, 1 mM EDTA] and stored at - 20 °C (Edwards et al. 1991).

### 2.6.2. Plasmid DNA purifications

A total of 1.5 ml of an overnight *E. coli* cell culture was added into an Eppendorf tube then centrifuged for 1 min at RCF 12,000 x *g* then the supernatant was decanted. The pellet was resuspended in 100 µl GTE [50 mM glucose, 25 mM Tris-Cl pH 8.0, 10 mM EDTA] and vortexed until the pellet was completely resuspended. Then, 200 µl of NaOH/SDS solution [0.2 M NaOH, 1% SDS (w/v)] was added and the tube was inverted several times, then 150 µl of 5 M potassium acetate (pH 4.8) was added and inverted several times. The tube was incubated on ice for 5 min then centrifuged down at RCF 12,000 x *g* for 1 min. After that, the supernatant was transferred into a fresh tube, 0.8 ml of 95 % ethanol was added and incubated in room temperature for 2 min. After spinning at RCF 12,000 x *g* for 1 min, the supernatant was removed and the pellet was washed with 0.5 ml of 70 % ethanol then centrifuged at RCF 12,000 x *g* for 1 min. The supernatant was then removed and the pellet was dried at 70 °C for 5 min, dissolved in 20 µl TE buffer [10 mM Tris-Cl (pH 7.5), 1 mM EDTA] and stored at -20 °C.

### 2.6.3. Restriction enzyme digests

Digestion of plasmid DNA (1-2 µg) or genomic DNA (up to 10 µg) with restriction endonucleases was routinely carried out in a reaction volume of 20 - 50 µl and contained restriction enzyme(s) [1 enzyme unit / 1 µg of linear DNA fragment, 5 units per µg plasmid DNA] and enzyme-specific buffer [1 x from 10 x stock]. Reactions were brought to the final volume using sterile dH<sub>2</sub>O. All restriction enzymes and buffers used in this study are illustrated in the table below. Digestion reactions were incubated for 3 h for plasmid digestions or overnight for genomic DNA digestions then deactivated by heating to the appropriate temperature as recommended by the manufacturer, or by gel purification of DNA fragments (Section 2.6.7) after electrophoresis (Section 2.6.6). Confirmation of the DNA digestion was carried out by running ~ 5 µl on a 1 % (w/v)

agarose gel. Table 4 shows the restriction enzymes and their buffers that were used in the study.

Enzyme	Buffer
Xba1	Tango Buffer
Pst1	O Buffer
Sal1	O Buffer
Bgl1	O Buffer
Sma1	Tango
T4 DNA ligase	10 X T4 DNA Ligase Buffer

Table 4: Restriction and modifying enzymes and buffers used in this study.

#### 2.6.4. DNA ligations

Restriction digested plasmid and insert DNA was ligated in a 20  $\mu$ l reaction volume. The usual vector to insert molar ratio was 1:3. A typical reaction contained 2  $\mu$ l of 10 x ligation buffer (400 mM Tris-HCl [pH 7.8], 100 mM MgCl<sub>2</sub>, 100 mM DTT, 5 mM ATP), 1  $\mu$ l of T4 DNA ligase (5 units per  $\mu$ l; Fermentas), DNA and dH<sub>2</sub>O up to the final volume. Ligations were incubated overnight at 16 °C before heat inactivation of the reaction at 70 °C for 10 min. Confirmation of the ligation was carried out by running ~5  $\mu$ l alongside a digested, non-ligated sample on a 1 % (w/v) agarose gel (section 2.6.6).

#### 2.6.5. Standard PCR reactions preparation

Routine PCR reactions contained 5  $\mu$ l 10 x DreamTaq™ PCR buffer (Fermentas), 1  $\mu$ l of each primer [10 pmol/ $\mu$ l], DNA template [minimum of 100 ng of genomic DNA or 10 ng of plasmid DNA], 200  $\mu$ M dNTPs and 0.2  $\mu$ l [1.5 units] of Taq polymerase (DreamTaq™, Fermentas). The reaction was brought to a total volume of 50  $\mu$ l with sterile dH<sub>2</sub>O. The reaction mixture was transferred into a 200  $\mu$ l PCR tube (AxyGen, Inc.) and placed in a thermal cycler (Gen Amp® PCR system 2700, Applied Biosystems).

A standard PCR cycle has three main stages: denaturation, annealing then extension. Cycles initiate with an introductory denaturation stage of 5 min at 94 °C then followed

by number of cycles consisting of denaturation [30 sec at 94 °C), annealing [30 sec at primer specific temperatures] (see Table 5) and extension stages [1 min at 74 °C). Then, a final extension step of 74 °C for 7 min to completed primer extension before holding at 10 °C. Negative control reactions [reactions containing dH<sub>2</sub>O instead of DNA] were run alongside the sample reactions. PCR products were ran on agarose gel electrophoresis and stored at - 20 °C until required.

Primer	Sequence (5' → 3')	T <sub>a</sub> (°C)	
PAP97-F	GCCAACGAACACATAAGC	58	PM19 forward
PAP986-R	CTTGGCCTGTAGCATAGTCTT	58	PM19 reverse
PROK-LB	GCGTGGACCGCTTGCTGCAACT	58	Left border of T-DNA
3A	GCAATTGATGGCGACGACA	58	PM19 forward

Table 5: Names, sequences and annealing temperatures (T<sub>a</sub>) of primers used in this study.

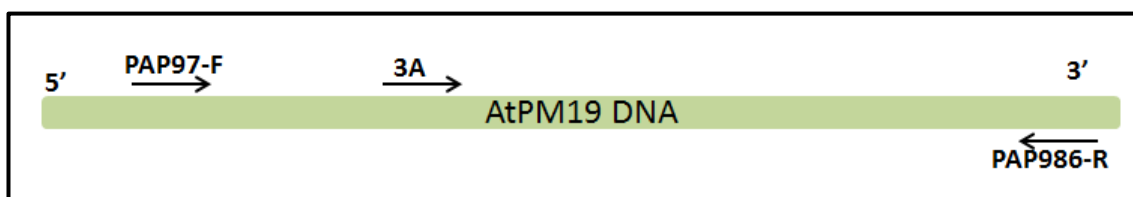


Figure 7: a graph of the primers used in this study.



### 2.6.6. Agarose gel electrophoresis of DNA

Routine DNA analyses were carried out by separating DNA fragments using the RunOne™ Electrophoresis Cell (EmbiTec). A 1 % (w/v) agarose solution in 0.5 x TBE [44.5 mM Tris-HCl, pH 8.0, 44.5 mM boric acid, 1 mM EDTA] was prepared by melting the agarose in a microwave oven. After cooling the gel below 60°C, ethidium bromide was added to concentration of 0.5 µg/ml. The gel then was poured into the gel platform and left to cool with a comb in place. After the gel had solidified, combs were slowly removed before placing the gel within the electrophoresis tank and immersing with 0.5 x TBE. DNA samples were mixed with 6 x loading buffer [60 % (v/v) glycerol, 60 mM EDTA, 0.09 % (w/v) bromophenol blue and 0.09 % (w/v) xylene cyanol, Fermentas] and loaded into the wells of the gel. Electrophoresis was carried out at 100 V for 25 min, or until the loading dye reaches the end of the gel front, before visualising the DNA with an ultra violet transilluminator (UVItec ltd). A DNA marker ( $\lambda$ HindIII, Fermentas) was run alongside DNA samples to give detectable and measurable fragments of 23130, 9416, 6557, 4361, 2322, 2027 and 564 bp on a 1 % (w/v) agarose gel. DNA gels were photographed using a UVP gel documentation system.

### 2.6.7. Gel purification of DNA

After separating DNA fragments and/or plasmid DNA on a 1 % (w/v) agarose gel, DNA was purified using a GeneJET™ gel extraction kit (Fermentas) following the manufacturer's instructions.

### 2.6.8. Preparation and transformation of E. coli competent cells:

The *E. coli* cell strain used was XL-1 Blue, the background is [*recA1*, *end A1*, *gyrA96 thi-1*, *hsdR17*, *supE44*, *relA1*, *lac* [*F'* *proABlacI<sup>t</sup>* *ZAM15Tn10 (Tet<sup>r</sup>)*]]. Efficient competent cells were prepared as described by (Inoue et al. 1990). 5 ml of LB plus 20 mM MgSO<sub>4</sub> was inoculated with a single colony of XL-1 Blue cells and grown overnight at 25 °C. This culture was then used to inoculate (1:50 dilution) 250 ml LB

plus 20 mM MgSO<sub>4</sub>. This culture was then grown at 25 °C to (OD<sub>600</sub> ≥ 0.4 ≤ 0.6). After that, cultures were stored on ice for 10 min before centrifugation (4 °C; RCF 600 x g; 10 min). The pellet was then resuspended in 80 ml of ice-cold transformation buffer [PIPES-HCl (pH 6.7), 15 mM CaCl<sub>2</sub>, 250 mM KCl, 55 mM MnCl<sub>2</sub>] and stored at 4 °C for 10 min before centrifugation (4 °C, RCF 600 x g, 10 min). Cells were resuspended in 20 ml pre-chilled transformation buffer [+ 1.5 ml dimethyl sulfoxide] and stored on ice for 10 min. Finally, cells were dispensed into pre-chilled Eppendorf tubes (200 µl volumes). Aliquots were frozen in liquid nitrogen and stored at - 70 °C until needed.

Competent *E. coli* cells were transformed using the heat shock method described by (Sambrook et al. 1989). Competent cells aliquots were removed from the - 70 °C freezer and thawed on ice. Up to 100 ng of plasmid DNA (1-20 µl) was added to the culture and gently mixed by inverting up and down then stored on ice for 30 min. Cells were then heat shocked for 2 min at 42 °C before immediately being put back on ice for another 5 min. Cells were allowed to recover by adding 1 ml of LB (without antibiotic) to the cells and incubated at 37 °C for 45 min. Cells were then harvested by spinning down the cells at RCF 2,400 x g for 3 min and resuspended in 50 µl of LB before plating onto LB plates (+ appropriate antibiotic) and incubating overnight at 37 °C.

## **2.7. RNA methods:**

### 2.7.1. Preparation and quantifying of total RNA from Arabidopsis tissues:

#### 2.7.2. From Arabidopsis leaves:

Plant tissues were ground in liquid nitrogen then transferred into pre-chilled Eppendorf tubes. Then, about equal volume of REB (RNA extraction buffer) [25 mM Tris, pH 8.0, 75 mM NaCl, 25 mM EDTA, 1 % SDS] and β-merceptoethanol solution [REB, merceptoethanol 700:50 µl] was added to the ground tissue then vortexed until homogenised. After that, 700µl of water-saturated phenol:chloroform (50:50 v:v) was added and vortexed then centrifuged at RCF 12,000 x g for 5 minutes. The upper layer

was transferred into a fresh tube and the phenol:chloroform step was repeated until no interface was seen. After that, an equal volume of chloroform was added into the tube, vortexed then centrifuged for 3 minutes at RCF 12,000 x g. The supernatant was transferred into a fresh Eppendorf tube and ¼ volume of DEPC treated 10 M LiCl was added gently and gently mixed and left at - 20 °C overnight. The sample was then centrifuged at RCF 12,000 x g for 30 minutes. The supernatant was decanted and the pellet was resuspended in 100 µl dH<sub>2</sub>O. Then the RNA sample was ethanol precipitated as follows. A 1/10 volume of DEPC-treated 3 M sodium acetate pH 5.8 was added to the tube. After that 2.5 × volume of ethanol 96% was added, then vortexed. This was centrifuged down for 15 min at RCF 12,000 x g and the supernatant was decanted. After a wash with 70 % ethanol samples were centrifuged down for 1 min and supernatant carefully decanted and pellets were dried at 37 °C. Then, the pellets were resuspended in 20 µl of dH<sub>2</sub>O and stored at - 70 °C.

### 2.7.3. From Arabidopsis seeds:

As outlined by (Meng and Feldman 2010) about 100 mg of dry seeds were ground in liquid nitrogen then directly added to a 15 ml tube containing 1.5 ml of extraction buffer [100 mM Tris-HCl pH 9.5] and mixed until homogenised. The mixture then was transferred into 2 ml tubes, vortexed for 3 min and centrifuged at maximum speed for 5 minutes before the supernatant was transferred to a fresh tube. A ½ volume of chloroform was added to the tube and vortexed for 5 min, then a ½ volume of water saturated phenol was added and the mix was vortexed for 2 min and centrifuged at RCF 12,000 x g for 15 min. The upper aqueous phase was removed to a fresh 1.5 ml tube and 90 µl of 3 M sodium acetate pH 5.2 and 600 µl of isopropanol was added and mixed. The samples were incubated at room temperature for 10 min and centrifuged for 10 minutes, the upper aqueous phase was removed and the pellet was washed with 1 ml of 70 % ethanol then centrifuged at RCF 12,000 x g for 10 min. The supernatant then was

discarded and the pellet was dried and resuspended in 1 ml TRIzol and vortexed until the pellet dissolved. Then 200  $\mu$ l of isopropanol was added and mixed by vigorously shaking the tube for 20 sec before the tubes were incubated at room temperature for 3 min then centrifuged at RCF 12,000 x g for 15 min. The upper phase was transferred into a fresh tube and 500  $\mu$ l of isopropanol was added and mixed then incubated at room temperature for 10 min then centrifuged at RCF 12,000 x g for 10 min. After discarding the supernatant, the pellet was washed with 1.2 ml of 70% ethanol before it was centrifuged at RCF 12,000 x g for 10 min. The supernatant then was decanted and the pellet was dried and dissolved in DEPC-treated sterile dH<sub>2</sub>O. A 10  $\mu$ l of DEPC-treated 3 M sodium acetate (pH 5.8) and 250  $\mu$ l of 96% ethanol was added to the sample and incubated at room temperature for 20 min then centrifuged at RCF 12,000 x g for 15 min. The pellet then was washed with 1.2 ml of 70% ethanol, centrifuged for 10 min, supernatant was discarded and pellet was dried. The pellet then was resuspended in 50  $\mu$ l of DEPC-treated sterile dH<sub>2</sub>O and stored at -70 °C for further analyses.

#### 2.7.4. Quantifying RNA concentration by spectrophotometer:

For measuring RNA concentration, readings were taken at wavelength of 260 nm.

1 OD (Optical Density) at 260 nm for RNA molecules = 40 ng/ $\mu$ l of RNA

If there is contamination with protein or phenol, accurate quantitation of the amount of RNA will not be possible, and RNase in the protein will degrade the RNA. In order to quantify the RNA, a 1  $\mu$ l sample was diluted in 400  $\mu$ l TE, so the dilution factor was 1:400. The 400  $\mu$ l was transferred into a spectrophotometer cuvette and absorbance between 320 and 220 nm measured. The RNA concentration read will then be:

$OD_{260} \times 40 \text{ ng}/\mu\text{l} \times \text{dilution factor}$

Clean RNA has an OD 260:280 ratio of 2, lower values suggest contamination with proteins.

#### 2.7.5. Preparation of RNA denaturing gel:

The RNA samples were analysed on denaturing gels. The RNA denaturing gel is made as follows: 1 g agarose, 80 ml dH<sub>2</sub>O, 10 ml of 10 × Mops buffer [200 mM MOPS, 50 mM Na acetate and 10 mM EDTA, pH 7.0] were added in a 250 ml flask and heated in a microwave until agarose was dissolved. After it cooled down to 60 °C 10 ml of formaldehyde was added to the mix then poured into an RNase free RNA tray with the comb in place. The gel was left at room temperature until it set.

#### 2.7.6. Northern blotting:

The northern blot is an approach by which gene expression can be detected by hybridisation to an RNA sample.

##### 2.7.6.1. Preparation of RNA probe:

The RNA probe used in this study was Digoxigenin labelled and made using T7 RNA polymerase. For northern blot analysis, an antisense probe was needed. For making the DNA template, the PM19 cDNA insert was amplified with M13F/R primers. Then, in a Eppendorf tube, 200 ng of the PCR product, 2 µl 5x RNA polymerase buffer, DTT to 30 mM, 0.5 µl RNase inhibitor, 1µl DIG RNA labelling mix and 1 µl RNA polymerase were added then incubated at 37 °C for 2 hours, then analysed on a TBE gel.

##### 2.7.6.2. Transferring RNA to a Membrane (Capillary Transfer Method):

The gel was soaked twice for 5 min in autoclaved 20× SSC buffer [3 M NaCl, 300 mM sodium citrate, pH 7] to clear formaldehyde from the gel that may cause transfer inhibition. A diagonally small cut on the top right angle of the gel was made to help orientate the gel. Then, the transfer blot was set up as follows, avoiding the formation of air bubbles between any two parts of the blot “sandwich”: 2 pieces of Whatman 3MM

paper soaked in 20× SSC was placed on top of a pad of tissues. A piece of positively charged nylon membrane (Roche) was cut to the size of the gel, make a diagonally small cut on the top left angle to match the cut made on the gel. The nylon membrane was soaked in sterile distilled water, then in 20× SSC buffer. The wet membrane was carefully placed on top of the Whatman paper. The gel then was placed on top of the nylon membrane facing downwards. A pipette can be rolled over the layers to remove all air bubbles. The blot assembly was completed by adding two sheets of Whatman 3MM paper, cut to the size of the gel. A bridge with Whatman 3MM paper was made to carry 20× SSC buffer from a tray to the blot sandwich. After that, the blot was left for 6 hours.

#### 2.7.6.3. Fixing RNA to membrane

Once the RNA had transferred to the nylon membrane, and the membrane was still damp, the RNA was fixed to the nylon membrane by a UV cross linker. The membrane was placed - with the RNA side facing up - on Whatman 3MM paper that has been soaked in 2 × SSC buffer and exposed to UV light with the cross-linker in automatic mode.

#### 2.7.6.4. Pre-hybridization

The membrane must not be allowed to dry at any time during pre-hybridization, hybridization or detection to avoid formation of high backgrounds. The membrane was placed between two nylon meshes and put into roller bottle containing 10 ml of pre-warmed hybridization buffer [6 M urea, 6 × SSC, 1% SDS, 50 mM Tris, pH 7.5] and placed in a rotating oven in a temperature of 68 °C for 30 min.

#### 2.7.6.5. Denaturation of the probe

The concentration of transcriptionally labelled RNA probe should be 100 ng of RNA probe per 1 ml of hybridization buffer. An appropriate amount of labelled probe was

added into an Eppendorf tube with 100 µl of sterile dH<sub>2</sub>O. The tube then was incubated on the heating block at 95 °C for 5 min to denature the RNA before chilling in ice. After that, the denatured probe was added to a tube containing 10 ml of pre-warmed hybridisation buffer and mixed by inversion.

#### 2.7.6.6. Hybridization

After removing the pre-hybridization buffer and adding the new one which contains the denatured probe, the tube was placed in the rotating oven at 68°C for 6-16 hours.

#### 2.7.6.7. Washing

After finishing the hybridization, the hybridization buffer was removed and preheated autoclaved 2 × SSC (low stringency buffer) [100 ml of 20 × SSC, 900 ml H<sub>2</sub>O, 0.1% SDS] was added and the tube placed back in the rotating oven at 68 °C for 20 min. After repeating this step, preheated autoclaved 0.1 × SSC (high stringency buffer) [5 ml of 20 × SSC, 995 ml H<sub>2</sub>O, 0.1% SDS] was added to the tube and incubate in rotating oven for 20 min at 68 °C and repeated once.

#### 2.7.6.8. Blocking

After hybridisation, the membrane was placed in a plastic bag and 10 ml of DEPC treated, autoclaved blocking buffer [100 mM malic acid, 1 M NaCl, pH 8, 0.3% Tween, 0.5% casein] was added, making sure air bubbles were removed and the bag was sealed and left at room temperature for 1 h. After that, anti-Digoxigenin antibody conjugated to alkaline phosphatase was centrifuged at RCF 12,000 x g for 5 min and 1µl was taken and added to 10 ml of blocking buffer and mixed. Then the blocking buffer was poured off and add fresh one containing anti-Digoxigenin was added and left at room temperature for 30 min.

#### 2.7.6.9. Washing

The blot was placed in small tray and autoclaved Dig1 buffer [100 mM Tris, 1 M NaCl, pH 8] was poured into the tray until covering the blot membrane and placed on the shaker at 45 rpm. This step was repeated for another three times. After that, the blot was washed with autoclaved Dig4 [100 mM Tris, 100 mM NaCl, pH 9.5] for 5 min before detection.

#### 2.7.6.10. Detection

After hybridising with anti-digoxigenin antibody, the blot was spread with 500 µl of CDP-star between two pieces of acetate sheet and put in the developing cassette. Then, in a dark room, the blot membrane was exposed to an X-ray film for 1 to 20 min - depending on signal intensity - and developed.

### **2.8. Characterization of mutants**

#### 2.8.1. Seed sterilization:

Seeds were added in an Eppendorf tube and 1 ml of [70% ethanol and 0.1 % solution] was added then the tube was inverted up and down for two minutes. The solution was then poured out and seeds were rinsed with 1 ml of 95% ethanol then poured off. After adding 0.5 ml of 95% ethanol until seeds had sunk, the seeds were pipetted and transferred into a filter paper and left until the ethanol evaporated. Seeds were then transferred into an Eppendorf tube.

#### 2.8.2. Sowing the seeds for germination percentage:

One hundred wild type, *pm19* mutant and 35S-*PM19-GFP* seeds were all sown on one square petri dish to minimize variations in growth conditions. Seeds were picked using a sterile 200µl tip then placed in the medium.

Seeds were allowed to germinate and grow for 7 days. Seeds that grew and showed roots and green leaves were counted as germinated seeds.



### 2.8.3. Drought experiments

Water loss and stomatal conductancy experiments was carried out as explained by (Verslues et al. 2006).

#### 2.8.3.1. Water loss:

Three leaves from healthy plants of each genotype (WT, pm19 and 35S-PM19) were cut and their weight were measured immediately (time 0). Then every 30 minutes their weight were measured and recorded. The readings were taken until 6 hours after cutting the leaves.

#### 2.8.3.2. Stomatal conductancy:

Seeds were grown as described in the section (plant growth conditions) in page 42. After 3 days the germinated seedlings were transferred into 76 mm size pots. In order to expose all of the genotypes to the same conditions, two pm19 seedlings (or 35S-PM19 seedlings) were planted beside two wildtype seedlings in the same pot. There were eight replicates from each pot. After 10 days four pots of each of the eight were exposed to drought for 7 days and four were watered as normal. After that, the stomatal conductancy of the control plants and the plants that were exposed to drought was measured (Figure 8).

Measurement of the stomatal conductancy was carried out using (Leaf Porometer) from (Decagon Devised). Since stomatal conductancy can be defined as is the amount of H<sub>2</sub>O that pass out from the leaf, the way Leaf Porometer works is that it measures the rate of that passage by measuring the difference between the humidity atmosphere and the vapor that pass out from the leaf. The Leaf Porometer consists of keyboard, which contains some controllers and a monitor, and a sensor head. After calibrating the devise as explained by the operator's manual directions, the readings were taken by clipping the sensor head on the leaf until the reading showed in the screen.

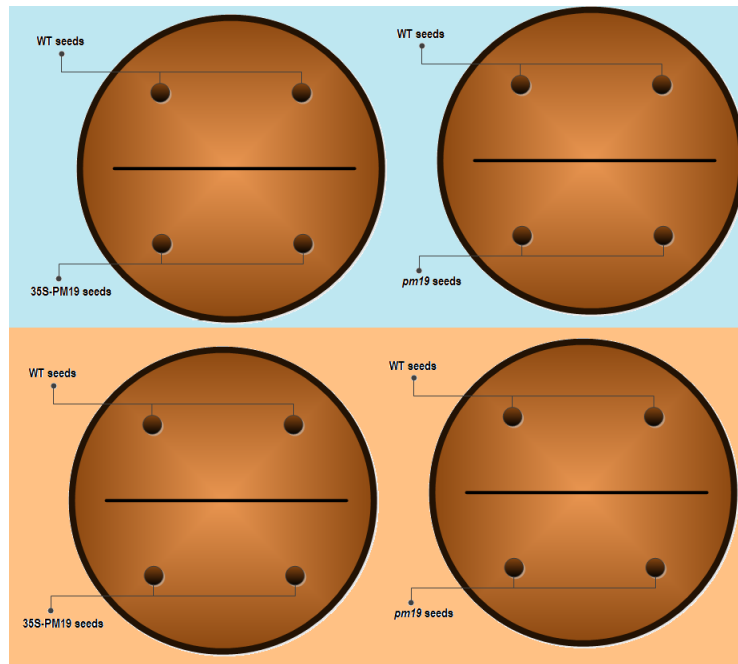


Figure 8: the picture explains the concept of the soil drying drought experiment. The pots in blue background represents the pots that were watered normally, while the light brown background represents the pots that were exposed to drought stress.

**2.9. The floral dip *Agrobacterium* plant transformation:**

Transformation of *Arabidopsis* plants was carried out using floral dip method as outlined by (Clough and Bent 1998) *Agrobacterium tumefaciens* strain carrying the gene of interest was grown in 400 ml LB culture with the appropriate antibiotics for about 3 days to an OD<sub>600</sub> of 0.8. Then, 5 % sucrose solution in addition to 500 µl/l of surfactant Silwet L-77 was also added to the solution and mixed well. Shoot tissues of healthy flowering *Arabidopsis* plants were dipped into the *Agrobacterium* solution for few seconds then covered with plastic bags for about 24 hours. Then the plants were grown in standard room conditions. After seeds become mature, watering was stopped and seeds were harvested, then screened. Screening was carried out on plant medium plates containing the appropriate antibiotic. Confirmation of transgenic plants was carried out by PCR of the genomic DNA of the potential transgenic plant, using the appropriate pair of primers.

**2.10. Staining GUS-expressing plants:**

The GUS staining of *Arabidopsis thaliana* seeds, seedlings and tissues were performed as described by (R.A. Jefferson et al. 1987). Tissues were immersed in freshly made staining solution [0.1 M NaPO<sub>4</sub> pH 7.0, 10.0 mM EDTA, 0.1% Triton X-100 (v/v), 1.0 mM K<sub>3</sub>Fe (CN)<sub>6</sub>, and 2.0 mM X-Gluc] and incubated at 37 °C overnight. Then, the staining solution was removed and washed several times with 70% ethanol, incubating the tissue overnight for each wash. The tissues become ready for observation when green chlorophyll was cleared.

**2.11. Yeast methods:****2.11.1. Extraction of DNA from yeast:**

As outlined by (Hoffman and Winston 1987) 10 ml yeast cultures were grown for 24-48 h in YPD, the cultures were centrifuged down at RCF 600 x g for 3 min. After decanting the supernatant, the cells were resuspended in 0.5 ml of distilled water and

transferred in a fresh Eppendorf tube. Then, the samples were centrifuged at RCF 12,000 x g for 1 min, the supernatant were decanted and the cells were vortexed briefly to resuspend the pellet in the residual liquid. After adding 200 µl lysis buffer [2% Triton x 100, 1% SDS, 100 mM Tris-Cl pH 8, 1 mM EDTA], 200 µl phenol chloroform and ~ 300 mg of glass beads (size 0.25 mm), sample were vortexed for 3 min. Then, 200 µl of TE [10 mM Tris, pH 8.0 with HCl, 1 mM EDTA] were added and the samples were centrifuged at RCF 12000 x g for 5 min and the aqueous (top) layer was transferred to a fresh tube. 1 ml of 96% ethanol was added to each sample and mixed gently by inversion. Then the samples were centrifuged down at RCF 12,000 x g for 2 min, the supernatant was decanted and pellets resuspended with 400 µl TE pH 8 and 3 µl RNase. Samples then were incubated for 5 minutes at 37° C. 10 µl of 4 M ammonium acetate plus 1 ml of 96% Ethanol was added to samples and mixed by inversion, then centrifuged at RCF 12,000 x g for 2 min. The supernatant was decanted and pellets were air dried, resuspended in 50 µl TE and stored in -20° C.

#### 2.11.2. Yeast Transformation (Electroporation):

Yeast cells were grown on YPD broth [tryptone 20 g/l, yeast extract without amino acids 10 g/l and dextrose 20g/l] to Optical Density of 600. Then, cells were spun at RCF 1600 x g for 5 min, and pellets were washed in an equal volume of ice-cold water. After that, cells were washed in 1/2 volume cold water then washed in 1/25 volume ice-cold 1M sorbitol. Cells then were treated with 25mM DTT for 10 min at room temperature then washed with 1M cold sorbitol. After that, cells were resuspended in 1/200 original volume cold 1M sorbitol then mixed with 50µl of cell suspension with 5µl DNA. Cell/DNA solutions immediately were tapped to the bottom of a 0.2cm cuvette and were exposed to electric pulse at 1.5kV for 5 milliseconds. Then, immediately 1ml of YPD/1M sorbitol solution was added and samples were allowed to recover at room

temperature for one hour. Cells were spun down and resuspended in 1ml 1M sorbitol then plated on selective media (containing no uacil).

**CHAPTER 3: RESULTS**

**3. RESULTS:**

In order to study the function of a protein, such as PM19 in this case, one of the important aspects to investigate is its significance, not only for the particular species from which it was obtained (*A. thaliana*) but also for the plant kingdom as a whole.

**3.1. PM19 in evolution:**

A standard protein BLAST (Basic Local Alignment Search Tool) search was carried out (Altschul et al. 1997) using the *AtPM19* amino acid sequence, as there is less redundancy embodied in the encoded amino acid sequence as compared to the redundancy in the DNA sequence of a gene, to find out the similar protein sequences in different organisms. The cut-off chosen for highly similar alignments was for those alignments that have a query cover of  $\geq 50\%$  and identity of  $\geq 60\%$ . Under this criterion the result showed 19 different plant species in the Genbank databases that have a highly similar protein to the encoded protein sequence from the *AtPM19* DNA sequence (see Table 6). It also showed that there are no similar proteins to PM19 in any other kingdom apart from plants. It must be born in mind that many organisms have not been fully sequenced, however given that full genomic sequences from all representative phyla are present in Genbank, it is unlikely that genes encoding PM19 homologues exist other than in green plants.

The blastp search also showed that *A. thaliana* genome has three different genes that encode proteins that have some similarity to AtPM19. Although the scores for those proteins were not as high as the set cut-off, they showed a high similarity to AtPM19 protein, suggesting AtPM19 protein might belong to a protein family rather than a single gene. The gene numbers and accession numbers are shown in (Table 7).

In order to analyse the degree of similarity of the identified sequences to PM19, seven sequences were chosen (shown in Table 7) to represent plant groups that are distinct in

terms of their ancestral roots, including all three members of the Arabidopsis family (see Figure 11). A multiple sequence alignment of those sequences was carried out using the protein sequence alignment tool (PRALINE multiple sequence alignment (<http://www.ibi.vu.nl/programs/pralinewww/>)) to show similarities in the overall sequence (Figure 9), the hydrophobicity (Figure 12) and the secondary structure between these sequences (Figure 14). Then, as can be seen by reference to the Cambridge University Plant Evolution Timeline (<http://www.ensemble.ac.uk/projects/plantsci/timeline/>) and in (Smith et al. 2010), the major groups of the plant kingdom in which homologues of the PM19 protein can be found, showing that the core of the PM19 protein is highly conserved throughout plant evolution for over four hundred million years (Figure 10).

Proteins are composed of a chain of amino acids. Each amino acid has different physio-chemical properties. These physio-chemical properties determine the function of the amino acid as a unit then accordingly the structure and function of the protein. Since the plant cell has different structures and each part of the cell has different physio-chemical properties, in order for the protein to be present and stable in that environment, it must be appropriately targeted and structured. In particular, the cellular plasma membrane is composed of a 5 nm thick lipid bilayer (Alberts et al. 2008).

The multiple sequence alignment of PM19 protein in (Figure 12) shows the hydrophobicity of the amino acids and whether they are identical or functionally conserved in the examined plant species. The total number of the highly conserved amino acids represents about 40% of the full protein sequence. Most of those highly conserved amino acid are non-polar hydrophobic (i.e. have low affinity to water). The prediction of the transmembrane tendency plot in Figure 13 indicates that AtPM19 is a four transmembrane domain protein.



Since the first 160 amino acids in the sequence alignment show hydrophobic properties with four conserved patches with hydrophilic properties, the hydrophobicity plot of the PM19 protein in Figure 12 indicates that PM19 might be a membrane protein with four transmembrane domains. The unconserved tail of the protein is hydrophilic, that is it is probably located outside the membrane domain (see Figure 9 and Figure 12).

Thus, within PM19 there are 4 transmembrane domains as can be seen in Figure 13. When compared with Figure 14 we can find that those four domains have an alpha helix structure. The reason for this is that these alpha helixes consume all of the hydrogen bonds such that there are no exposed polar groups - that have hydrophilic properties- to bind with water. This, in turn, might have a significant role in stabilising the protein in its location in the plasma membrane and then in the protein function.

The alignments show that the conserved amino acids are highly specific in terms of their properties within the PM19 multiple protein sequence alignment (see Figure 9, Figure 12 and Figure 14). For instance, the basic amino acids (R and K) are highly conserved in their location in the sequence (for example amino acid number 7 in the sequence alignment). Moreover, isoleucine (I) (amino acid number 122 in the sequence) is not only identical in its location outside the membrane domain due to its hydrophobicity but it also located in a zone of beta strand.

This high degree of specificity and consistency in the protein structure throughout plant evolution indicate that PM19 as whole has vital functions for plant life. In addition, some particular amino acids in the PM19 amino acid sequence seem to play an important role, as they are conserved throughout evolution. For example, some amino acids in PM19 protein may function as anchors to hold the protein in its location in the membrane (Lodish et al. 2008b). This can be noticed by observing the conserved negatively charged amino acids arginine, histidine and lysine. It is also clear that this

specificity in the conservation and in the location of the amino acid is not simply associated with the structural features concerning the location of the protein in the plasma membrane. The conservation disappeared when the plasma membrane protein AtKCO1 was included in the multiple protein sequence alignment. The AtKCO1 protein has 6 transmembrane domains.

Figure 12 also show that the last 40 amino acids of the PM19 protein are not at all conserved and are hydrophilic. This indicates that they are probably not as functionally significant as the first 160 amino acids and are not located in the transmembrane domain.

<b>Organism</b>
<i>Arabidopsis thaliana</i>
<i>Arabidopsis lyrata subsp. lyrata</i>
<i>Arachis hypogaea</i>
<i>Lotus japonicus</i>
<i>Glycine max</i>
<i>Populus trichocarpa</i>
<i>Vitis vinifera</i>
<i>Cucumis sativus</i>
<i>Ricinus communis</i>
<i>Sorghum bicolor</i>
<i>Zea mays</i>
<i>Oryza sativa</i>
<i>Triticum aestivum</i>
<i>Hordeum vulgare</i>
<i>Brachypodium distachyon</i>
<i>Picea sitchensis</i>
<i>Prunus dulcis</i>
<i>Selaginella moellendorffii</i>
<i>Physcomitrella spp.</i>

Table 6: The identified species after a protein BLAST search using AtPM19 amino acid sequence. It shows the wide variety of plant species that has a PM19-like protein. The cut-off of highly similar sequences was those that have a query cover value of  $\geq 50\%$  and an identity of  $\geq 60\%$ .

Species Latin name	Common name	Gene number	Accession number
<i>Arabidopsis thaliana</i>	Arabidopsis	AT1G04560 (AtPM19)	NP_563710
<i>Arabidopsis thaliana</i>	Arabidopsis	AT5G18970	NP_197398
<i>Arabidopsis thaliana</i>	Arabidopsis	AT1G29520	NP_174245
<i>Oryza sativa</i>	Rice		NP_001059485
<i>Hordeum vulgare</i>	Barley		AF218627.1
<i>Picea sitchensis</i>	Pine tree		ADE76757
<i>Selaginella moellendorffii</i>	Club moss		XP_002960681
<i>Physcomitrella patens subsp. patens</i>	Moss		XP_001767555
<i>Arabidopsis thaliana</i>	Arabidopsis	AT5G55630 (AtKCO1)	NM_124945

Table 7: The scientific names, the accession numbers and sequences of the protein sequences used in the protein sequence alignment and in the phylogenetic tree. in addition to the sequence of KCO1, the K<sup>+</sup> transporter in *Arabidopsis thaliana*.



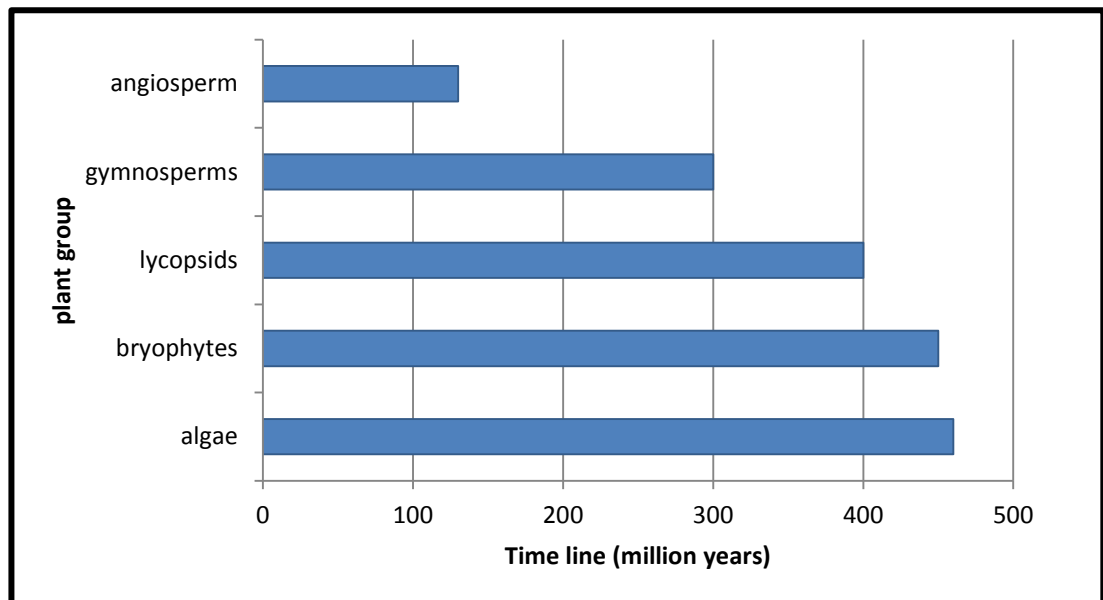


Figure 10: The PM19 protein sequence is conserved in plant groups for over four hundred million years. It is found in different plant groups, namely flowering plants (angiosperms), pines (gymnosperms), club mosses (lycopsids), and mosses (bryophytes). On the other hand PM19 protein does not exist in algae.

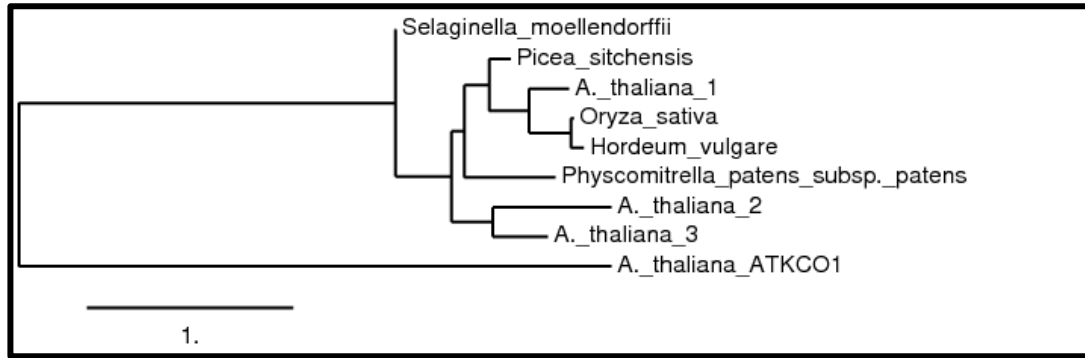


Figure 11: A phylogenetic tree comparing the amino acids sequences of PM19 from representative plant species, and illustrating that although the *A. thaliana* PM19 protein may share common ancestors with higher plants such as rice, there are also roots that are shared with other more primitive plants like mosses, club mosses, and pine trees (Dereeper et al., 2008). The figure also shows that PM19 protein is not closely aligned to the *A. thaliana* membrane protein KCO1. This indicates that PM19 protein is conserved not only in one family of plants but rather in all different plant families. PM19 is represented as *A. thaliana\_1*. The line at the bottom is the scale bar showing the distance between species.

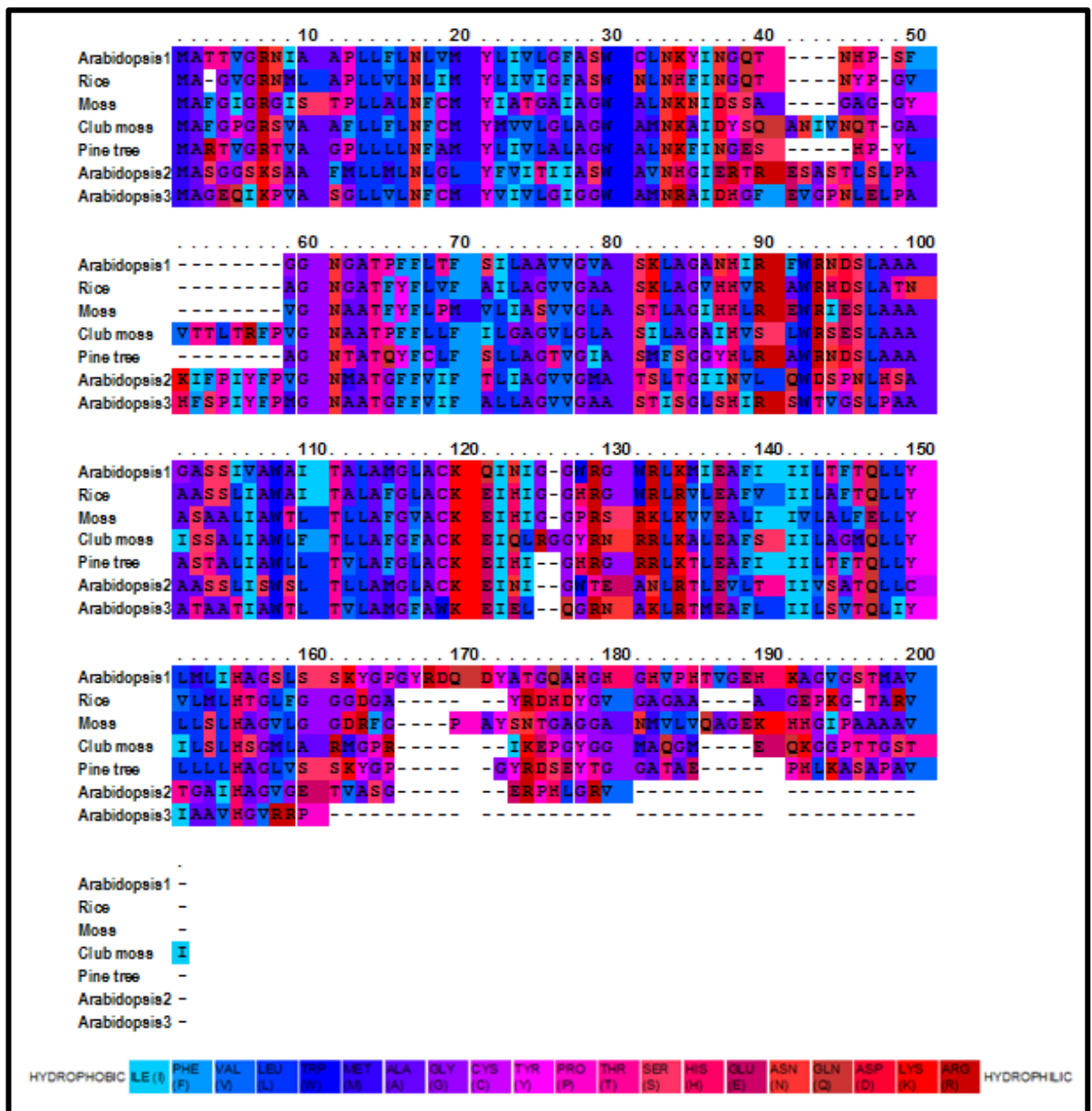


Figure 12: PM19 multiple protein sequence alignment for different plant species showing the hydrophobicity of the amino acids. The alignment was carried out using PRALINE alignment tool (<http://www.ibi.vu.nl/programs/pralinewww/>) (Simossis and Heringa 2005). Dark red colour shows hydrophilic regions in the amino acid sequences while blue colours show hydrophobic regions of the protein.



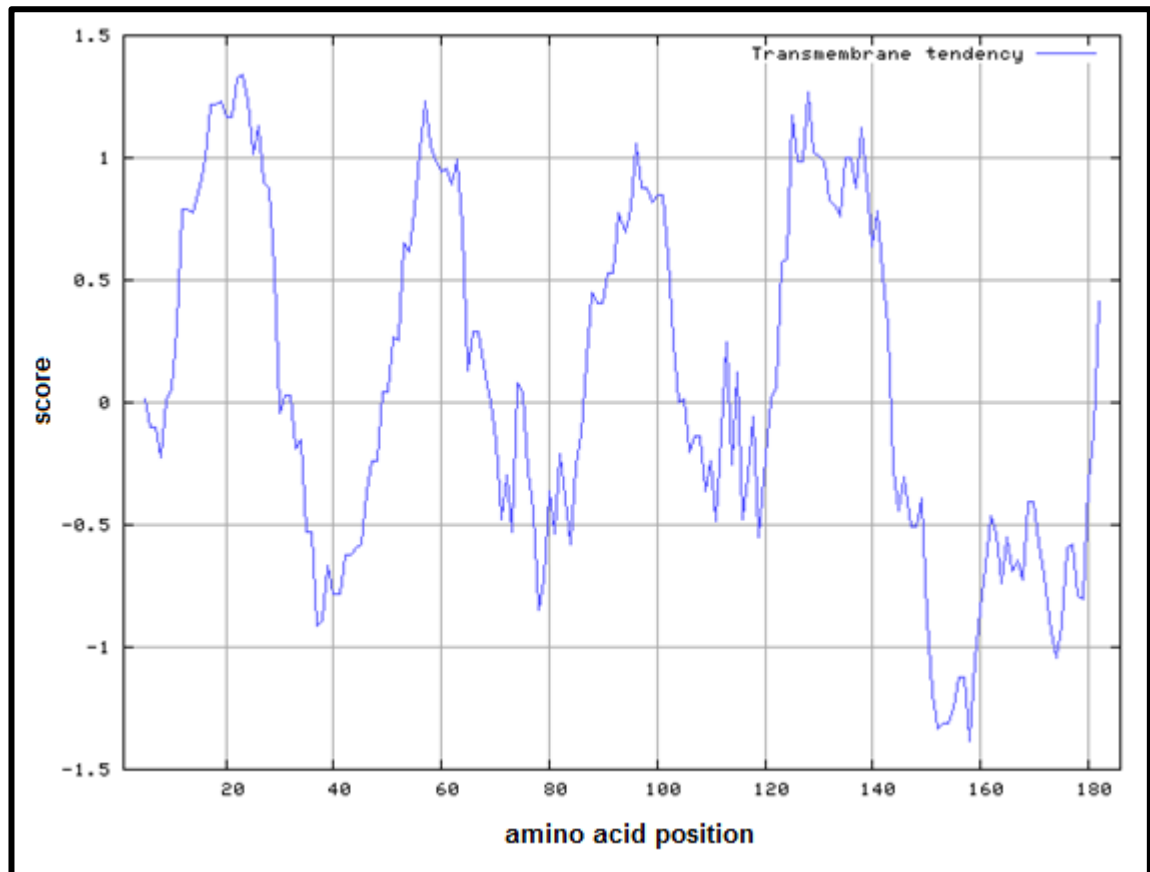


Figure 13: Predicted transmembrane tendency of AtPM19. The vertical axis represents the transmembrane tendency score, while the horizontal axis shows the position of the amino acids. The higher the score means the more hydrophobic properties the amino acid window has, while the lower the score means the higher the hydrophilic properties the window has. This strongly suggests that AtPM19 protein is a four domain transmembrane protein which is a consistent result with that in Figure 12. The program used to generate this figure was PROTSCALE (<http://web.expasy.org/protscale/>) (Gasteiger et al. 2005).

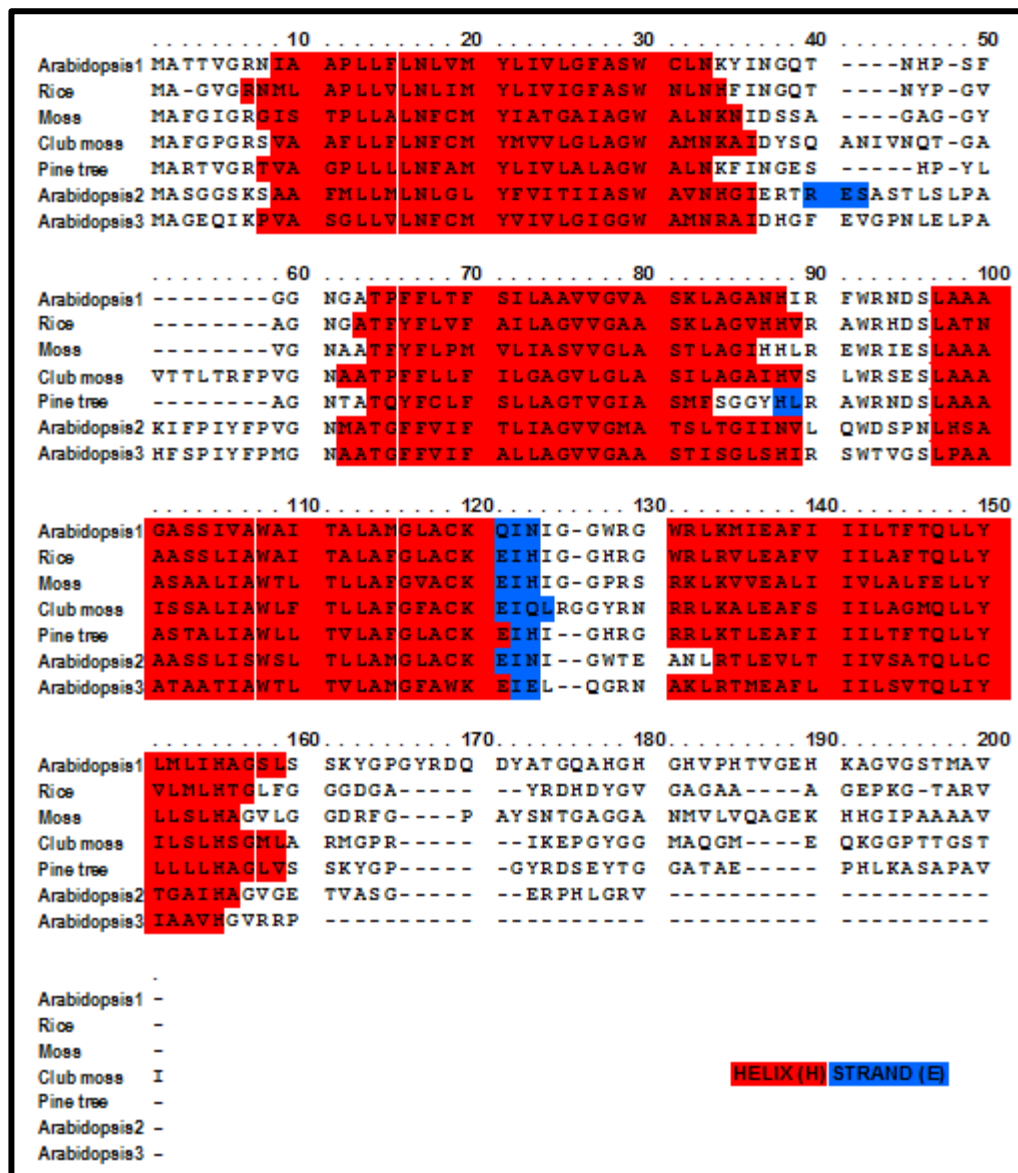


Figure 14: PM19 multiple protein sequence alignment for different plant species showing the secondary structure of the amino acids. The alignment was carried out using PRALINE alignment tool (Simossis and Heringa 2005). Red colour shows alpha helix regions in the amino acid sequences while blue colour shows strand regions of the protein. The alpha helix regions coincide with the hydrophobic regions shown in Figure 12.

**3.2. Prediction of protein localization:**

Until now the protein location of PM19 in the cell is not confirmed. However bioinformatics tools such as PSORT (<http://psort.hgc.jp/form.html>) can predict the possible location of the protein in the cell. By analysing the amino acid sequence of the AtPM19 protein the final result showed that AtPM19 can be located in the plasma membrane with a probability of 0.640 as compared to a certainty of 0.460, 0.370 and 0.100 for Golgi body, ER membrane and ER lumen respectively.

### 3.3. PM19 expression pattern

In order to know when in respect to the development stages of the plant and in what tissue(s) *PM19* is expressed, plants bearing the *PM19* promoter-GUS transcriptional fusion (*PM19::GUS*) transgenic plants made by (Pons 2005) were analysed. A transcriptional fusion is a construct made by the fusion of a reporter gene without its promoter and the promoter of a gene of interest (Richard A Jefferson et al. 1987). Bioinformatics analysis based on publically available microarray data such as (Hruz et al. 2008) and (Toronto 2013), suggests that *PM19* is highly expressed in seeds and seedlings. In addition, analysis of the publically available microarray data shows that *PM19* expression is seen in leaves of *A. thaliana* under drought stress (Hruz et al. 2008). Although the DNA microarray approach is designed to help analysing biological observations, data has to be supported by in vivo-based observations (on the real plant) (D'Ambrosio et al. 2005).

(Pons 2005) made a *AtPM19* promoter -GUS fusion using 1255 bp of upstream *AtPM19* promoter sequence (Figure 15). This construct was introduced into *Arabidopsis thaliana* plants. GUS ( $\beta$ -glucuronidase) is a molecular biological reporter gene and allows one to determine patterns of gene expression in the plant. The enzyme  $\beta$ -glucuronidase is stable and can be detected in transgenic plants that have *GUS* expression driven by the promoter of the gene of interest, meaning in this case that *GUS* will only be expressed when *PM19* gene expresses.

Transgenic *A. thaliana* bearing the *PM19::GUS* fusion were stained for GUS enzyme activity in the dry seeds as well as at different development stages as outlined in (section 12) the materials and methods chapter.

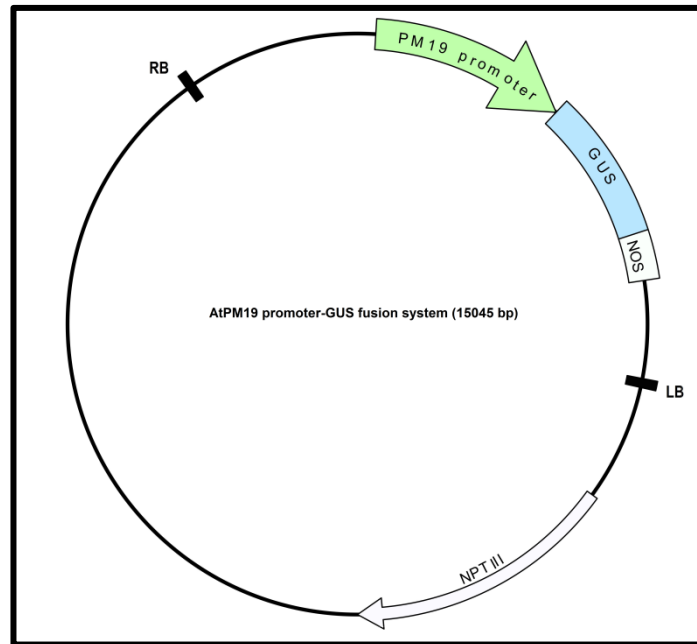


Figure 15: A schematic map of the PM19 promoter-GUS system made by (Pons 2005). *PM19* promoter is cloned in the binary vector pPR97 (Szabados et al. 1995) to control the expression of *GUS*, while NOS terminates this expression. The selectable marker is kanamycin.

### 3.3.1. PM19 protein expression in different stages of plant life:

*PM19::GUS* seeds were germinated in plant media. After different periods of time the seedlings were stained for GUS activity. Dry transgenic seeds showed strong expression of GUS in the cotyledons (

Figure 16), though seeds after 3 days on plant media showed the highest intensity of GUS expression. Transgenic seedlings aged 7 days old showed a clear distinct blue colour in the cotyledons (Figure 17). Those transgenic seedlings also showed high levels of GUS activity protein in roots (Figure 18).

GUS activity in 11 days old transgenic seedlings (Figure 19) and (Figure 20) was not apparent in tissues that had developed post germination. The roots were clear from any blue colour apart from the root tips, where there were some remaining GUS activity.

The cotyledons showed a strong blue colour while the new emerging leaves were clear, showing no GUS activity.

At day 15 after sowing the transgenic seeds in plant media, there was no GUS activity, neither in the leaves nor in the roots of the samples, indicating that *AtPM19* gene expression has stopped by day 15 (Figure 21) and (Figure 22). The results observed are in constancy with the bioinformatics data shown in (Toronto 2013) and (Hruz et al. 2008).



Figure 16: Crushed dry seeds of Columbia (0) wild type (top) and *PM19::GUS* (bottom) plant stained for GUS activity. There is no GUS activity in the wild type seeds. The bluish colour in the bottom picture is GUS activity in the cotyledons. 90 % of *PM19::GUS* seeds that were stained showed GUS activity in the embryonic cotyledons (N = 30).

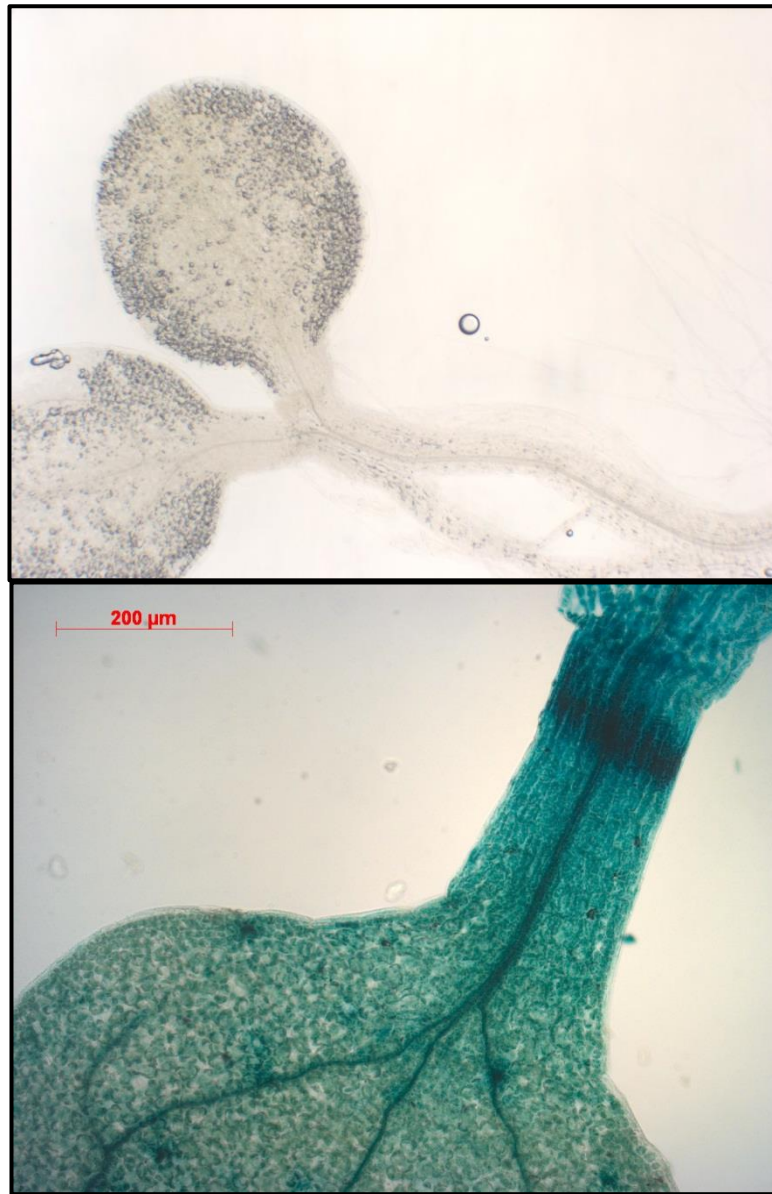


Figure 17: Cotyledons of wild type (top) and *PM19::GUS* (bottom) plant stained for GUS activity after 7 days in plant media. There is no GUS activity in the wild type cotyledons while there is high level of GUS activity in the *PM19::GUS* seedlings.



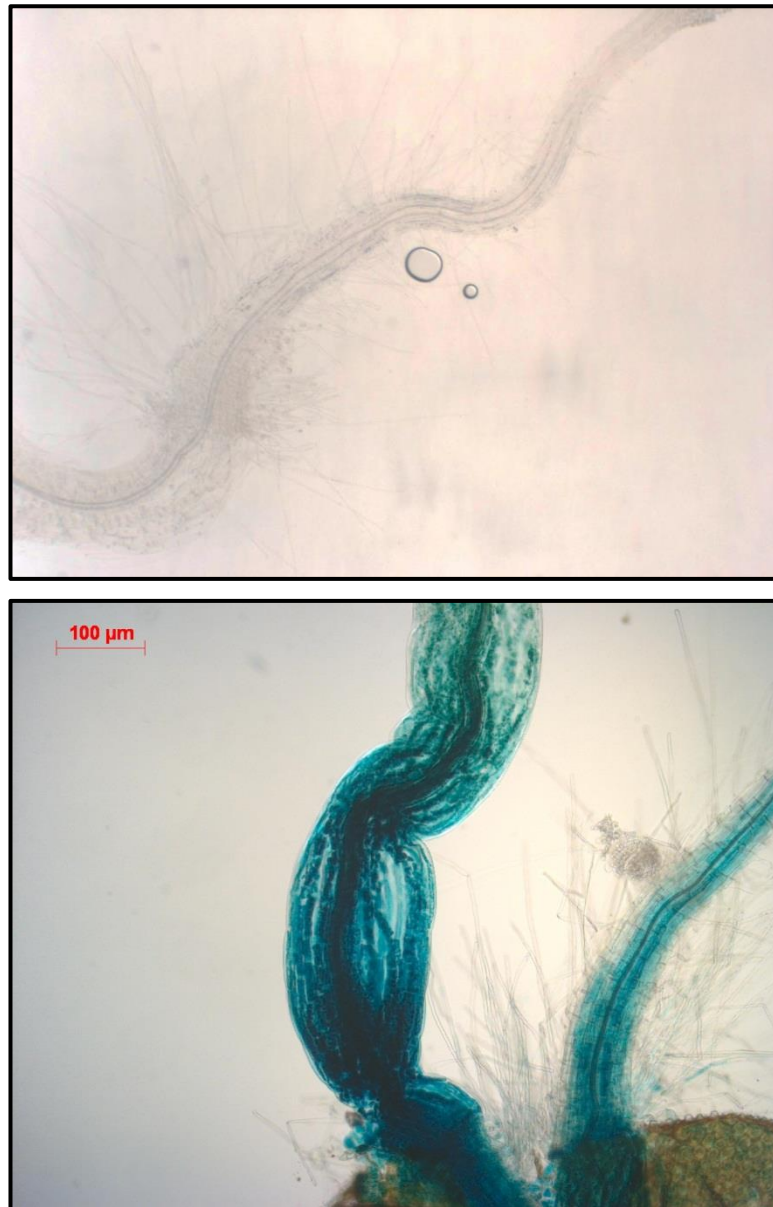


Figure 18: Primary roots of *PM19::GUS* plant stained for GUS activity after 7 days in plant media. *GUS* is highly active in the roots.

Primary roots of wild type (top) and *PM19::GUS* (bottom) plant stained for GUS activity after 7 days in plant media. There is no GUS activity in the wild type cotyledons while there is high level of GUS activity in the *PM19::GUS* seedlings.



Figure 19: Primary root of *PM19::GUS* plant stained for GUS activity after 11 days in plant media. The root tip is showing activity of *GUS*, however there is no further expression in the main body of the root.

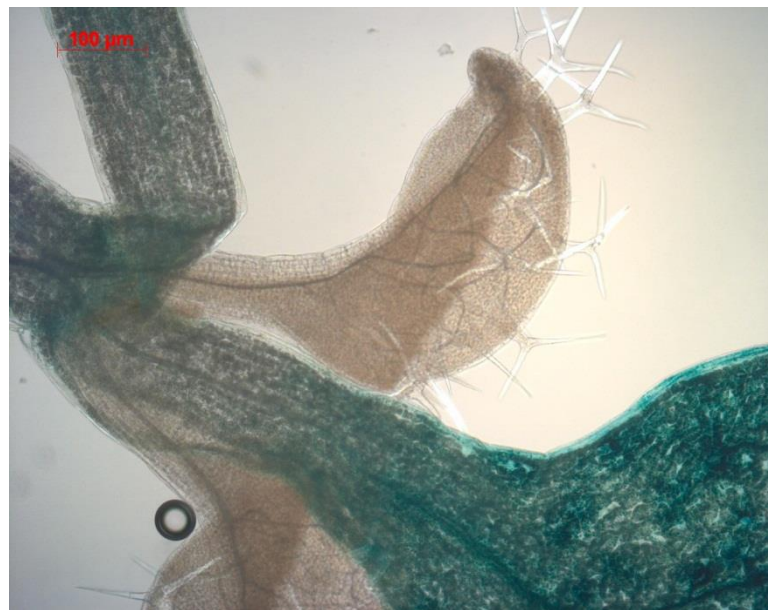


Figure 20: cotyledon and leaves of *PM19::GUS* plant stained for GUS activity after 11 days in plant media. The cotyledon is still showing GUS activity, however there is no activity in the leaves.

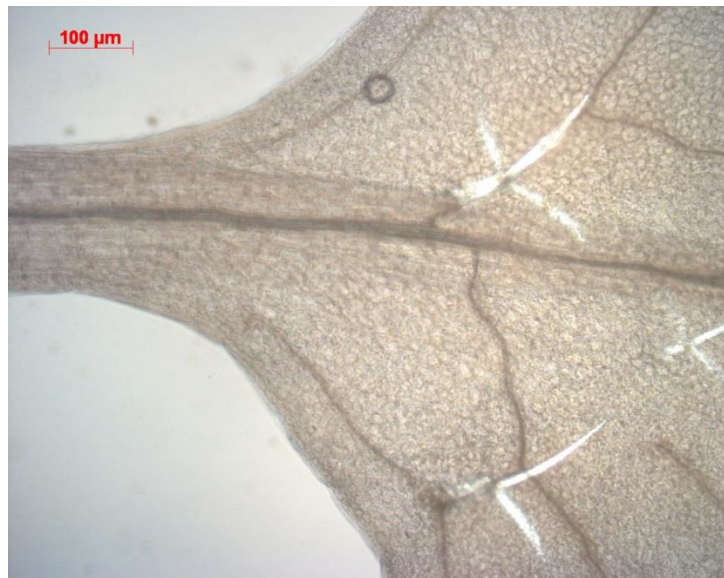


Figure 21: Leaf of *PM19::GUS* plant stained for GUS activity after 15 days in plant media. The leaf is not showing any GUS activity.



Figure 22: Root of *PM19::GUS* plant stained for GUS activity after 15 days in plant media. The tissue is not showing any GUS activity.

### 3.3.2. *PM19::GUS* fusion expression in plants under drought stress:

Data from the (Hruz et al. 2008) database indicated that there might be expression of *AtPM19* gene in leaves of drought stressed plants. Trying to confirm this data *PM19::GUS* containing seeds were grown in two separate pots. These pots were watered normally for 14 days. After that one of those pots was left without watering to

impose drought stress on the transgenic plants, while continuing watering the other pot as a control. Seven days later leaves from the drought stressed plants and the control plants were stained for GUS activity.

There was no blue colour in the control leaf samples while leaf samples from drought stressed plants showed light blue GUS staining (Figure 23), indicating GUS enzyme activity in drought stressed leaves and thus confirming that *AtPM19* gene expression is drought-inducible.

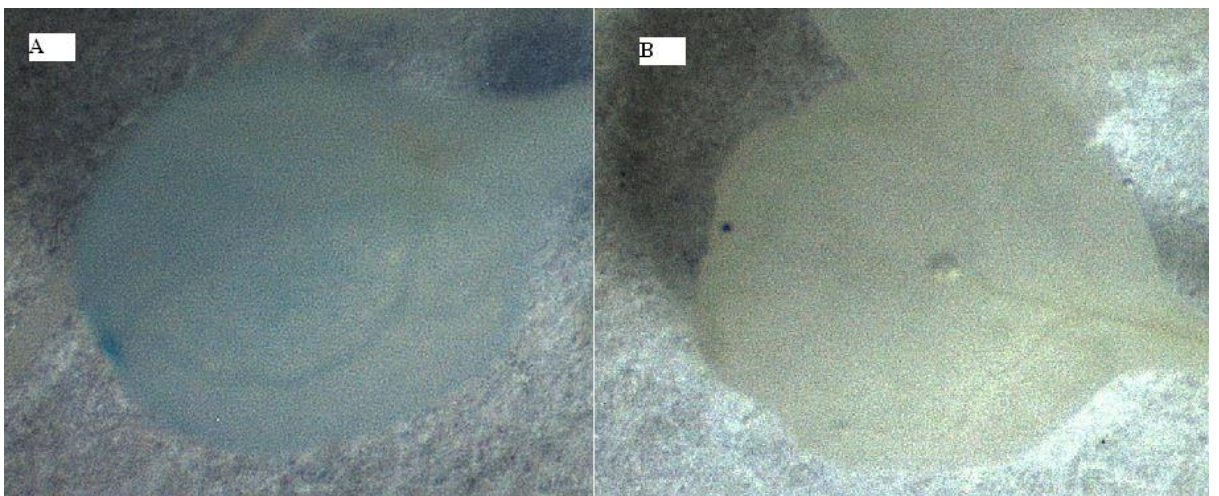


Figure 23: leaves from 2 weeks old *PM19::GUS A. thaliana* plants stained for GUS activity. A) A leaf after 7 days under drought. B) A leaf from a normally watered plant. Leaf A shows blue colouration, indicating an expression of *AtPM19*.

### 3.4. PM19 protein localisation in the cell:

To localise the protein at the cellular level a “translational” fusion system was used. A translational fusion is a recombinant DNA construct containing a promoter - such as the CaMV 35S cauliflower mosaic virus reporter promoter sequence, and a reporter gene sequence (such as GFP) fused to the N or C terminal of the encoded protein of the gene of interest. By this way, both the gene of interest as well as the reporter gene are driven by the strong promoter. By such an approach the intracellular location of the expression can be detected by observing the reporter gene expression, as the GFP fusion will be targeted to cellular locations by the sequence information encoded in the PM19 protein sequence. In this construct the GFP sequence is located at the C terminal of the translated PM19 sequence and there is no stop codon in between PM19 and GFP, thus the protein is a chimaeric fusion protein. Figure 24 illustrates the translational fusion construct between *PM19* and *GFP* that (Pons 2005) successfully made in *E. coli*.

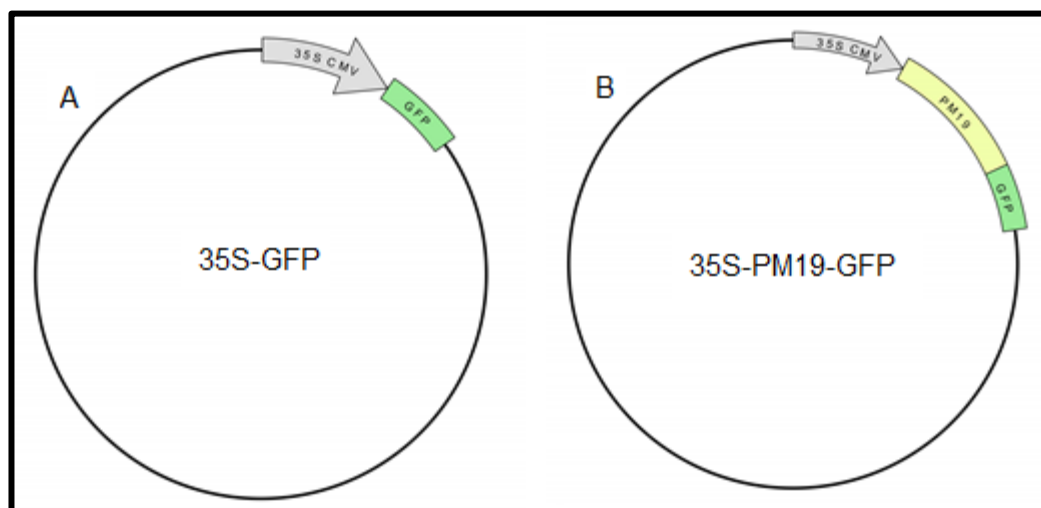


Figure 24: the figure shows the plasmids used for the localisation experiments of PM19 protein in the plant cell. (A) is a control plasmid where GFP is expressed without the control of PM19 while (B) GFP localisation is directed by PM19.

#### 3.4.1. Transformation of *A. thaliana* plants:

The construct produced by Pons was transformed into *A. thaliana* wild type plants. To do that the construct had to be transformed first into *Agrobacterium tumefaciens* (strain EHA105). The construct was introduced into *A. tumefaciens* by triparental mating. After that, the correct *A. tumefaciens* transformed colonies (containing *35S::GFP* as a control, and *35S::PM19-GFP*) were confirmed by growing a colony in an LB plate containing two antibiotics: kanamycin for the selection of the plasmid that contains 35S-PM19-GFP and rifampicin for the *Agrobacterium* selection. Then one colony was cultured in a liquid LB media containing kanamycin and rifampicin.

Wild type *A. thaliana* plants were transformed by *Agrobacterium tumefaciens* mediated transformation (explained in the materials and methods chapter section 11) and positive transformants were selected and grown for seed collection.

#### 3.4.2. AtPM19-GFP expression analysis

Transgenic *A. thaliana* containing *35S::GFP* were used as control not only to make sure GFP protein can be observed in the plant but also to ensure that the plants can grow normally with no other effect that the construct may make to the plant development.

Examined roots from plants containing *35S::GFP* showed free GFP in the cellular membrane, cytoplasm and in the nucleus (Figure 25). However, examination of the roots from *35S::PM19-GFP* plants under the confocal microscope showed a GFP signal only in the plasma membrane of the cells (Figure 26). This confirms that PM19 is localised in the plasma membrane of the cell.

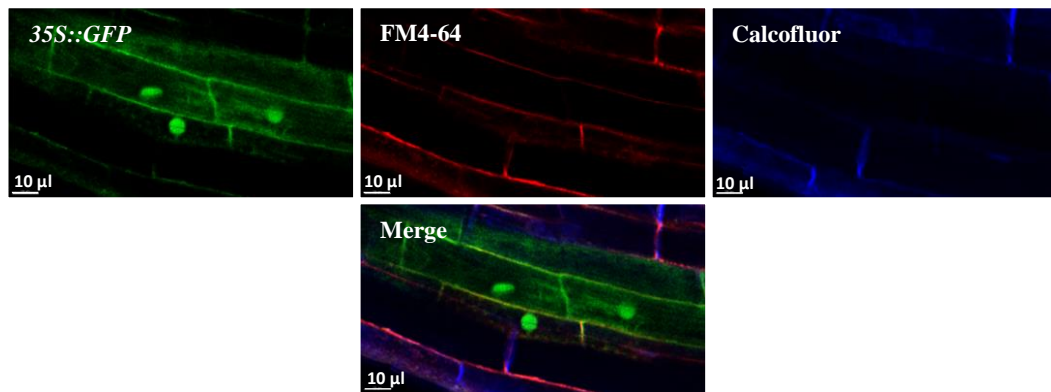


Figure 25: Confocal microscopy of *A. thaliana* root cells from transformed plants with *35S::GFP*. GFP appears in green colour showing expression in the cytoplasm and the nucleus. The red colour is a specific stain (FM4-64) for the cell plasma membrane. Calcofluor-white is a cell wall specific stain. Yellow colour appears when green and red colours overlap. GFP excitation wavelength was 488 nm, emission 500-550 nm. Calcofluor excitation wavelength was 405 nm and emission 420-450 nm. FM4-64 excitation wavelength was in 561 nm emission 650-740 nm. The size of the bar is 10 μm.

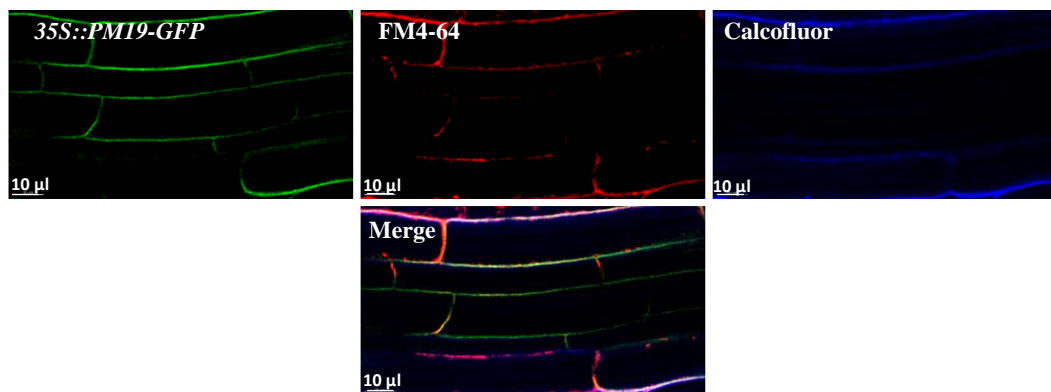


Figure 26: Confocal microscopy of *A. thaliana* root cells from transformed plants with *35S::PM19-GFP*. GFP appears in green colour showing expression only in the cellular plasma membrane. The red colour is a specific stain (FM4-64) for cell plasma membrane staining, while the blue colour is a calcofluor dye to stain the cell wall. GFP excitation wavelength was 488 nm, emission 500-550 nm. Calcofluor excitation wavelength was 405 nm and emission 420-450 nm. FM4-64 excitation wavelength was in 561 nm emission 650-740 nm. The size of bar is 10 μm.

### 3.4.3. Obtaining homozygous 35S::PM19-GFP

Further experiments, such as cross breeding of the *atpm19* mutant (see later) with *35S::PM19-GFP* plants, need homozygous *35S::PM19-GFP* plants. In order to prepare those plants, PCR was carried using genomic DNA of individual T<sub>1</sub> *35S::PM19-GFP* plants as a DNA template with the PAP986 and 3A primers. The samples that contained *35S::PM19-GFP* showed two bands; the lower one is the *AtPM19* cDNA that is fused with the *GFP* while the upper band is the genomic *AtPM19* (see Figure 27). Then, seeds from plant number 3 was collected and planted for further examination. Plant number 3 was chosen because it showed two strong intensity bands in the gel electrophoresis suggesting that the gene may be homozygous in this plant. A PCR reaction was carried out using the T<sub>2</sub> *35S::PM19-GFP* plants to provide DNA template along with 986 and 3A primers. All of the samples showed that they contain two bands (Figure 28), the upper one is the genomic *AtPM19* gene (1113 bp) while the lower one is the *AtPM19* cDNA (855 bp), meaning they are all homozygous .

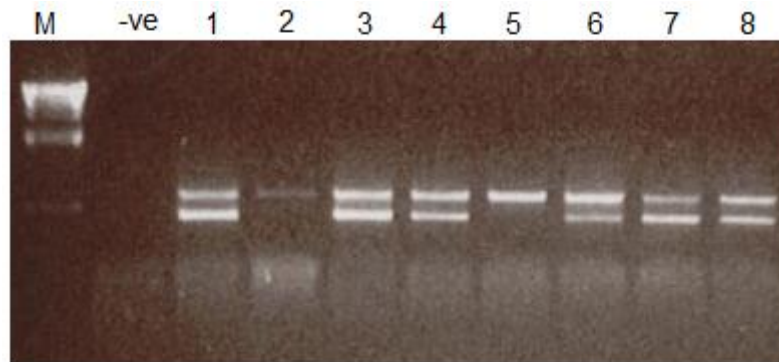


Figure 27: 1% agarose gel electrophoresis for PCR amplifications based on genomic DNA from T<sub>1</sub> *35S::PM19-GFP* plants. M: 2  $\mu$ l of  $\lambda$ HindIII DNA marker. -ve: negative control 1-8: PCR results from different *35S::PM19-GFP* plants using PAP986/3A primers. The photo is showing some homozygous plants and some wildtype. Samples number 2 and 5 show only the genomic *AtPM19* band (1113 bp), while samples 1,3,4,6,7 and 8 show two bands; the genomic *AtPM19* and *AtPM19* cDNA band (855 bp).



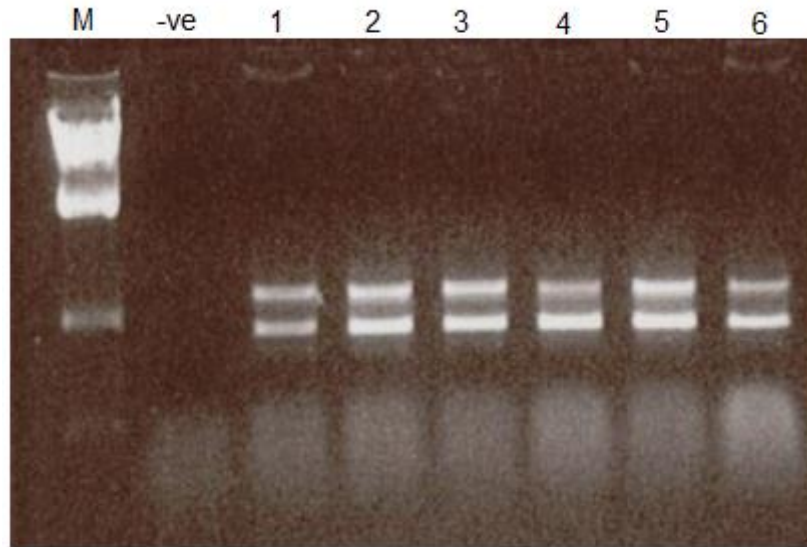


Figure 28: 1% agarose gel electrophoresis for PCR amplifications based on genomic DNA from *35S::PM19-GFP* plants. M: 2  $\mu$ l of  $\lambda$ HindIII DNA marker. -ve: negative control 1-6: PCR results from F3 *35S::PM19-GFP* plants using PAP986/3A primers. The photo is showing all plants to contain the wildtype gene and the *35S::PM19-GFP* gene, confirming the plants as homozygous.

### **3.5. Molecular biological analysis of the transgenic plants:**

To understand the function of the AtPM19 protein, wild type *A. thaliana* plants, *atpm19* mutant and plants containing overexpressed *AtPM19* were compared with each other for their behaviour under different conditions. For this reason, the mutation of the *AtPM19* gene and the overexpression of *AtPM19* have to be confirmed.

#### **3.5.1. PCR confirmation of the insertion mutation of AtPM19 DNA**

Interrogation of the SALK T-DNA insertion database (<http://signal.salk.edu/cgi-bin/tdnaexpress>) revealed the existence of an *Arabidopsis* line with a T-DNA insertion in the exon of the *AtPM19* gene (the T-DNA clone is: SALK\_075435.31.95.x). PCR reactions were carried out using wild type *A. thaliana* genomic DNA and the genomic DNA of the *atpm19* mutant in *A. thaliana* in order to confirm the mutation. The used primers were PAP97 and PAP986, which are *PM19* specific primers and the T-DNA left border primer (see Table 8). As shown in Figure 29, the samples containing wild type DNA showed a band when *PM19* primers were used. However there were no bands shown when the T-DNA primer was used with PAP97 and PAP986 primers. On the other hand, the samples containing *atpm19* mutant DNA showed no band when the *PM19* primers were used. However, a band appeared when the T-DNA left border primer was used along with each of the *PM19* primers (see Table 8 and Figure 29). This confirms that at least two T-DNA fragments were inserted back to back into the *AtPM19* gene (see Figure 30).

Sample	DNA template	Primer 1	Primer 2	Band
1	WT	PAP97(F)	PAP986(R)	Showed a band
2	WT	pROK-LB	PAP97(F)	No bands
3	WT	pROK-LB	PAP986(R)	No bands
4	<i>pm19</i>	PAP97(F)	PAP986(R)	No bands
5	<i>pm19</i>	pROK-LB	PAP97(F)	Showed a band
6	<i>pm19</i>	pROK-LB	PAP986(R)	Showed a band

Table 8: The PCR reactions carried out to confirm the presence and the orientation of the inserted T-DNA in the *AtPM19* gene. (F): is the forward *AtPM19* primer, (R): is the reverse *AtPM19* primer (pROK-LB): is the T-DNA left border primer.



Figure 29: Gel electrophoresis photo showing PCR products produced using genomic DNA of wild type and mutant *AtPM19* *A. thaliana* plants. Wells from left: M)  $\lambda$ HindIII DNA marker, 1) Wild type genomic DNA, primer used: PAP97/PAP986, 2) Wild type genomic DNA, primer used: pROK-LB/PAP97, 3) Wild type genomic DNA, primer used: pROK-LB/PAP986, 4) Mutant *AtPM19* genomic DNA, primer used: PAP97-PAP986, 5) Mutant *AtPM19* genomic DNA, primer used: pROK-LB/PAP97 and 6) Mutant *AtPM19* genomic DNA, primer used: pROK-LB/PAP986. This confirms that two T-DNA fragments were inserted into the exon regions of the *AtPM19*. The left borders of both of the T-DNA inserts are positioned to the peripheries as shown in Figure 30.

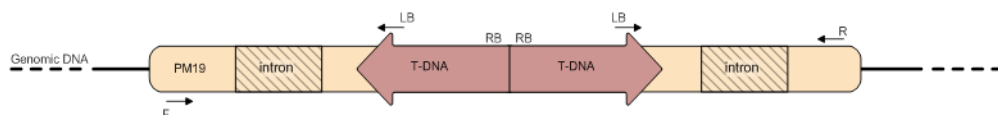


Figure 30: A schematic graphic of the mutant *atpm19* gene in the genomic DNA of *A. thaliana*. At least two T-DNA sequences are inserted back to back into the wild type *AtPM19* gene.

3.5.2. Sequencing the mutant AtPM19 gene:

Another confirmation of the insertion of the T-DNA was carried out. The two PCR amplicons 5 and 6 (see Figure 29) were sequenced using pROK-LB/PAP97 and pROK-LB/PAP986 primers (one primer per sequence). The grey shading (below) shows the T-DNA sequence and the rest of the sequence is *AtPM19* genomic DNA. This confirms that the two T-DNA were inserted in the *AtPM19* genomic DNA as illustrated in (Figure 30).

3.5.3. Left border/forward:

NGGNCCCATGCCCTTCCATTAGATCATCACCGAGCAAGTTAGTTTACGTGTT  
 TGTTGCAAAGAGAAGAAAGGNTTCGAGATAGCAAAAGAGTAAACTAGAT  
 CTTTAGGAGAAGGTAAAAGAAGCAATTGATGGCGACGACAGTGGGAAGAA  
 ACATAGCAGCACCAATTGCTGTTCTTGAATCTTGTTATGTACCTGATTGTGCTT  
 GGTTTTGCAAGTTGGTGTCTCAATAAATACATCAACGGCCAAACTAACCACC  
 CAAGTAAATTTATTTTTCTCTTTCTCTCTAGCTATTTATATGGTCATGTAGCT  
 GATCTAGTGAATTACTAAGAATATTAGTAATGTTTGAATAGGTTTTGGAGG  
 CAATGGAGCAACACCGTTCTTCTTGACGTTTTTCGATATTGGCGGCTGTGGTA  
 GGAGTAGCGTCGAAGTTGGCCGGAGCAAATCATATTAGGTTTTGGAGGAAT  
 GATAGTTTAGCCGCTGCTGGAGCTTCTTCCATCGTGGAAACAAATTGACGC  
**TTAGACA**ACTTAATAACACATTGCGGACGTTTTTAATGTACTGGGGTGG  
**TTTTTCTTTT**CACCAGTGAGACGGGCAACAGCTGATTGCCCTT**CACCGC**  
**CTGGCCCTGAGAGAGTTGCAGCAAGCGGTCCACGCANN**

3.5.4. Left border/reverse:

NTCGGGCANATTTGCTGCTGAGTGGACCGGCATGGATCAACATGAAGGTAG  
 AGAAGCTGCGTGAACGTCAAATGATAATGAAGGCTTCAATCATCTTCAGT  
 CTCCATCCTCTCCATCCTCCTATGTTTATTTGTTTGCATGCCAACCTTTCATC  
 AAAATTAAGTTTATTATAACATTTACCAAACACTGACACTTCCATGCATCTA  
 TATAAAGAAGTTCACAAAATATCCAAAACCAAGTTTTAAAGAAAAATAGTC  
 GTCAAAAATTAGCACTTCATGAGATTTAATAGGACATCATAAATAAAGTAA  
 TTACCCCATGGCAAGAGCTGTGATAGCCCAT**TGACGCTTAGACA**ACTTAA  
**TAACACATTGCGGACGTTTTTAATGTACTGGGGTGGTTTTTCTTTT**CAC  
**CAGTGAGACGGGCAACAGCTGATTGCCCTT**CACCGCCTGGCCCTGAGA  
**GAGTTGCAGCAAGCGGGTCCACGCANN**

### 3.5.5. Northern blot confirmation of the silencing of *AtPM19* gene expression:

Although it was confirmed that *AtPM19* gene has a T-DNA insertion, in order to confirm there is no expression of the gene, *AtPM19* mRNA must not appear in a northern blot.

After extracting the RNA from wild type and mutant *atpm19* seeds and running the samples in an RNA denaturing gel the RNA samples were seen to be of good quality. Then the gel was blotted on a membrane, and hybridized to a digoxigenin labelled antisense RNA probe. After incubation with an alkaline phosphatase conjugated anti digoxigenin antibody, *PM19* mRNA was detected on an X-ray film. The wild type RNA sample showed an approximately 1000 b band while the mutant *atpm19* showed no band confirming the silencing of the *AtPM19* gene (Figure 31).

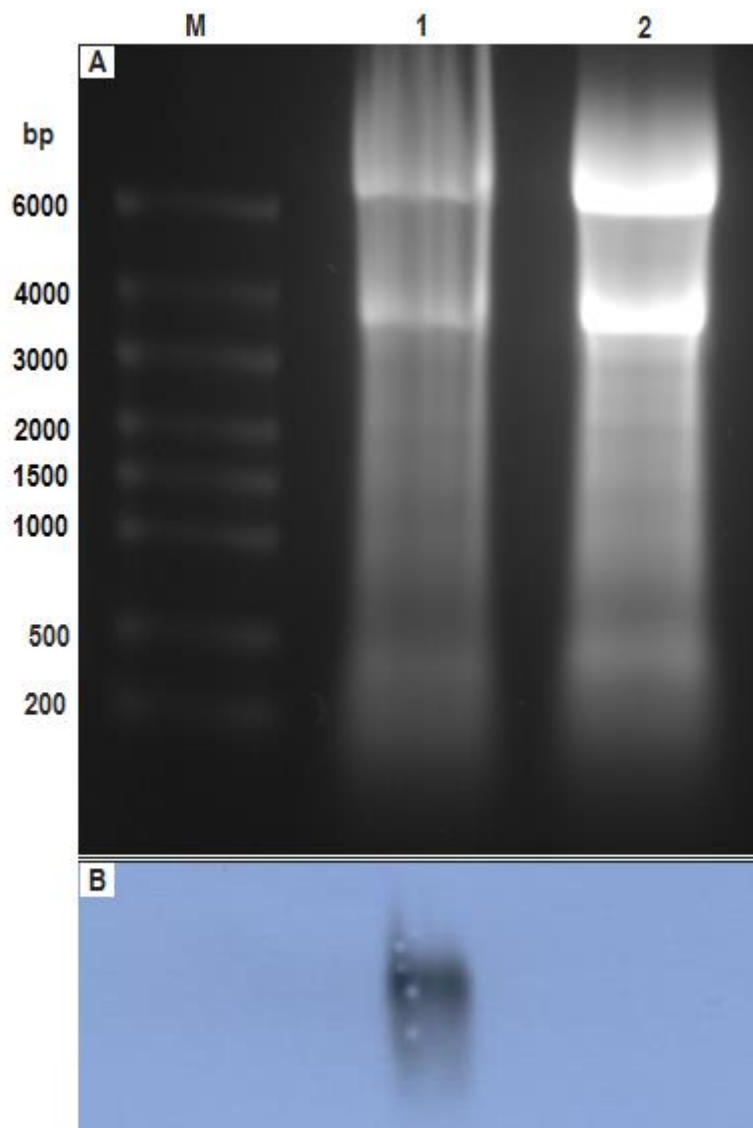


Figure 31: Northern blot for RNA extracted from wildtype and *atpm19* mutant from seeds. Wells M, 1, and 2 are RNA ladder, wildtype and mutant *AtPM19* respectively. A) Shows ethidium bromide stained RNA denaturing gel while B) is the X-ray film. The band under the wildtype shows that *AtPM19* was detected in wildtype seed RNA. No bands are seen for the mutant *atpm19* confirming that *AtPM19* RNA is not expressed in the mutant seeds.

#### 3.5.6. Overexpression of *AtPM19* gene:

In order to help understanding the role of PM19 protein it is essential to make sure that the protein is expressed all the time. This can be achieved by controlling the expression of *AtPM19* by a The CaMV 35S promoter as it is a very strong constitutive promoter. The plasmid of choice was PbinAR as it contains the 35S promoter and it is a binary vector (i.e. it can replicates in two hosts *E. coli* and *Agrobacterium*). The plan of the

cloning is explained in Figure 32. A PCR confirmation was carried out showing that the gene was successfully transferred to *Arabidopsis* plants (Figure 33). When the expression of 35S-*AtPM19* was analysed by northern blot (Figure 34) it detected no signal for the 35S-*AtPM19*. However, the expression of 35S-GFP-*AtPM19* was detected. Therefore, 35S-GFP-*AtPM19* plants were used to show the overexpressed PM19.

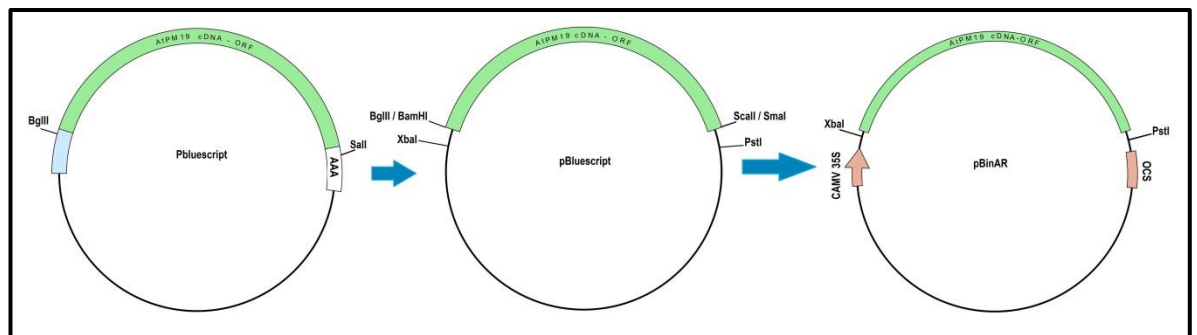


Figure 32: Cloning plan for overexpression of the *AtPM19* ORF into a binary vector. The original *AtPM19* cDNA was in pBluescript SK and has a poly(A) tail attached to the 3' end, in addition to extra nucleotides 5' to the ATG start codon. The fragment containing the open reading frame was cut with *Bgl*III and *Sca*I, which are located just to the outer sides of *AtPM19* cDNA ORF fragment. This results in obtaining the required fragment without the poly (A) tail. This fragment was ligated over the *Bam*HI and *Sca*I restriction sites in pBluescript KS plasmid vector. *Bam*HI and *Sma*I sites are compatible with *Bgl*III and *Sca*I. Then, a digestion reaction to pBluescript KS plasmid vector with *Xba*I and *Pst*I releases the *AtPM19* open reading frame. The plasmid vector pBinAR also contains *Xba*I and *Pst*I sites within the multiple cloning sites where the cDNA fragment was ligated, thus permitting expression by the CAMV 35S promoter in pBinAR.

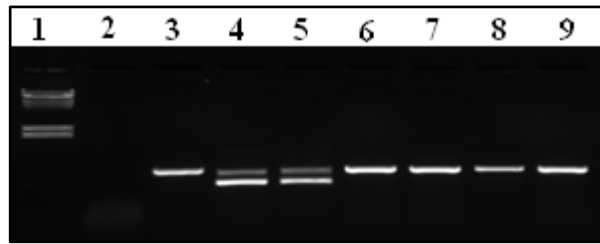


Figure 33: Confirmation of the transformed *Arabidopsis* plants with the pBinAR plasmid DNA carrying the 35S::*PM19* fragment. Primers used were: 3A and PAP986. Well 1)  $\lambda$ HindIII DNA marker. 2) Negative control. 4,5) Positively transformed plants. 3,6,7,8 and 9) not transformed plants. Wells 4 and 5 have two fragments: the upper fragment is the wildtype genomic *AtPM19*, while the lower one is the *AtPM19* cDNA transgene.

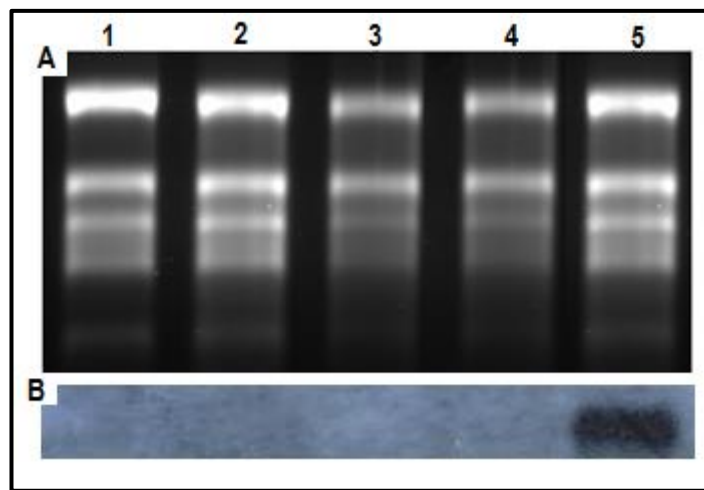


Figure 34: A) RNA denaturing gel of total RNA from leaves of different genotypes of *A. thaliana* plants. Wells are 1) WT, 2) 35S::*AtPM19*, 3) 35S::*AtPM19*, 4) 35S::*GFP* and 5) 35S::*GFP-AtPM19*.

B) DIG Northern blot of the RNA and hybridization was carried out for the testing of the expression of 35S::*AtPM19*. 1) WT, 2) 35S-*AtPM19*, 3) 35S-*AtPM19*, 4) 35S-*GFP* and 5) 35S-*GFP-AtPM19*. As can be seen, only the 35S-*AtPM19*-*GFP* RNA is expressed in the leaves. The 35S- *AtPM19* RNA is not expressed despite the gene having been successfully transformed into the plant genome.



**3.6. Physiological analysis of *AtPM19* under different abiotic stresses:****3.6.1. Analysis of the germination percentage of wildtype and *atpm19* mutants under different abiotic stresses:**

The literature shows that some  $K^+$  ion transporters in plants are plasma membrane proteins with four transmembrane domains such as the channels TWIK, TREK, TASK and TRAAK (Shieh et al. 2000). This hypothesis was the basis for designing experiments to answer whether *AtPM19* protein is an ion transporter. Germination experiment was carried out where the ion tolerance in the wild type, mutant *atpm19* and the *35S::PM19-GFP A. thaliana* genotypes was examined (see materials and methods section 10.1). One hundred seeds from each genotype were sown in different concentrations of different ions. Drought tolerance experiments were also carried out by exposing the seeds to low water availability media; for instance, seeds were grown on mannitol. Experiments that assess the effect of abscisic acid on germination were also carried out.

**3.6.2. Alkali metals**

The alkali metals,  $Na^+$ ,  $K^+$ ,  $Li^+$ ,  $Cs^+$ , and  $Rb^+$  were chosen for testing *AtPM19* protein ion transport capacity. On media containing those metals, seeds expressing *35S::PM19-GFP* showed higher germination percentage than the wild type and the mutant *atpm19*. The mutant *atpm19*, on the other hand, showed a lower germination percentage on media containing different concentrations of alkali metals. The differences in the germination percentage between the three genotypes were very clear under enhanced  $Na^+$  concentrations, but the effect is relatively small when  $K^+$  was used in the medium. The figures 35, 36, 37, 38, 39, 40, 41 and 42 show the germinations experiments on water, KCl, NaCl, Mannitol, ABA, CsCl, LiCl and RbCl respectively. Under control conditions in which agar and 0.5 MS medium alone was used, there was no difference in germination between any of the lines, with 100% germination within one week. However, on medium composed of agar and water only, all lines showed reduced

germination with *atpm19* showed a lower germination (20%) than the wildtype (60%) (Figure 35). These observations suggest that PM19 protein might have a role in cation homeostasis. The reduced germination of the mutant on water-based medium suggests that PM19 facilitates the uptake of ions during germination, perhaps in order to drive osmotic expansion of the cells during germination. However both the wild type *A. thaliana* seedlings and those seedlings containing overexpressed AtPM19 protein were able to germinate and grow even when surrounded with relatively high  $\text{Na}^+$  concentrations which the mutant PM19 protein seedlings could not tolerate, suggesting that PM19 is acting to remove  $\text{Na}^+$  from the cell. Seeds with *35S::PM19-GFP* showed a much higher ability than the wild type to germinate specifically on media containing an  $\text{Na}^+$  concentration as high as 100 mM, and *35S::PM19-GFP* seeds exposed to 150 mM of  $\text{Na}^+$  germinated almost 4 fold better than the wild type, with the mutant *atpm19* seeds showed no germination (Figure 36 and Figure 37).

Interestingly, *Atpm19* seeds showed a reduced germination percentage than the wildtype or the overexpressed line when grown in the presence of the toxic metal  $\text{Cs}^+$  (Figure 40), again suggesting that PM19 has a role in exporting cations from the cell. Although in other studies, *Arabidopsis* germination was observed when using  $\text{Li}^+$  concentrations as high as 15 mM (Bueso et al. 2007), in this study lithium was found to be lethal to all genotypes at lower concentrations such as 5 mM, with no difference between the lines (Figure 41). The *35S::PM19-GFP* seeds behaved similarly to the wild type seeds when grown on 5 mM and 10 mM  $\text{RbCl}$  with higher sensitivity of the mutant *atpm19* seeds (Figure 42), a result similar to that seen for caesium. It is worth mentioning here that rubidium is found naturally in the environment and in fact it sometimes used as an analogue for  $\text{K}^+$  to trace its absorption by the cell membranes (Läuchli and Epstein 1970).

### 3.6.3. Low water availability

In order to induce water stress, seeds were grown on different media with different concentrations of mannitol that induces osmotic stress on cells. Seeds with *35S::PM19-GFP* showed higher germination percentage than the wild type and mutant *atpm19* seeds when grown on as high as 200 mM mannitol. However, on 300 mM mannitol the *atpm19* seeds germinated two fold more than the *35S::PM19-GFP* seeds (Figure 38), thus the picture here is less clear cut.

### 3.6.4. Abscisic acid

The data from (Koike et al. 1997) show an ABA induced expression of the AWPM19 protein (the wheat AtPM19 protein homologue), thus germination of Arabidopsis on different concentrations of ABA was carried out to obtain evidence on the role of the AtPM19 protein with respect to ABA. The seeds containing *35S::PM19-GFP* showed a germination percentage of more than the double of the wild type seeds on low ABA concentrations. The concentration of 0.5  $\mu$ M ABA, however, was enough to decrease the germination percentage of all of the genotypes to below 10% (Figure 39).

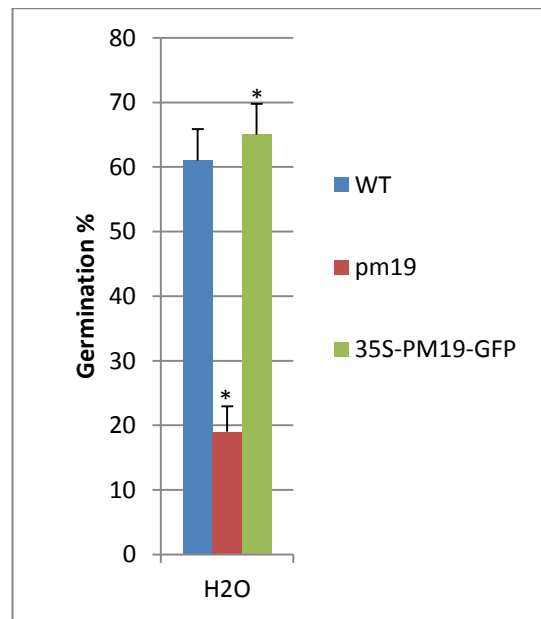


Figure 35: Germination percentage of wild type, mutant *atpm19* and *35S::PM19-GFP* seeds on media containing H<sub>2</sub>O. Seeds containing *35S::PM19-GFP* germinated more than the wild type while the germination percentage of mutant *atpm19* seeds was the third of the wild type. Since this is a binomial distribution, the error bars was based on the standard error of the germination percentage using this formula  $\sqrt{(pq/n)}$ , where  $p$  is percentage of germinated seeds  $q$  is the percentage of not germinated seeds and  $n = 100$ . (\*) Means there is a significance difference between the two genotypes based on Chi-squared test. Chi-squared formula is  $(O - E)/\sqrt{E}$ , where  $O$  is the Observed value and  $E$  is the expected value. If the result is  $\geq \pm 2$  then there is a significant difference.

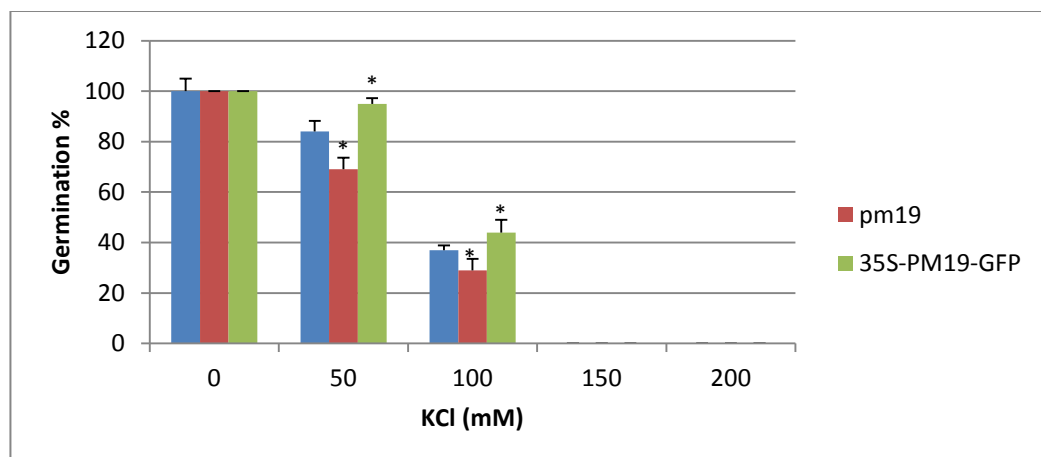


Figure 36: Germination percentage of wild type, mutant *atpm19* and *35S::PM19-GFP* seeds on media containing different concentrations of KCl. Seeds containing *35S::PM19-GFP* germinated more than both the wild type and the mutant *atpm19*

seeds. Since this is a binomial distribution, the error bars was based on the standard error of the germination percentage using this formula  $\sqrt{(pq/n)}$ , where  $p$  is percentage of germinated seeds  $q$  is the percentage of not germinated seeds and  $n = 100$ . (\*) Means there is a significance difference between the two genotypes based on Chi-squared test. Chi-squared formula is  $(O - E)/\sqrt{E}$ , where  $O$  is the Observed value and  $E$  is the expected value. If the result is  $\geq \pm 2$  then there is a significant difference.

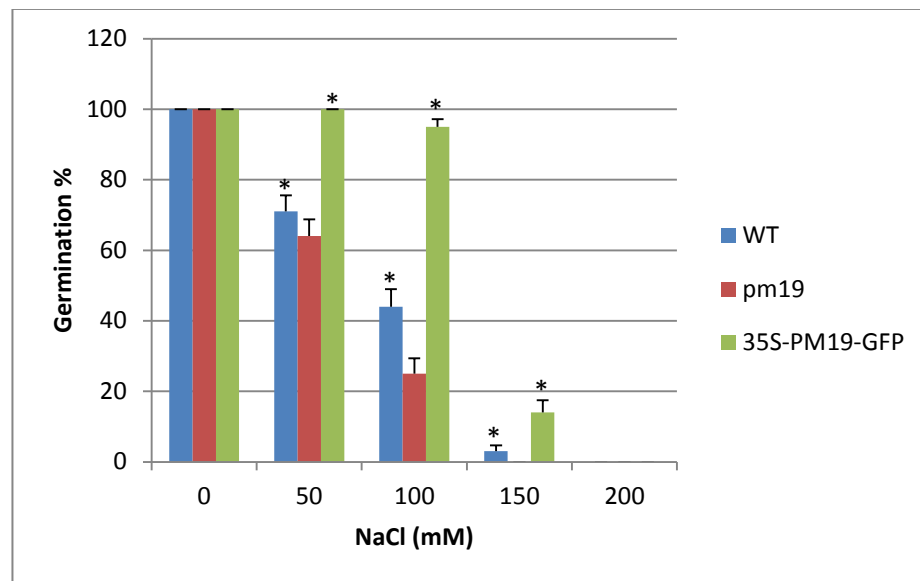


Figure 37: Germination percentage of wild type, mutant *atpm19* and *35S::PM19-GFP* seeds on media containing different concentrations of NaCl. Seeds containing *35S::PM19-GFP* show higher germination percentage than the wild type and mutant *atpm19* seeds showed lower germination. Since this is a binomial distribution, the error bars was based on the standard error of the germination percentage using this formula  $\sqrt{(pq/n)}$ , where  $p$  is percentage of germinated seeds  $q$  is the percentage of not germinated seeds and  $n = 100$ . (\*) Means there is a significance difference between the two genotypes based on Chi-squared test. Chi-squared formula is  $(O - E)/\sqrt{E}$ , where  $O$  is the Observed value and  $E$  is the expected value. If the result is  $\geq \pm 2$  then there is a significant difference.

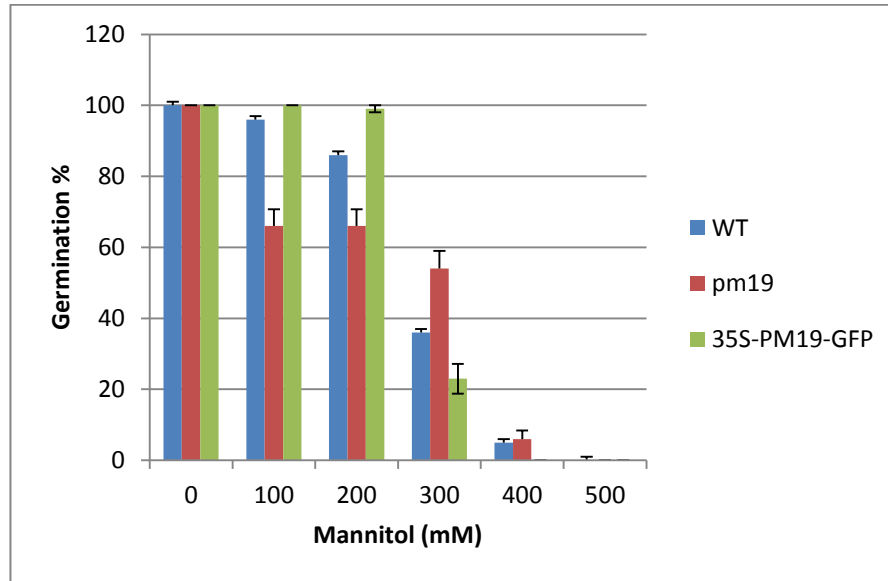


Figure 38: Germination percentage of wild type, mutant *atpm19* and *35S::PM19-GFP* seeds on media containing different concentrations of mannitol. Seeds containing *35S::PM19-GFP* show higher germination percentage than the wild type as well as the mutant *atpm19* seeds on media containing mannitol concentrations of 100 mM and 200 mM. However, when grown on 300 mM mannitol the germination of *atpm19* seeds double of the germination of *35S::PM19-GFP* seeds. Since this is a binomial distribution, the error bars was based on the standard error of the germination percentage using this formula  $\sqrt{(pq/n)}$ , where  $p$  is of germinated seeds,  $q$  is the percentage of not germinated seeds and  $n = 100$ .

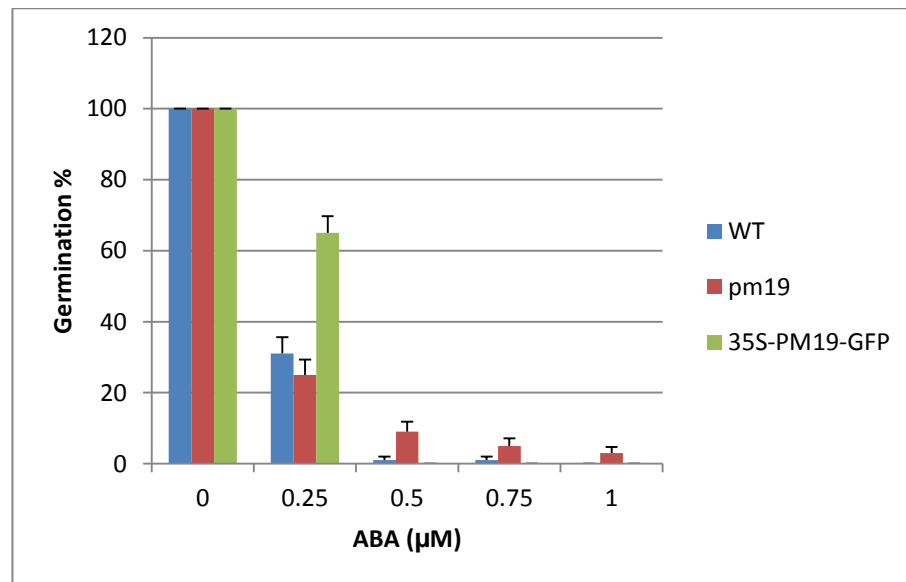


Figure 39: Germination percentage of wild type, mutant *atpm19* and *35S::PM19-GFP* seeds on media containing different concentrations of ABA. Seeds expressing *35S::PM19-GFP* show higher germination percentage than the wild type and mutant *atpm19* seeds on plant media containing ABA concentration of 0.25 μM. However, when grown on 0.5 μM ABA and higher the germination percentage of all lines was very low. Since this is a binomial distribution, the error bars was based on the standard error of the germination percentage using this formula  $\sqrt{(pq/n)}$ , where  $p$  is percentage of germinated seeds  $q$  is number of not germinated seeds and  $n = 100$ .

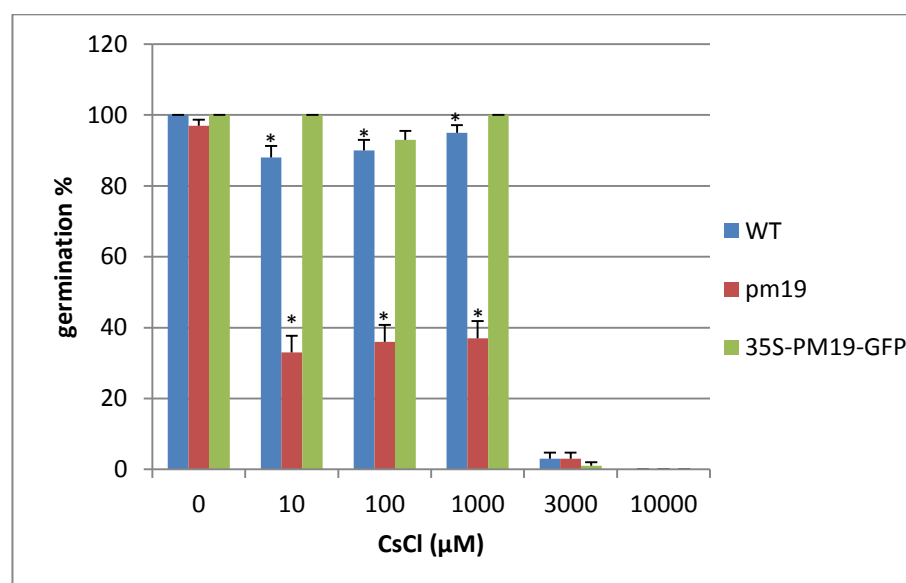


Figure 40: Germination percentage of wild type, mutant *atpm19* and *35S::PM19-GFP* seeds on media containing different concentrations of CsCl. Seeds containing *35S::PM19-GFP* showed higher germination percentage than the wild type as well as

the mutant *atpm19* seeds. Since this is a binomial distribution, the error bars was based on the standard error of the germination percentage using this formula  $\sqrt{(pq/n)}$ , where  $p$  is percentage of germinated seeds  $q$  is the percentage of not germinated seeds and  $n = 100$ . (\*) Means there is a significance difference between the two genotypes based on Chi-squared test. Chi-squared formula is  $(O - E)/\sqrt{E}$ , where  $O$  is the Observed value and  $E$  is the expected value. If the result is  $\geq \pm 2$  then there is a significant difference.

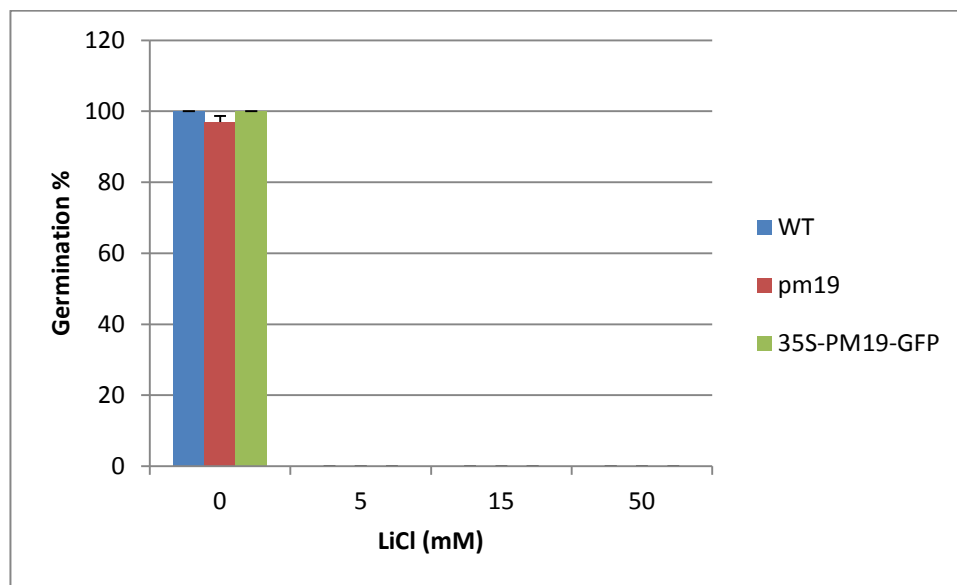


Figure 41: Germination percentage of wild type, mutant *atpm19* and *35S::PM19-GFP* seeds on media containing different concentrations of LiCl. All seeds of the different genotypes showed no germination when grown on 5 mM LiCl and above. Since this is a binomial distribution, the error bars was based on the standard error of the germination percentage using this formula  $\sqrt{(pq/n)}$ , where  $p$  is percentage of germinated seeds  $q$  is number of not germinated seeds and  $n = 100$ .



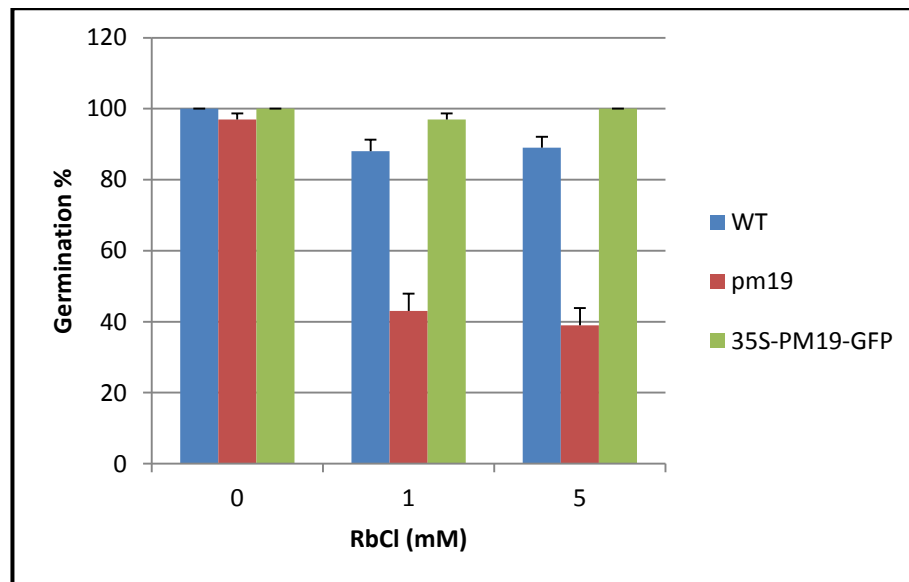


Figure 42: Germination percentage of wild type, mutant *atpm19* and *35S::PM19-GFP* seeds on media containing different concentrations of RbCl. Germination percentage of wild type and *35S::PM19-GFP* seeds showed similar germination percentage. However, the mutant *atpm19* seeds were more sensitive. Since this is a binomial distribution, the error bars was based on the standard error of the germination percentage using this formula  $\sqrt{(pq/n)}$ , where  $p$  is percentage of germinated seeds  $q$  is number of not germinated seeds and  $n = 100$ .

### 3.6.5. Stomatal conductancy:

Germination experiments showed that the plants that overexpressed *AtPM19* were able to show higher germination percentages on high concentrations of sodium chloride (Figure 37) and potassium chloride (Figure 36) and on mannitol (Figure 38). In addition, *AtPM19* gene expression was observed on *Arabidopsis* leaves that were exposed to drought (Figure 23). It is also reported that  $K^+$  concentration of the guard cell has a major role on the opening and closure of the stomata (Roelfsema and Hedrich 2005). Collectively, this suggests that the *AtPM19* protein might have a role as an ion transporter and in turn help on the opening and closure of the stomata. In order to investigate this possibility, stomatal conductance was measured in plants with differing levels of *AtPM19* expression whilst undergoing drought stress.

Under both conditions; normal watering and drought, the highest stomatal conductancy observed (i.e. greatest extent of stomatal opening) was on the *35S::PM19-GFP* plants. The mutant *atpm19*, however, showed the least conductance when exposed to drought. The readings for the stomatal conductancy were taken as explained in the instructions for the instrument, however, there were high fluctuation in the readings. Never the less, the differences in mean conductancy between control and drought was significantly different between the wildtype and the overexpression lines.

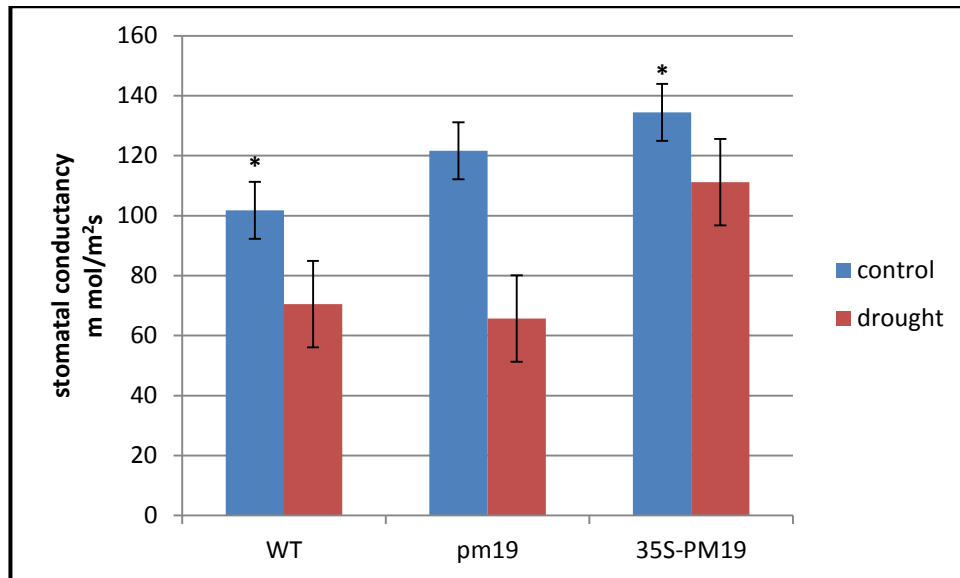


Figure 43: Stomatal conductance of wildtype, mutant *atpm19* and *35S::PM19-GFP* plants under normal watering and drought conditions. The conductance is lower in drought conditions as the stomata apparatus close the passage of water. The mutant *atpm19* plants show the lowest conductance rate in drought conditions when compared with the wild type and the *35S::PM19-GFP* plants while the *35S::PM19-GFP* conductance was the highest. Analysis of variance of all the readings showed a significance difference between the wild type and the *35S::PM19-GFP* plants when watered normally ( $p < 0.05$ ). The error bars based on standard errors ( $n = 5$ ).

3.6.6. Analysis of leaf weight loss:

One of the physiological phenotypes was the leaf weight loss over a period of time to obtain answers on whether PM19 has an effect on the cells' capacity to withhold water. The weights of the leaves of the three genotypes were measured at time 0 then every 30 minutes over 6 hours. The linear regression trend lines show that the overexpressed plants have a slightly more tendency to resist water loss than the wild type and the mutant *pm19* (Figure 44).

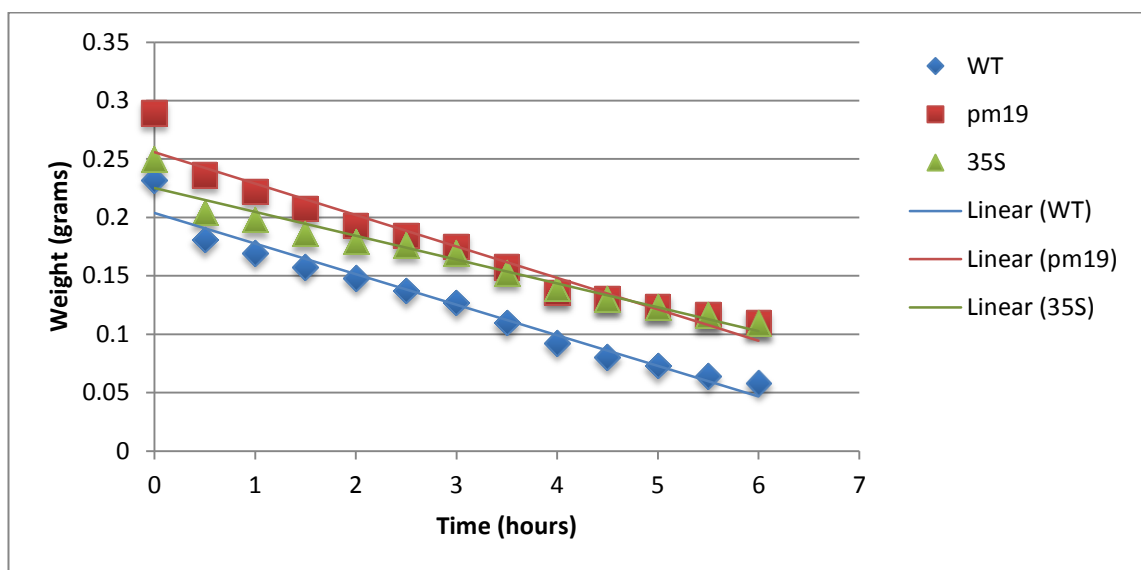


Figure 44: leaf weight loss over 6 hours. There was no significant difference on the weight loss rate between the wild type, the mutant *atpm19* and the *35S::PM19-GFP* leaves.

### **3.7. Yeast functional complementation:**

Although the results of the germination experiments gave an idea about the function of PM19 protein, the absolute function has not been answered at yet. A yeast mutant functional complementation approach was chosen to answer that query. (Bertl et al. 2003) worked on yeast mutants that exhibit changes in potassium uptake. In this study it was attempted to recover the loss of function by insertion of *AtPM19* in those mutants. Although the yeast strains used in this project WT (ply343), *trk1Δ* (PLY234) and *tok1Δ* (PLY238) were obtained by personal communication with (Bertl et al. 2003), yeast mutants are also available in database centres such as the Saccharomyces Genome Database (SGD). Functional complementation can be explained as an attempt to recover the lost function of a known gene or genes due to a mutation by the insertion of a gene of an unknown function. This approach helps to identify the function of PM19 protein.

#### **3.7.1. Cloning of *AtPM19* into yeast plasmid vector**

The original *AtPM19* cDNA was in pBluescript SK and has a poly(A) tail attached to the 3' end, in addition to the 3' and 5' untranslated region. This needs to be removed prior to expression in yeast. The fragment was cut with *Bgl*III and *Sca*I, which are located just to the outer sides of *AtPM19* cDNA fragment. This results in obtaining the required fragment without the poly(A) tail. The plasmid yeast expression vector used to insert the gene encoding *AtPM19* protein was pYES2, containing URA3 gene as a selectable marker for yeast and a galactose inducible promoter. A digestion reaction of the pBluescript SK plasmid vector containing *AtPM19* with *Xba*I and *Bam*HI released the *AtPM19* cDNA. The yeast vector pYES2 also contains *Xba*I and *Bam*HI sites within the multiple cloning sites where the cDNA fragment can be ligated.

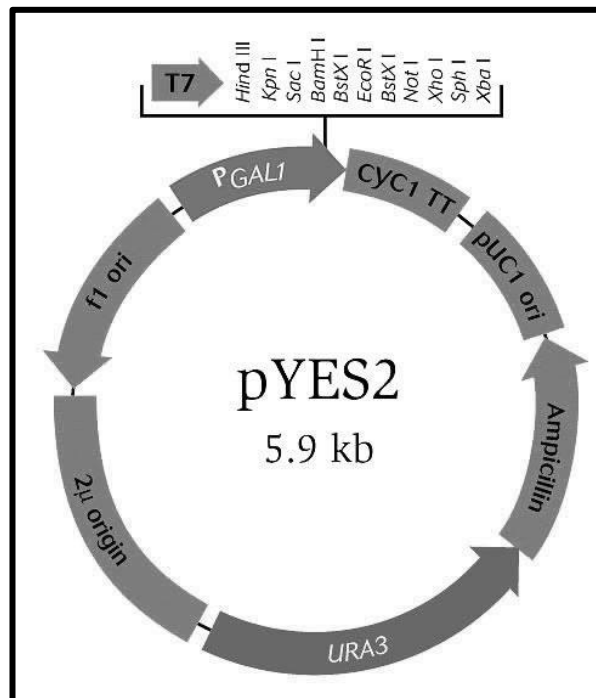


Figure 45: The plasmid vector used to insert *AtPM19* cDNA into. The plasmid contains the selectable marker *URA3* for selection in yeast. Obtained from <https://products.invitrogen.com/ivgn/product/V82520> on 29/4/2013

3.7.2. Confirmation of pYES2-PM19 cloning [digestion with *Xba*I+*Bam*HI]:

After the construct been made and transformed into *E. coli*, 13 colonies were picked and grown in LB broth separately then plasmid minipreps were carried out to test the construct by endonuclease digestion. There is a unique site for each of *Bam*HI and *Xba*I sites in the construct that contains pYES2 and *AtPM19*. By doing a digest reaction using *Bam*HI and *Xba*I endonuclease enzymes the *AtPM19* cDNA fragment (561 bp) dropped from the construct as shown below in Figure 46.

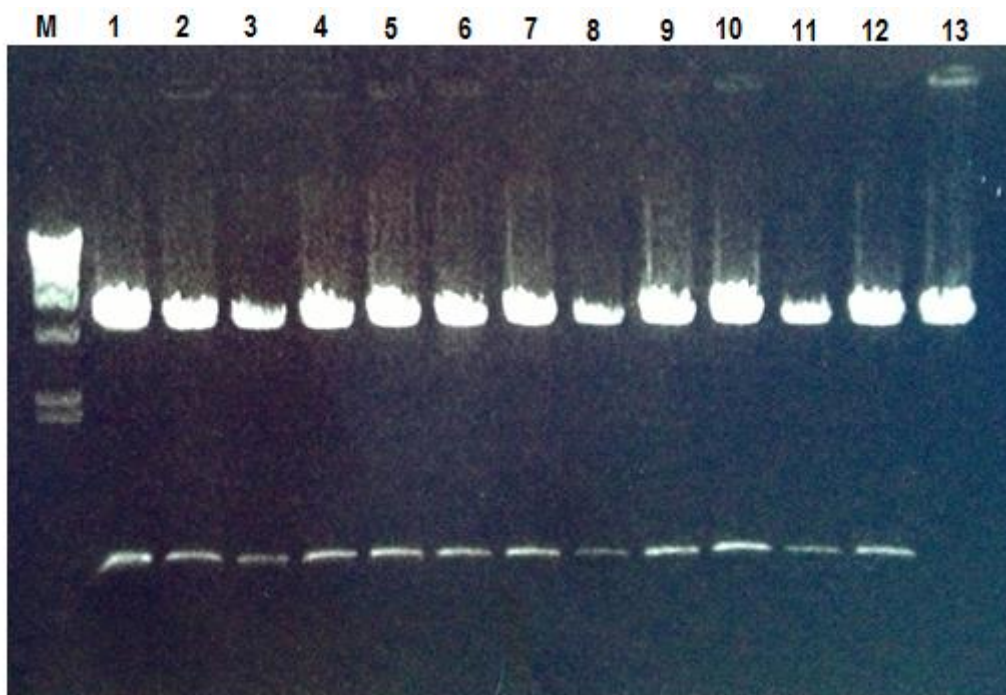


Figure 46: a photo of a DNA gel electrophoresis showing DNA fragments of YES2-*AtPM19* construct after digestion with *Xba*I and *Bam*HI. (M) is  $\lambda$ HindIII DNA ladder, wells from (1) to (13) are the digestion reaction products. The upper fragment (5.9 kb) is pYES2 while the smaller fragment (561 kb) is the *AtPM19* cDNA. This confirms that PM19 was inserted successfully into pYES2 plasmid vector.

### 3.7.3. Transformation of the yeast vector pYES2 containing *AtPM19* into yeast strains:

Then the YES2-*AtPM19* construct was transformed into the yeast strains by electroporation transformation (see materials and methods section 13.2).

### 3.7.4. Yeast in SDAP media containing 75 mM NaCl pH 5.8:

A number of experimental trials were carried out to screen for the potassium phenotype of the yeast mutants to help understand the role of *AtPM19* protein. The SDAP media as outlined by (Bertl et al. 2003) was used with K<sup>+</sup> content as low as 0.1 mM KCl, but there was no growth was obtained (Figure 47-A). Bertl et al (2003) showed that *trk1* do not grow on SDAP media containing potassium lower than 0.1 mM. It was expected that cloning *AtPM19* into the yeast strains used by (Bertl et al 2003) can recover the loss of growth. Since the results obtained from the germination experiments showed a distinctly high germination percentage of the wild type seedlings and those seedlings containing *35S::PM19-GFP* on high concentrations of NaCl, 75 mM NaCl was added in SDAP media to grow the wild type, *trk1* and *trk2* yeast mutants with and without *AtPM19* gene. The mutant yeast cells and the mutant yeast containing the pYES2 vector were tested to confirm if there are no nonspecific phenotypes. The control yeast mutants cells along with the YES2-*AtPM19* construct were diluted into four dilutions ( $10^0$ ,  $10^{-1}$ ,  $10^{-2}$  and  $10^{-3}$ ) then spotted on the media and incubated at 28 °C for 3-5 days (Figure 47). There was no growth of the *trk1*, nor the *trk1*-pYES2 strain on SDAP media containing 0 mM KCl, 75mM NaCl and pH 5.83 (see Figure 47-B), however when *AtPM19* was inserted, *trk1* containing *AtPM19* showed recovery of the loss of growth of yeast *trk1* mutant. This suggests that *AtPM19* is a possible sodium ion outward transporter.



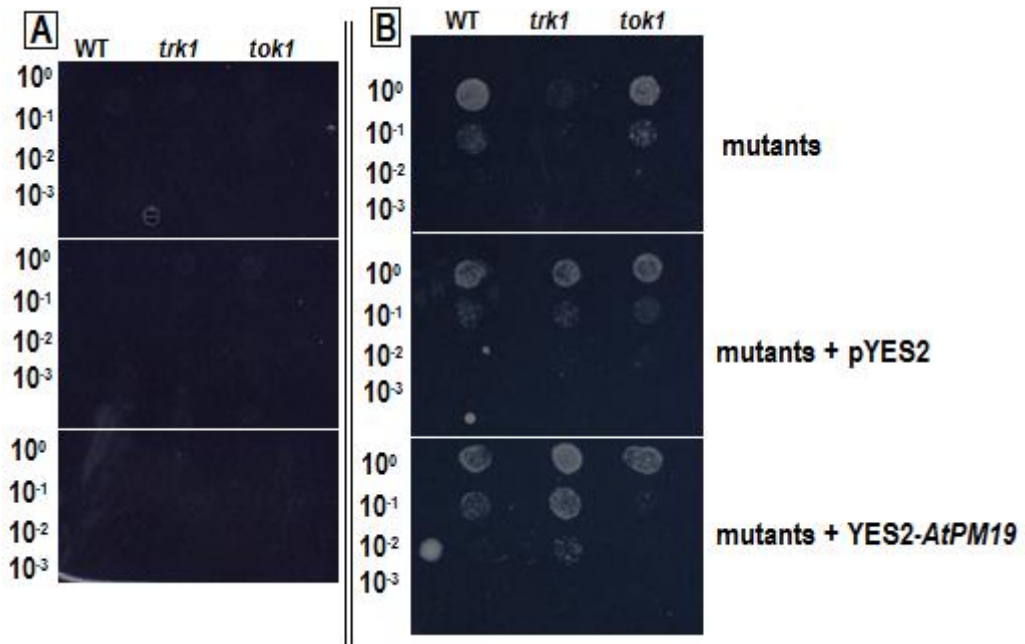


Figure 47: (A): WT yeast, *trk1* and *tok1* mutants, mutants with pYES2 vector and with YES2-*AtPM19* were diluted to  $10^0$ ,  $10^{-1}$ ,  $10^{-2}$  and  $10^{-3}$  then spotted on SDAP media containing 0 mM KCl at pH 5.83. The wild type as well as the mutants did not show any growth and the presence of the *AtPM19* gene did not change growth of the yeast mutants. (B): A combination of WT, *trk1* and *tok1* mutants, mutants with pYES2 vector and mutants with YES2-*AtPM19* were diluted to  $10^0$ ,  $10^{-1}$ ,  $10^{-2}$  and  $10^{-3}$  then spotted on SDAP media containing 0 mM KCl and 75mM NaCl pH 5.83. The loss of growth shown by *trk1* mutants was recovered by expression of the *AtPM19* gene. This indicates that *AtPM19* may have a role in  $\text{Na}^+$  outward transport.

**CHAPTER 4: DISCUSSION**

**4. DISCUSSION:**

The findings presented in this thesis on the *A. thaliana* PM19 protein are discussed in this chapter. Specifically the molecular characterisation, the effect of alkali metals on the *pm19* knockout and PM19 overexpression plants and the functional complementation on yeast mutants are discussed and analysed.

**4.1. Molecular characterization of the *A. thaliana* PM19 gene and its expression:**

Koike and his team (1997) were the first to characterise the PM19 protein. This was when they showed that there is an accumulation of a 19 kDa plasma membrane protein in wheat cell culture when freezing tolerance was induced by ABA treatment.

In these experiments the suspension cultured cells obtained from winter wheat (*Triticum aestivum*) immature embryos were treated with ABA for 7 days then freezing tolerance was measured by measuring the electrolytes leakage from frozen and thawed cultures. The cultures that were treated with 50  $\mu$ M ABA showed the highest freezing tolerance. A comparison of expression patterns of plasma membrane proteins from the wheat cultures in the presence and absence of ABA showed that the highest intensity increase for the membrane proteins was observed for a 19 kDa polypeptide. Further analysis of this protein revealed that it is an integral plasma membrane protein, which was purified and the N-terminal amino acid sequence was determined, which allowed the cDNA to be cloned. A hydropathy plot of the winter wheat 19 kDa (AWPM-19) amino acid sequence showed that the protein is a putative integrative membrane protein with 4 transmembrane domains, suggesting that it might be involved in what they described as "ionic interaction", but exactly what was meant by this is not clear (Koike et al. 1997).

The comparison of the amino acid sequence of AWPM-19 with its close homologue in soybean revealed that 60.8% of the amino acids were identical. The similarity between the two species, AWPM-19 and the soybean GmPM3 protein, suggested that is not a

protein that is specific to monocotyledonous plants but present also among dicotyledonous plant species as well (Koike et al. 1997). Although Koike et al. (1997) deduced a structure for the AWPM-19 protein (four transmembrane domain protein), however, their findings did not suggest a particular function of AWPM-19.

Ranford et al. (2002) carried out a study to isolate embryo genes associated with dormancy in dormant oat. By screening the dormant wild oat embryo cDNA library with cDNA made from dormant and non-dormant barley mRNA so as to pick out differentially expressed conserved sequences, one of the detected oat clones showed a homology to the *AWPM-19* isolated by (Koike et al. 1997). Further analysis of a full-length barley cDNA and its deduced amino acid product showed 92.8% identity to the wheat PM19 protein. It also showed high homology with amino acid sequences encoded by clones obtained from dry seeds of *Arabidopsis thaliana* (clone *PAPIII*), rice embryos (*Oryza sativa*) and immature soybean cotyledons (*Glycine max*). Ranford et al. (2002) found no further similarities with other protein or DNA sequences in the databases (Ranford et al. 2002). Although neither of the works of Koike et al. (1997) and Ranford et al. (2002) established a function for PM19, however, assumptions can be made from their findings. For instance, the conservation of the protein in different plant species can indicate the inherent and evolutionarily conserved significance of PM19 to plant physiology. Moreover, the findings of Koike et al. (1997) that the expression of PM19 increased when cells were exposed to 50  $\mu$ M ABA then showed maximum freezing tolerance suggest that the expression of PM19 is associated with the tolerance of abiotic stress and low water availability. In addition, the findings of Ranford et al. (2002) that PM19 is expressed more during embryo development and germination argue for a role in desiccation tolerance, or the mechanisms associated with water uptake or ionic homeostasis during germination. Since the protein sequence is also highly conserved in

the model plant *Arabidopsis*, this meant that the tools and resources afforded by *Arabidopsis* could be used to investigate the function of this highly conserved membrane protein.

Investigation of protein functions can be conducted by different tools. For example, studies such as (Shi et al. 2002) showed that *SOS1* (a plasma membrane sodium export protein) has been investigated using number of biotechnological investigation tools. For instance, the subcellular location of the putative plasma membrane protein was studied using translational fusion with GFP in addition to transcriptional fusion of the subject protein promoter with GUS. Moreover, Shi et al. (2002) carried out a complementation of the *Saccharomyces cerevisiae* Na<sup>+</sup> and K<sup>+</sup> transport mutants (*nha1*, *nhx1*, *trk1* and *trk2*). When these were grown on arginine phosphate medium containing 70 mM NaCl, the *nha1 nhx1* double mutant yeast cells did not grow, However, when the *SOS1* gene was expressed in those mutants it was able to recover the loss of function indicating it is functional as an Na<sup>+</sup> efflux protein (Shi et al. 2002).

More recently, in order to study the mechanisms that mediate plant copper (Cu) distribution, Gracia-Molina et al. (2013) carried out functional complementation of yeast mutants lacking genes responsible for high-affinity copper transport. The gene *COPT6*, a member of the conserved family of CTR/COPT Cu transport proteins in *Arabidopsis* that are responsible for Cu distribution, was able to recover the loss of growth phenotype in the *ctr1Δctr3Δ* yeast strain that lacks high-affinity Cu transport at the plasma membrane. This finding indicates that *COPT6* is a Cu transporter in *Arabidopsis* (Garcia-Molina et al. 2013). Thus complementation of yeast mutants can be a powerful means of establishing function of plant genes.

In this thesis, a BLAST search of the *A. thaliana* PM19 amino acid sequence was carried out to find out closely related homologues. The cut-off value for highly similar

sequences was those that have a query cover value of  $\geq 50\%$  and an identity of  $\geq 60\%$ . This resulted in 19 different species only from the plant kingdom being picked out, all of which were terrestrial plants belonging to gymnosperms - such as conifers - and angiosperms (flowering plants) such as rice (*Oryza sativa*) and soybean (*Glycine max*). Thus PM19 is not represented in the animal kingdom, nor in the bacteria or archaea. Despite being present in representatives of the major plant groups, it is not found in any of the algae that have been fully sequenced (Turmel et al. 1999).

For further bioinformatics analysis, five amino acid sequences were chosen to represent the major plant groups. The represented groups are flowering plants (angiosperms), pines (gymnosperms), club mosses (lycopsids) and mosses (bryophytes). A protein sequence alignment of the PM19 protein homologues found in those groups was undertaken to understand the degree of conservation of PM19 protein over evolutionary time. These findings are in agreement with (Koike et al. 1997), the conclusion is that the AWPM-19 is a protein common to monocots and dicots in higher plants, but not found elsewhere in living organisms.

Furthermore, the PM19 protein sequences alignment showed that it is highly conserved in all of these plant groups. Algae (generally aquatic plants) existed 200 million years before the existence of terrestrial plants (Smith et al. 2010). Terrestrial plants, such as mosses, conquered the land more than 400 million years ago. The amino acid sequence alignment of the AtPM19 protein along with its number of homologues from plant species representing major groups of the plant kingdom all show high homology to each other over the core transmembrane domains but the homology breaks down at the C terminal domain. However, no homologues were found in algae. This shows that not only that the PM19 protein is highly conserved throughout plant evolution for over four hundred million years, but also suggests that AtPM19 may have a vital role in the plant

ability to survive in water-deficient environments, since algae are associated with aqueous environments and the groups with PM19 are predominantly land plants. Such a role might be for example involved in the uptake of essential nutrient for plant development or associated with the adaptation with low water availability, as for example in seed desiccation. It is of note that the C terminal portion of the PM19 protein is variable in length, is not conserved and has no discernible structural features. Nevertheless, all of the PM19 proteins do have a C terminal domain, suggesting that such a domain is required for the function of the protein, but this function may be structural in nature rather than playing an active physiological role of some kind.

The BLAST search also showed two other amino acid sequences in *Arabidopsis* that are homologous to PM19 (AT5G18970 and AT1G29520). An amino acid multiple sequence alignment analysis using the online PRALINE sequence analysis programme (<http://www.ibi.vu.nl/programs/pralinewww/>) showed that those two amino acid sequences are also highly similar in terms of their secondary structure. For example, all of the three proteins have four alpha helix regions in a very similar location in the amino acid sequence. This suggests that PM19 is actually represented by a small (3) gene family in *Arabidopsis*.

However, bioinformatics data from publically available microarray experiments on the eplant browser (<http://bar.utoronto.ca/eplant/>) (Toronto 2013) showed that the *AtPM19* homologue gene (AT5G18970) is expressed in the ovary tissues rather than in the seeds as in the subject protein of this study. The third homologue gene in *A. thaliana* (AT1G29520) is found to be expressed in the epidermis of the stem. There might be a link between *AtPM19* and the protein encoded by gene (AT5G18970) since the ovary is where the seed is produced. However, more investigation of mutants in those genes is needed to understand if there might be a functional relation between them.

The hydrophathy plot for the AtPM19 amino acid sequence that was carried out in this study suggests that the protein is a membrane protein with 4 transmembrane domains which is in consistence with the conclusions of Koike et al. (1997) obtained from AWPM-19. The four transmembrane spanning topology of AtPM19 is a feature of number of different proteins such as the vacuolar potassium (VK) channels that belongs to the tandem-pore K<sup>+</sup> (TPK) channel family (Ward et al. 2009, Chen et al. 2008).

Potassium ion channels contain ion conduction pore loops. Those pore loops are short polypeptide chains that loop into one side of the membrane. The ion conduction pore loops of potassium channels share a common feature that they contain GYG sequence at the end of the channel's loop (Ward et al. 2009). Since this conserved GYG sequence is not found in AtPM19 this suggest that AtPM19 is not a conventional potassium ion channel.

As far as the amino acids sequence alignment of PM19 proteins homologues (Figure 9), it shows high conservation in a wide region within the amino acid sequences with many conserved amino acids indicating that the locations of the amino acids are functionally significant rather than simply complying with the required structural requirements for a hydrophobic transmembrane domain. In addition, since the level of conservation is highest within the putative transmembrane domains rather than the connecting sequences, this is indicative that the key to the function of PM19 lies within the four transmembrane domains. Furthermore, the hydrophobicity alignment of the PM19 protein homologues shows that they maintain four very similar hydrophobic regions in their amino acid sequences (explained in more detail in section 1 of the results chapter). Since hydrophobic amino acids must be within the membrane domain to avoid contact with water, the reason of the location of these conserved amino acids is likely to be to anchor the protein sequence in its location.



Koike et al. (1997) have obtained the full cDNA sequence after the first thirty-six N-terminal amino acid sequence was determined. Since this N-terminal amino acid sequence was obtained from the mature protein within the membrane and is conserved in all of the aligned PM19 homologues, this indicates that the signal sequence is retained and not cleaved after the translation of the protein and translocation to its target location in the plasma membrane of the cell.

**4.2. AtPM19 protein localisation:**

Bioinformatic prediction of AtPM19 protein location in the cell using the bioinformatics tool PSORT showed a certainty of 0.640 out of 1 that AtPM19 protein is located in the plasma membrane as compared to a certainty of 0.460, 0.370 and 0.100 for Golgi body, ER membrane and ER lumen respectively. This prediction is backed up by experimental evidence as follows.

Koike et al. (1997) gave tangible evidence that PM19 is a possible integral plasma membrane protein after washing the membrane preparation with salt and finding that it is not soluble. In this study, the location of a GFP fusion version of the protein in the cell was determined by confocal microscopy. After the successful transformation of the *35S::AtPM19-GFP* construct - made by (Pons 2005) - into *A. thaliana* wild type Columbia (0) plants, AtPM19 protein was observed under confocal microscope to be expressed in the plasma membrane of the plant cells. The control *35S::GFP* containing tissues showed fluorescence in the nucleus in addition to the cytosol (see Figure 25 and Figure 26 in the results chapter). These observations confirm that the subcellular location of the PM19 protein is in the plasma membrane of the plant cell, and not in the cytosol or in any of the cellular organelles.

So far, these findings show that AtPM19 is very likely to be expressed in the plasma membrane of the cell. However, the orientation of the N-terminus of the protein (intracellular or extracellular) is not yet clear. This orientation might be determined by using *A. thaliana* protoplast cells containing *35S::AtPM19-GFP* along with protoplast cells from the wild type *A. thaliana* and as a control, *A. thaliana* containing *35S::GFP*. The protoplast cells could be treated with 50 µg/ml of proteinase K to degrade the protein residue in the outer side of the protoplast. Then, proteinase K would be deactivated by adding (0.5 mM) of PMSF and incubating the sample at 70 °C for 5 min.

After fractionating the protein in a 1 dimensional SDS-PAGE gel, western blotting of the gel on a nitrocellulose membrane and hybridization of the membrane with an antibody directed against GFP would be carried out. If GFP on the C terminal of the protein is on the exterior of the cell, it would be destroyed by Proteinase K, whereas if the C terminal were to be intracellular, GFP would be protected from proteolysis.

As far as the stage of the expression of AtPM19 in terms of plant development and in terms of the location in the plant tissues, the online data base (Hruz et al. 2008) that is based on microarray studies showed that *AtPM19* is expressed in seeds, seedlings and in mature leaves under drought stress. However, this needed further *in vivo* confirmation studies. The expression investigation in this study using transgenic *A. thaliana* seeds containing the *AtPM19 promoter:GUS* construct showed high GUS activity in seeds and seedlings. This GUS activity was even observed in the root tip of seedlings of the age of 11 days, but it is not clear if this is residual GUS or new activity, as GUS is a very stable protein and might be retained in cells for a period of time. The GUS activity was not detected in the mature leaves in seedlings of 11 days in plant media. However, when the mature plants were subjected to drought, low levels of GUS activity was seen in the leaves (see the section number 3.3 PM19 expression pattern in the results chapter). These observations are in consistence with the observations in the microarray based studies (Hruz et al. 2008, Toronto 2013). It would be preferable to corroborate this finding by RT-PCR analysis to quantify the protein expression more precisely.

The high expression of *AtPM19* in seedlings tissues and perhaps in the root tip expression might suggest that PM19 plays a role in seedling development, one possibility being in the regulation of nutrient uptake. The expression of PM19 in leaves under drought stress shows that it is also possible that AtPM19 is involved in the regulation of the plant drought stress tolerance responses, a process in which the

regulation of ion uptake and release from the cell play an important role. Investigations into the physiological behaviour of AtPM19 protein in *A. thaliana* seedlings for a better understanding of the function of the AtPM19 protein are discussed in the next section.

As explained earlier (see sections 3.5.1, 3.5.2 and 3.5.3 in the results chapter) the mutant *atpm19 Arabidopsis thaliana* line was examined to confirm that the *AtPM19* gene is not expressed. The PCR reactions set with PM19 specific primers (PAP986 and PAP97) and T-DNA left border primer (pROK-LB) showed that two T-DNAs are inserted in the *AtPM19* gene. In addition a northern blot of RNA extracted from wild type and mutant *atpm19 Arabidopsis* seeds showed an approximately 1000 base band for the wild type, while the mutant *atpm19* showed no band, confirming the silencing of the *AtPM19* gene.

Complementation of the mutant *atpm19 Arabidopsis* by crossing with a plant containing the overexpressed form of the *AtPM19* gene would support and validated the findings in the germination experiments. After the crossed plants are obtained, it will be essential to obtain plants containing homozygous *atpm19* mutant with the *ATPM19* transgene to use them for the complementation investigation. These experiments are being performed while this thesis is written.

**4.3. Physiological analysis of germination:**

So far, it has been established that PM19 is a very highly conserved protein found in all land plants. It is highly expressed in the germinating seedling, is localised in the plasma membrane and can be induced by drought. In order to investigate the role of the AtPM19 protein, germination experiments were carried out, since seeds and seedlings are the tissues with the highest levels of *AtPM19* gene expression. Wild type *A. thaliana* seeds, mutant *atpm19* containing seeds and seeds containing over-expressed *AtPM19* were grown on media containing different concentration of Na<sup>+</sup>, K<sup>+</sup>, Li<sup>+</sup>, Cs<sup>+</sup>, and Rb<sup>+</sup> ions added to media based on MS salts. In addition the three genotypes were germinated in media containing only water (no MS salts). The criterion for germination that was considered here was the emergence of green and healthy cotyledons.

When seeds were grown on media containing only water the mutant *atpm19* seedlings showed less than 20% germination (Figure 35). On the other hand, the overexpressed *AtPM19* protein containing seeds showed germination up to 65% while the control showed 61% germination. Although this might suggest that *AtPM19* protein helps the cell to take up water during germination, the mechanism of this process is yet to be investigated. The reduced germination of wildtype seeds on water based media compared to media with high levels of salts such as MS media might indicate that salts in general are required for high levels of germination in *Arabidopsis*, and perhaps other seeds. One explanation might be that uptake of ions increases the osmotic potential of the cell, thus driving cell expansion through increased water uptake.

The germination of seeds on media containing 50 mM and 100 mM KCl showed an enhanced sensitivity of the mutant *atpm19* as compared to the wildtype, while the seeds that contain over-expressed *AtPM19* showed higher germination than the wild type seedlings. In addition, there was an enhanced germination of seedlings containing

*35S::PM19-GFP* on media containing 100 mM NaCl (Figure 37). The germination percentages of the wild type and the mutant *pm19* seeds were 44% and 25% respectively. It was reported that 75 mM NaCl is enough to inhibit *Arabidopsis* seed germination (Koornneef et al. 2004). This suggests that PM19 protein might be involved in the efflux of  $\text{Na}^+$ . Absence of the protein in the mutant would cause toxic levels of Na to accumulate whereas overexpression of PM19 would help the plant survive on toxic levels of salt.

A caesium concentration of more than 200  $\mu\text{M}$  is reported to be toxic to plant cells (Hampton et al. 2004), however, seeds containing *35S::PM19-GFP* were able to show 100% germination on media containing 1000  $\mu\text{M}$  CsCl, which is more than the wild type plants, that showed 95% germination. On the other hand, the mutant *atpm19* was much more sensitive to  $\text{Cs}^+$ , showing only 37% germination at 1000  $\mu\text{M}$  Cs. This result also suggests that the AtPM19 protein is involved in the efflux mechanism of ions. Although Bueso et al. (2007) reported that some *Arabidopsis* germination was observed when using  $\text{Li}^+$  concentrations as high as 15 mM, in this study 5 mM of lithium was found to be inhibitory to all genotypes, with no difference between the genotypes. The germination percentage of wild type, *pm19* mutant and seeds containing *35S::PM19-GFP* on 5 mM rubidium showed 89%, 39% and 100% respectively, which is similar to what was found for potassium, albeit at much higher concentrations.

Testing the sensitivity of *Arabidopsis* mutants to different salts has been a useful method. In 1998, Zhu and his team carried out similar experiments in order to isolate and investigate the sensitivity of *sos* mutants to salts. Zhu et al. (1998) screened 267,000 mutant *Arabidopsis* plants. They measured the sensitivity of the plants by exposing the 5 days seedlings to different concentrations of NaCl, KCl, LiCl, CsCl and mannitol (Zhu et al. 1998). As a part of his study, Tezuka et al. (2013) investigated the sensitivity

to sodium and of physiological differences between two *Arabidopsis* ABA-insensitive mutant lines; (*abi5-1*) and the salt-tolerant (*mh31*) mutant. When Tezuka et al. (2013) exposed *Arabidopsis* seeds to different concentrations of NaCl they found that the *abi5-1* can grow on 175 mM NaCl concentration more than the salt-tolerant (*mh31*) mutant. After number of subsequent crossings between wild type, *mh31* and *abi5-1* plants in addition to ABA and NaCl sensitivity assays Tezuka et al. (2013) indicated that *mh31* is a new *abi5* allele (Tezuka et al. 2013).

The stomatal apparatus functions by the increase of the turgidity of the guard cells which takes place as a result of water intake by these cells. Water uptake is highly influenced by the ion concentration across the plasma membrane and the vacuolar membrane of guard cells. K<sup>+</sup> intake is essential to increase the electric potential, which in turn causes water uptake, takes place via H<sup>+</sup>/K<sup>+</sup> antiporters (Roelfsema and Hedrich 2005).

By comparing the stomatal conductancy of leaves of the wild type *A. thaliana* with the that from leaves of plants containing the mutant *atpm19* and those containing *35S::PM19-GFP*, it is possible to understand the whether there is an effect of AtPM19 protein on the guard cells. The results showed that when the plants are under drought stress, the average stomatal conductancy in the mutant *atpm19* leaves is lower than those in the wild type and the overexpressed *AtPM19* (Figure 43). The overexpressed *AtPM19* showed the highest average stomatal conductancy under normal and in drought conditions. Analysis of variance of all the readings showed statistical significance between the wild type and the *35S::PM19-GFP* plants that were watered normally.

Assuming the validity of the stomatal conductancy findings, the stomata of the plants containing *35S::PM19-GFP* showed a higher conductancy meaning they were more opened when AtPM19 is overexpressed. However, the mutant *atpm19* plants should

therefore have shown a lower conductancy than the wild type, which was not the case.

This may indicate that the effect is subtle and more replicates may be needed.



**4.4. Yeast functional complementation:**

The findings so far indicate that the function of AtPM19 is as a possible efflux ion transporter. Yet, in order to gain further evidence for this view and to pin point specifically at the metal/s that it transports, further specific investigations on yeast mutants were carried out. The genes *TRK1* and *TOK1* encode potassium specific transport proteins. Bertl et al. (2003) showed that yeast *trk1* mutant cells do not grow on SDAP media with low KCl (0.1 mM) (Bertl et al. 2003). In addition, yeast *tok1* mutants showed strong growth on SDAP media containing 100 mM CsCl and 100 mM KCl (Bertl et al. 2003), since they do not import the cesium. The transformation of *AtPM19* under control of the inducible Gal promoter into the yeast mutants WT (ply343), *trk1Δ* (PLY234) and *tok1Δ* (PLY238) was carried out in order to test if *AtMP19* would complement the yeast mutant phenotype.

In order to recover the phenotype from the yeast mutants *trk1* and *tok1*, numbers of trial experiments based on Bertl et al. (2003) were carried out. For example, three sets of genotypes were examined; first, the untransformed WT, *trk1* and *tok1* yeast mutants, second, genotypes containing the pYes2 vector on its own, third, the genotypes containing the Yes2-AtPM19 construct. These sets of genotypes were tested for growth on SDAP media containing different concentration of K<sup>+</sup>, Cs<sup>+</sup> and Li<sup>+</sup> and different pH values as in Bertl et al. (2003). These trials showed no recovery of the wildtype phenotype in either case.

Blumwald et al. (2000) pointed out that some K<sup>+</sup> plant cellular membrane transporters, such as the high-affinity K<sup>+</sup> transporter proteins (HKT), can transport sodium as well. HKT are activated at external K<sup>+</sup> concentrations as low as micromolar ranges (Blumwald et al. 2000). The germination experiments (see section 6.1.1 in the results chapter) showed high germination percentage of the wild type seedlings and seedlings

containing *35S::PM19-GFP* on high concentrations of NaCl, in contrast to the *pm19* mutant, in which germination was inhibited. In order to understand the role of AtPM19 in the NaCl tolerance, a concentration of 75 mM NaCl was used in SDAP media to grow the wild type, *trk1*, *trk2* and *tok1* yeast mutants with and without *AtPM19* gene. There was no growth of the *trk1*, nor the *trk1*-pYES2 (vector) strain on concentrations of 0 mM KCl, 75 mM NaCl at pH 5.83. When *AtPM19* was inserted, it was able to recover the loss of growth of the yeast *trk1* mutant (Figure 47), suggesting that AtPM19 may be a sodium efflux transporter. However the phenotype could not be obtained when the experiment was repeated.

The *Ena1* protein is a yeast ATPase Na<sup>+</sup> detoxification transporter (Arino et al. 2010), and the *enal* mutant yeast cells are highly sensitive to NaCl in the medium. Transformation of *AtPM19* into yeast *enal* mutant was carried out to investigate whether AtPM19 can complement the *enal* phenotype. However there were no observed growth when the yeast *Ena1* mutant containing AtPM19 was spotted on media containing between 50 and 500 mM NaCl and galactose (to induce transgene expression).

The finding that was obtained from the *enal* yeast mutant is in contradiction with the previous finding that was obtained from the *trk1* yeast mutant. The reason for that might be because although Bertl et al. (2003) were able to show growth phenotypes on media lacking K<sup>+</sup> by using yeast strains lacking TRK1, TRK2 and TOK1 proteins, those yeast mutants are not necessarily ideal for testing this phenotype for AtPM19 function. The reason for this seems that AtPM19 contains four transmembrane domains while TRK1 encodes a protein that contains 12 transmembrane domains (Gaber et al. 1988). So further research need to be undertaken to resolved this. For instance, since germination

experiments showed higher tolerance to Na<sup>+</sup>, complementation of more low affinity and other high affinity sodium transport yeast mutants with AtPM19 can be carried out.

**4.5. Conclusions:**

In conclusion, the in silico as well as the in vivo findings of the *Arabidopsis thaliana* PM19 showed that it is conserved protein in plant kingdom indicating its significance. In addition, the findings show that it very likely to be a plasma membrane protein with four transmembrane domains. Furthermore, AtPM19 protein plays a pivotal role during the germination and development of the *A. thaliana* seedlings. Germination of *A. thaliana* seeds on media containing relatively high concentrations of salt, in addition of their ability to grow on Caesium, showed that AtPM19 is an ion exporter.

More investigation on yeast mutants would help to elucidate the function of AtPM19 more specifically. For instance, since Nha1 is the only described sodium and potassium plasma membrane exporter, combining different concentrations of KCl along with NaCl would help understand the function of AtPM19. The mutant *atpm19* *A. thaliana* seeds showed high sensitivity to NaCl which is in contrast to the seeds containing overexpressed *AtPM19*, however, a recovery of the loss of phenotype by cross breeding the mutant plants with the overexpressed *AtPM19* ones would validate this finding.

**5. REFERENCES:**

- AbuQamar, S., Luo, H., Laluk, K., Mickelbart, M. V. and Mengiste, T. (2009)  
'Crosstalk between biotic and abiotic stress responses in tomato is mediated by  
the AIM1 transcription factor', *The Plant Journal*, Volume 58, Issue 2, 348-360.
- Alberts, B. (2004) *Essential Cell Biology 2: interactive*, Garland Science.
- Alberts, B., Johnson, A., Lewis, J., Raff, M., Roberts, K. and Walter, P. (2008)  
*Molecular Biology Of The Cell, New York: Garland Science*, 5th edition ed.
- Altschul, S. F., Madden, T. L., Schäffer, A. A., Zhang, J., Zhang, Z., Miller, W. and  
Lipman, D. J. (1997) 'Gapped BLAST and PSI-BLAST: a new generation of  
protein database search programs', *Nucleic acids research*, 25(17), 3389-3402.
- Araus, J., Slafer, G., Reynolds, M. and Royo, C. (2002) 'Plant breeding and drought in  
C3 cereals: what should we breed for?', *Annals of Botany*, 89(7), 925-940.
- Ashley, M., Grant, M. and Grabov, A. (2006) 'Plant responses to potassium  
deficiencies: a role for potassium transport proteins', *Journal of Experimental  
Botany*, 57(2), 425-436.
- Bartels, D., Hanke, C., Schneider, K., Michel, D. and Salamini, F. (1992) 'A  
desiccation-related Elip-like gene from the resurrection plant *Craterostigma  
plantagineum* is regulated by light and ABA', *The EMBO journal*, 11(8), 2771.

- Bertl, A., Ramos, J., Ludwig, J., Lichtenberg-Fraté, H., Reid, J., Bihler, H., Calero, F., Martínez, P. and Ljungdahl, P. O. (2003) 'Characterization of potassium transport in wild-type and isogenic yeast strains carrying all combinations of *trk1*, *trk2* and *tok1* null mutations', *Molecular microbiology*, 47(3), 767-780.
- Bewley, J. D. (1997) 'Seed germination and dormancy.', *The Plant Cell*, 9(7), 1055.
- Birch, R. G. (1997) 'Plant transformation: problems and strategies for practical application', *Annual review of plant biology*, 48(1), 297-326.
- Blatt, M. (2008) 'Ion Transport at the Plant Plasma Membrane', *eLS*.
- Blumwald, E. (2000) 'Sodium transport and salt tolerance in plants', *Current opinion in cell biology*, 12(4), 431-434.
- Blumwald, E., Aharon, G. S. and Apse, M. P. (2000) 'Sodium transport in plant cells', *Biochimica et Biophysica Acta-Biomembranes-Including Reviews on Biomembranes*, 1465(1), 140-151.
- Boyer, J. S. (1982) 'Plant productivity and environment', *Science*, 218(4571), 443-448.

- Bray, E. A. (1997) 'Plant responses to water deficit', *Trends in Plant Science*, 2(2), 48-54.
- Brisson, N., Paszkowski, J., Penswick, J., Gronenborn, B., Potrykus, I. and Hohn, T. (1984) 'Expression of a bacterial gene in plants by using a viral vector', *Nature*, (310), 511-514.
- Britto, D. T. and Kronzucker, H. J. (2008) 'Cellular mechanisms of potassium transport in plants', *Physiologia Plantarum*, 133(4), 637-650.
- Bueso, E., Alejandro, S., Carbonell, P., Perez-Amador, M. A., Fayos, J., Bellés, J. M., Rodriguez, P. L. and Serrano, R. (2007) 'The lithium tolerance of the *Arabidopsis cat2* mutant reveals a cross-talk between oxidative stress and ethylene', *The Plant Journal*, 52(6), 1052-1065.
- Castro, P. and Huber, M. E. (1992) 'Marine Biology. Mosby-Year Book', *Inc., Saint Louis, Missouri*.
- Cereghino, G. P. L. and Cregg, J. M. (1999) 'Applications of yeast in biotechnology: protein production and genetic analysis', *Current Opinion in Biotechnology*, 10(5), 422-427.
- Chen, Y. A. and Scheller, R. H. (2001) 'SNARE-mediated membrane fusion', *Nature Reviews Molecular Cell Biology*, 2(2), 98-106.

- Chen, Y. F., Wang, Y. and Wu, W. H. (2008) 'Membrane transporters for nitrogen, phosphate and potassium uptake in plants', *Journal of integrative plant biology*, 50(7), 835-848.
- Christou, P. (1992) 'Genetic transformation of crop plants using microprojectile bombardment', *The Plant Journal*, 2(3), 275-281.
- Clough, S. and Bent, A. (1998) 'Floral dip: a simplified method for *Agrobacterium* mediated transformation of *Arabidopsis thaliana*', *The Plant Journal*, 16(6), 735-743.
- Cushman, J. C. and Bohnert, H. J. (2000) 'Genomic approaches to plant stress tolerance', *Current opinion in plant biology*, 3(2), 117-124.
- D'Ambrosio, C., Gatta, L. and Bonini, S. (2005) 'The future of microarray technology: networking the genome search', *Allergy*, 60(10), 1219-1226.
- Davison, J. (1999) 'Genetic exchange between bacteria in the environment', *Plasmid*, 42(2), 73-91.
- Duffus, J. H., Nordberg, M. and Templeton, D. M. (2007) 'Glossary of terms used in toxicology, (IUPAC recommendations 2007)', *Pure and Applied Chemistry*, 79(7), 1153-1344.



- Edwards, K., Johnstone, C. and Thompson, C. (1991) 'A simple and rapid method for the preparation of plant genomic DNA for PCR analysis.', *Nucleic acids research*, 19(6), 1349.
- Elmahi, H., Espartero, J., Aguilar Portero, M., Quintero, F. J. and Pardo, J. M. (2010) 'The SOS system is essential for the salt tolerance of rice', *XVII Congress of the Federation of European Societies of Plant Biology*.
- Epstein, E., Rains, D. and Elzam, O. (1963) 'Resolution of dual mechanisms of potassium absorption by barley roots', *Proceedings of the National Academy of Sciences of the United States of America*, 49(5), 684.
- Finkelstein, R. R., Gampala, S. S. and Rock, C. D. (2002) 'Abscisic acid signaling in seeds and seedlings', *The Plant Cell Online*, 14(suppl 1), S15-S45.
- Fox, T. C. and Guerinot, M. L. (1998) 'Molecular biology of cation transport in plants', *Annual review of plant biology*, 49(1), 669-696.
- Gaber, R. F., Styles, C. A. and Fink, G. R. (1988) 'TRK1 encodes a plasma membrane protein required for high-affinity potassium transport in *Saccharomyces cerevisiae*', *Molecular and cellular biology*, 8(7), 2848-2859.
- Gambale, F. and Uozumi, N. (2006) 'Properties of Shaker-type potassium channels in higher plants', *The Journal of membrane biology*, 210(1), 1-19.

- Garcia-Molina, A., Andrés-Colás, N., Perea-García, A., Neumann, U., Dodani, S. C., Huijser, P., Peñarrubia, L. and Puig, S. (2013) 'The Arabidopsis COPT6 transport protein functions in copper distribution under copper-deficient conditions', *Plant and Cell Physiology*.
- Gasser, C. S. and Fraley, R. T. (1989) 'Genetically engineering plants for crop improvement', *Science*, 244(4910), 1293-1299.
- Gasteiger, E., Hoogland, C., Gattiker, A., Duvaud, S. e., Wilkins, M. R., Appel, R. D. and Bairoch, A. (2005) 'Protein identification and analysis tools on the ExPASy server', *The proteomics protocols handbook*, 571-607.
- Gelvin, S. B. (2003) 'Agrobacterium-mediated plant transformation: the biology behind the “gene-jockeying” tool', *Microbiology and Molecular Biology Reviews*, 67(1), 16-37.
- Glass, A. D. (1983) 'Regulation of ion transport', *Annual Review of Plant Physiology*, 34(1), 311-326.
- Grabov, A. (2007) 'Plant KT/KUP/HAK potassium transporters: single family–multiple functions', *Annals of Botany*, 99(6), 1035-1041.
- Grefen, C., Honsbein, A. and Blatt, M. R. (2011) 'Ion transport, membrane traffic and cellular volume control', *Current opinion in plant biology*, 14(3), 332-339.

- Hampton, C. R., Bowen, H. C., Broadley, M. R., Hammond, J. P., Mead, A., Payne, K. A., Pritchard, J. and White, P. J. (2004) 'Cesium toxicity in Arabidopsis', *Plant Physiology*, 136(3), 3824-3837.
- Hansen, G. and Wright, M. S. (1999) 'Recent advances in the transformation of plants', *Trends in Plant Science*, 4(6), 226-231.
- Hilder, V. A., Gatehouse, A. M., Sheerman, S. E., Barker, R. F. and Boulter, D. (1987) 'A novel mechanism of insect resistance engineered into tobacco', *Nature*, 330(6144), 160-163.
- Hoffman, C. S. and Winston, F. (1987) 'A ten-minute DNA preparation from yeast efficiently releases autonomous plasmids for transformiaon of *Escherichia coli*', *Gene*, 57(2), 267-272.
- Hooykaas, P. J. and Schilperoort, R. A. (1992) 'Agrobacterium and plant genetic engineering' in *10 Years Plant Molecular Biology*, Springer, 15-38.
- Hruz, T., Laule, O., Szabo, G., Wessendorp, F., Bleuler, S., Oertle, L., Widmayer, P., Gruissem, W. and Zimmermann, P. (2008) 'Genevestigator V3: a reference expression database for the meta-analysis of transcriptomes', *Advances in Bioinformatics*, 2008, 5.

- Huang, G.-T., Ma, S.-L., Bai, L.-P., Zhang, L., Ma, H., Jia, P., Liu, J., Zhong, M. and Guo, Z.-F. (2012) 'Signal transduction during cold, salt, and drought stresses in plants', *Molecular biology reports*, 39(2), 969-987.
- Hundertmark, M. and Hinch, D. K. (2008) 'LEA (late embryogenesis abundant) proteins and their encoding genes in *Arabidopsis thaliana*', *BMC genomics*, 9(1), 118.
- Hynes, R. O. (1976) 'Cell surface proteins and malignant transformation', *Biochimica et Biophysica Acta (BBA)-Reviews on Cancer*, 458(1), 73-107.
- Ingram, J. and Bartels, D. (1996) 'The molecular basis of dehydration tolerance in plants', *Annual review of plant biology*, 47(1), 377-403.
- Initiative, A. G. (2000) 'Analysis of the genome sequence of the flowering plant *Arabidopsis thaliana*', *Nature*, 408(6814), 796.
- Inoue, H., Nojima, H. and Okayama, H. (1990) 'High efficiency transformation of *Escherichia coli* with plasmids', *Gene*, 96(1), 23.
- Jefferson, R. A., Kavanagh, T. A. and Bevan, M. W. (1987) 'GUS fusions: beta-glucuronidase as a sensitive and versatile gene fusion marker in higher plants', *The EMBO journal*, 6(13), 3901.

- Jefferson, R. A., Kavanagh, T. A. and Bevan, M. W. (1987) 'GUS fusions: beta-glucuronidase as a sensitive and versatile gene fusion marker in higher plants.', *The EMBO journal*, 6(13), 3901.
- Johansson, I., Karlsson, M., Johanson, U., Larsson, C. and Kjellbom, P. (2000) 'The role of aquaporins in cellular and whole plant water balance', *Biochimica et Biophysica Acta-Biomembranes-Including Reviews on Biomembranes*, 1465(1), 324-342.
- Jones, G. V. and Davis, R. E. (2000) 'Climate influences on grapevine phenology, grape composition, and wine production and quality for Bordeaux, France', *American Journal of Enology and Viticulture*, 51(3), 249-261.
- Kammerloher, W., Fischer, U., Piechottka, G. P. and Schäffner, A. R. (1994) 'Water channels in the plant plasma membrane cloned by immunoselection from a mammalian expression system', *The Plant Journal*, 6(2), 187-199.
- Keinan, A. and Clark, A. G. (2012) 'Recent explosive human population growth has resulted in an excess of rare genetic variants', *Science*, 336(6082), 740-743.
- Klee, H., Horsch, R. and Rogers, S. (1987) 'Agrobacterium-mediated plant transformation and its further applications to plant biology', *Annual Review of Plant Physiology*, 38(1), 467-486.

- Klein, T., Gradziel, T., Fromm, M. and Sanford, J. (1988) 'Factors influencing gene delivery into *Zea mays* cells by high-velocity microprojectiles', *Nature Biotechnology*, 6(5), 559-563.
- Klein, T. M., Wolf, E., Wu, R. and Sanford, J. (1987) 'High-velocity microprojectiles for delivering nucleic acids into living cells', *Nature*, 327(6117), 70-73.
- Kline, K. G., Sussman, M. R. and Jones, A. M. (2010) 'Abscisic acid receptors', *Plant Physiology*, 154(2), 479-482.
- Koike, M., Takezawa, D., Arakawa, K. and Yoshida, S. (1997) 'Accumulation of 19-kDa plasma membrane polypeptide during induction of freezing tolerance in wheat suspension-cultured cells by abscisic acid', *Plant and Cell Physiology*, 38(6), 707-716.
- Komatsu, S. (2008) 'Plasma membrane proteome in Arabidopsis and rice', *Proteomics*, 8(19), 4137-4145.
- Koornneef, M., Alonso-Blanco, C. and Vreugdenhil, D. (2004) 'Naturally occurring genetic variation in *Arabidopsis thaliana*', *Annual review of plant biology*, 55, 141-172.
- Koornneef, M., Bentsink, L. and Hilhorst, H. (2002) 'Seed dormancy and germination', *Current opinion in plant biology*, 5(1), 33-36.

- Lal, R., Uphoff, N., Stewart, B. A. and Hansen, D. O. (2005) *Climate change and global food security*, Taylor & Francis Group.
- Läuchli, A. and Epstein, E. (1970) 'Transport of potassium and rubidium in plant roots: the significance of calcium', *Plant Physiology*, 45(5), 639.
- Leung, J. and Giraudat, J. (1998) 'Abscisic acid signal transduction', *Annual review of plant biology*, 49(1), 199-222.
- Li, B. and Foley, M. (1997) 'Genetic and molecular control of seed dormancy', *Trends in Plant Science*, 2(10), 384-389.
- Lodish, H., Berk, A., Kaiser, C. A., Krieger, M., Scott, M. P., Bretscher, A., Ploegh, H. and Matsudaira, P. (2008a) *Molecular Cell Biology*, Fifth ed., New York: Freeman.
- Lodish, H., Berk, A., Matsudaira, P., Kaiser, C. A., Krieger, M., Scott, M. P., Zipursky, S. L. and Darnell, J. (2008b) *Molecular Cell Biology*, Fifth ed., New York: Freeman.
- Lodish, H., Berk, A., Zipursky, S. L., Matsudaira, P., Baltimore, D. and Darnell, J. (2000) *Molecular cell biology*, New York, Freeman.

- Lüthje, S., Hopff, D., Schmitt, A., Meisrimler, C.-N. and Menckhoff, L. (2009) 'Hunting for low abundant redox proteins in plant plasma membranes', *Journal of proteomics*, 72(3), 475-483.
- Maathuis, F. J. and Sanders, D. (1996) 'Mechanisms of potassium absorption by higher plant roots', *Physiologia Plantarum*, 96(1), 158-168.
- Marin, E., Nussaume, L., Quesada, A., Gonneau, M., Sotta, B., Hugueney, P., Frey, A. and Marion-Poll, A. (1996) 'Molecular identification of zeaxanthin epoxidase of *Nicotiana plumbaginifolia*, a gene involved in abscisic acid biosynthesis and corresponding to the ABA locus of *Arabidopsis thaliana*', *The EMBO journal*, 15(10), 2331.
- Marschner, H., Kuiper, P. and Kylin, A. (1981) 'Genotypic differences in the response of sugar beet plants to replacement of potassium by sodium', *Physiologia Plantarum*, 51(2), 239-244.
- Mäser, P., Gierth, M. and Schroeder, J. I. (2002) 'Molecular mechanisms of potassium and sodium uptake in plants', *Plant and Soil*, 247(1), 43-54.
- Maurel, C. and Chrispeels, M. J. (2001) 'Aquaporins. A molecular entry into plant water relations', *Plant Physiology*, 125(1), 135-138.
- McCarty, D. R. (1995) 'Genetic control and integration of maturation and germination pathways in seed development', *Annual review of plant biology*, 46(1), 71-93.



- Meinke, D. W., Cherry, J. M., Dean, C., Rounsley, S. D. and Koornneef, M. (1998) '*Arabidopsis thaliana*: a model plant for genome analysis', *Science*, 282(5389), 662-682.
- Meng, L. and Feldman, L. (2010) 'A rapid TRIzol-based two-step method for DNA-free RNA extraction from *Arabidopsis* siliques and dry seeds', *Biotechnology Journal*, 5(2), 183-186.
- Mengel, K. and Arneke, W. W. (1982) 'Effect of potassium on the water potential, the pressure potential, the osmotic potential and cell elongation in leaves of *Phaseolus vulgaris*', *Physiologia Plantarum*, 54(4), 402-408.
- Meyerowitz, E. M. and Somerville, C. R. (1994) *Arabidopsis*, Cold Spring Harbor Laboratory Press.
- Miki, B. and McHugh, S. (2004) 'Selectable marker genes in transgenic plants: applications, alternatives and biosafety', *Journal of Biotechnology*, 107(3), 193-232.
- Mittler, R. (2006) 'Abiotic stress, the field environment and stress combination', *Trends in Plant Science*, 11(1), 15-19.

- Mueckler, M. (1994) 'Facilitative glucose transporters', *European Journal of Biochemistry*, 219(3), 713-725.
- Munns, R. and Tester, M. (2008) 'Mechanisms of salinity tolerance', *Annual review of plant biology*, 59, 651-681.
- Nakai, K. (1991) 'Predicting various targeting signals in amino acid sequences', *Bulletin of the Institute for Chemical Research, Kyoto University*, 69(3), 269-291.
- Nakai, K. (2000) 'Protein sorting signals and prediction of subcellular localization', *Advances in protein chemistry*, 54, 277-344.
- Pachauri, R. K. and Reisinger, A. (2007) 'Climate Change 2007: Synthesis Report. Contribution of Working Groups I, II and III to the Fourth Assessment Report of the Intergovernmental Panel on Climate Change', *Intergovernmental Panel on Climate Change*.
- Palmgren, M. G. (2001) 'Plant plasma membrane H<sup>+</sup>-ATPases: powerhouses for nutrient uptake', *Annual review of plant biology*, 52(1), 817-845.
- Parry, M. L. (2007) *Climate Change 2007: Impacts, Adaptation and Vulnerability: Working Group II Contribution to the Fourth Assessment Report of the IPCC Intergovernmental Panel on Climate Change*, Cambridge University Press.

Peleg, Z. and Blumwald, E. (2011) 'Hormone balance and abiotic stress tolerance in crop plants', *Current opinion in plant biology*, 14(3), 290-295.

Piao, S., Ciais, P., Huang, Y., Shen, Z., Peng, S., Li, J., Zhou, L., Liu, H., Ma, Y. and Ding, Y. (2010) 'The impacts of climate change on water resources and agriculture in China', *Nature*, 467(7311), 43-51.

Pons (2005) *Studies into the location and function of AtPM19, a putative membrane protein in Arabidopsis thaliana*, unpublished thesis Heriot-Watt University.

Potrykus, I. (1991) 'Gene transfer to plants: assessment of published approaches and results', *Annual review of plant biology*, 42(1), 205-225.

Pyo, Y. J., Gierth, M., Schroeder, J. I. and Cho, M. H. (2010) 'High-affinity K<sup>+</sup> transport in Arabidopsis: AtHAK5 and AKT1 are vital for seedling establishment and postgermination growth under low-potassium conditions', *Plant Physiology*, 153(2), 863-875.

Raghavendra, A. S., Gonugunta, V. K., Christmann, A. and Grill, E. (2010) 'ABA perception and signalling', *Trends in Plant Science*, 15(7), 395-401.

Rock, C. and Quatrano, R. (1995) 'The role of hormones during seed development', *Plant hormones: physiology, biochemistry and molecular biology*, 2, 671-697.

- Rodríguez-Navarro, A. and Rubio, F. (2006) 'High-affinity potassium and sodium transport systems in plants', *Journal of Experimental Botany*, 57(5), 1149-1160.
- Roelfsema, M. R. G. and Hedrich, R. (2005) 'In the light of stomatal opening: new insights into 'the Watergate'', *New Phytologist*, 167(3), 665-691.
- Romanos, M. A., Scorer, C. A. and Clare, J. J. (1992) 'Foreign gene expression in yeast: a review', *Yeast*, 8(6), 423-488.
- Sambrook, J., Fritsch, E. F. and Maniatis, T. (1989) *Molecular cloning*, New York: Cold Spring Harbor Laboratory Press
- Sanford, J. C. (1988) 'The biolistic process', *Trends in Biotechnology*, 6(12), 299-302.
- Shi, H., Ishitani, M., Kim, C. and Zhu, J.-K. (2000) 'The *Arabidopsis thaliana* salt tolerance gene SOS1 encodes a putative Na<sup>+</sup>/H<sup>+</sup> antiporter', *Proceedings of the National Academy of Sciences*, 97(12), 6896-6901.
- Shi, H., Quintero, F. J., Pardo, J. M. and Zhu, J.-K. (2002) 'The putative plasma membrane Na<sup>+</sup>/H<sup>+</sup> antiporter SOS1 controls long-distance Na<sup>+</sup> transport in plants', *The Plant Cell Online*, 14(2), 465-477.

- Shieh, C.-C., Coghlan, M., Sullivan, J. P. and Gopalakrishnan, M. (2000) 'Potassium channels: molecular defects, diseases, and therapeutic opportunities', *Pharmacological reviews*, 52(4), 557-594.
- Shillito, R. (1999) 'Methods of genetic transformation: electroporation and polyethylene glycol treatment' in *Molecular Improvement of Cereal Crops*, Springer, 9-20.
- Simossis, V. A. and Heringa, J. (2005) 'PRALINE: a multiple sequence alignment toolbox that integrates homology-extended and secondary structure information', *Nucleic acids research*, 33(suppl 2), W289-W294.
- Singer, S. (1990) 'The structure and insertion of integral proteins in membranes', *Annual review of cell biology*, 6(1), 247-296.
- Smith, A. M., Coupland, G., Dolan, L., Harberd, N., Jones, J., Martin, C., Sablowski, R. and Amey, A. (2010) *Plant Biology*, Garland Science.
- Smith, H. O., Gwinn, M. L. and Salzberg, S. L. (1999) 'DNA uptake signal sequences in naturally transformable bacteria', *Research in microbiology*, 150(9), 603-616.
- Spalding, E. P., Hirsch, R. E., Lewis, D. R., Qi, Z., Sussman, M. R. and Lewis, B. D. (1999) 'Potassium uptake supporting plant growth in the absence of AKT1 channel activity inhibition by ammonium and stimulation by sodium', *The Journal of general physiology*, 113(6), 909-918.

- Suelter, C. (1970) 'Enzymes activated by monovalent cations', *Science*, 168(3933), 789-795.
- Sychrova, H. (2004) 'Yeast as a model organism to study transport and homeostasis of alkali metal cations', *Physiological research*, 53, 91-98.
- Szabados, L., Charrier, B., Kondorosi, A., de Bruijn, F. J. and Ratet, P. (1995) 'New plant promoter and enhancer testing vectors', *Molecular Breeding*, 1(4), 419-423.
- Szczerba, M. W., Britto, D. T. and Kronzucker, H. J. (2009) 'K<sup>+</sup> transport in plants: physiology and molecular biology', *Journal of plant physiology*, 166(5), 447-466.
- Tezuka, K., Taji, T., Hayashi, T. and Sakata, Y. (2013) 'A novel *abi5* allele reveals the importance of the conserved Ala in the C3 domain for regulation of downstream genes and salt tolerance during germination in *Arabidopsis*', *Plant signaling & behavior*, 8(3), e23455.
- Thompson, K. and Jones, A. (1999) 'Human population density and prediction of local plant extinction in Britain', *Conservation Biology*, 13(1), 185-189.
- Toronto, U. o. (2013) 'ePlant Browser', [online], available: <http://bar.utoronto.ca/eplant/> [accessed 18/2/2013].

- Turmel, M., Otis, C. and Lemieux, C. (1999) 'The complete chloroplast DNA sequence of the green alga *Nephroselmis olivacea*: insights into the architecture of ancestral chloroplast genomes', *Proceedings of the National Academy of Sciences*, 96(18), 10248-10253.
- Tzfira, T. and Citovsky, V. (2003) 'The Agrobacterium-plant cell interaction. Taking biology lessons from a bug', *Plant Physiology*, 133(3), 943-947.
- Verslues, P., Agarwal, M., Katiyar-Agarwal, S., Zhu, J. and Zhu, J. (2006) 'Methods and concepts in quantifying resistance to drought, salt and freezing, abiotic stresses that affect plant water status.', *Plant J*, 45(4), 523-39.
- Véry, A.-A. and Sentenac, H. (2003) 'Molecular mechanisms and regulation of K<sup>+</sup> transport in higher plants', *Annual review of plant biology*, 54(1), 575-603.
- Wang, W., Vinocur, B. and Altman, A. (2003) 'Plant responses to drought, salinity and extreme temperatures: towards genetic engineering for stress tolerance', *Planta*, 218(1), 1-14.
- Wang, Y., Shaikh, S. A. and Tajkhorshid, E. (2010) 'Exploring transmembrane diffusion pathways with molecular dynamics', *Physiology*, 25(3), 142-154.
- Ward, J. M., Mäser, P. and Schroeder, J. I. (2009) 'Plant ion channels: gene families, physiology, and functional genomics analyses', *Annual Review of Physiology*, 71, 59-82.

- Wegner, L. H. and Raschke, K. (1994) 'Ion channels in the xylem parenchyma of barley roots (A procedure to isolate protoplasts from this tissue and a patch-clamp exploration of salt passageways into xylem vessels)', *Plant Physiology*, 105(3), 799-813.
- Weiner, J. J., Peterson, F. C., Volkman, B. F. and Cutler, S. R. (2010) 'Structural and functional insights into core ABA signaling', *Current opinion in plant biology*, 13(5), 495-502.
- Wendelboe-Nelson, C. and Morris, P. C. (2012) 'Proteins linked to drought tolerance revealed by DIGE analysis of drought resistant and susceptible barley varieties', *Proteomics*, 12(22), 3374-3385.
- Xiong, J. (2006) *Essential bioinformatics*, Cambridge University Press.
- Xiong, L. and Zhu, J. K. (2002) 'Molecular and genetic aspects of plant responses to osmotic stress', *Plant, cell & environment*, 25(2), 131-139.
- Yamaguchi-Shinozaki, K. and Shinozaki, K. (1994) 'A novel cis-acting element in an Arabidopsis gene is involved in responsiveness to drought, low-temperature, or high-salt stress', *The Plant Cell Online*, 6(2), 251-264.
- Zhu, J.-K. (2001) 'Plant salt tolerance', *Trends in Plant Science*, 6(2), 66-71.



Zhu, J.-K. (2002) 'Salt and drought stress signal transduction in plants', *Annual review of plant biology*, 53, 247.

Zhu, J.-K., Liu, J. and Xiong, L. (1998) 'Genetic analysis of salt tolerance in Arabidopsis: evidence for a critical role of potassium nutrition', *The Plant Cell Online*, 10(7), 1181-1191.